BME464: Medical Imaging

John DiCecco, PhD

Department of Electrical, Computer, and Biomedical Engineering
University of Rhode Island
Kingston, RI USA
diceccoj@ele.uri.edu

December 2, 2021

Introduction

Medical Imaging Systems (*The Physics of Medical Imaging*, Webb)

- Conventional X-rays
- Nuclear Medicine
  - Imaging of radiopharmaceuticals
- Diagnostic Ultrasound
- Magnetic Resonance Imaging (MRI)
- Medical Image Processing
  - Backprojection, Radon Transform, Convolution, filtering, etc.
- Computer Requirements

Student Image Processing Project (More later)

Grading Exam 1, Exam 2, Exam 3 (final ... also the last exam) 33% each

Why Imaging?

- Heart disease: 659,041
- Cancer: 599,601
- Accidents (unintentional injuries): 173,040
- Chronic lower respiratory diseases: 156,979
- Stroke (cerebrovascular diseases): 150,005
- Alzheimer's disease: 121,499
- Diabetes: 87,647
- Influenza and Pneumonia: 49,783 (2019 data, SARS-Cov-2 changes this with 377,883)
- Nephritis, nephrotic syndrome, and nephrosis: 51,565
- Intentional self-harm (suicide): 47,511 (2019 data)
- Septicemia: 35,539
- Chronic liver disease: 33,539
- Essential hypertension and hypertensive renal disease: 27,477
- Parkinsons disease: 23,107
- Pneumonitis due to solids and liquids: 18,090
- All other causes: about 600,000

History of Medical Imaging

- 1895 - Discovery of x-rays (Wilhelm Röntgen)
- 1905 - Subtraction Radiogram (DSA)
- 1917 - Radon Transform
- 1937 - Xeroradiograhpy (patent)
- 1946 - NMR principle
- 1950 - Scintillation imaging (γ-camera)
- 1952 - 2D Ultrasound Imaging
- 1953 - Positron Tomography
- 1957 - Anger (γ) camera using Sodium Iodide Crystals
- 1958 - X-ray CT
- 1961 - Oldendorf - laboratory X-ray CT
- 1963 - SPET (analog)
- 1971 - SPECT
- 1972 - First commercial X-ray CT (Ambrose and Hounsfield)
  - 1979 - Nobel prize to Hounsfield and Cormack
- 1976 - MRI (Mansfield & Maudsley) - ex-vivo finger
  - 1978 - Commercial version
- 1982 - Impedance Tomography

THINK BIG WE DO™

Cardiology

- Cardiac Ultrasound Images - Echo and Doppler
  - Non-invasive but poor resolution
  - Mitral (bicuspid), tricuspid valve regurgitation, flow
- Angiogram - Catheterization
  - Percutaneous Transluminal Coronary Angioplasty (PTCA)
  - AKA Balloon Angioplasty

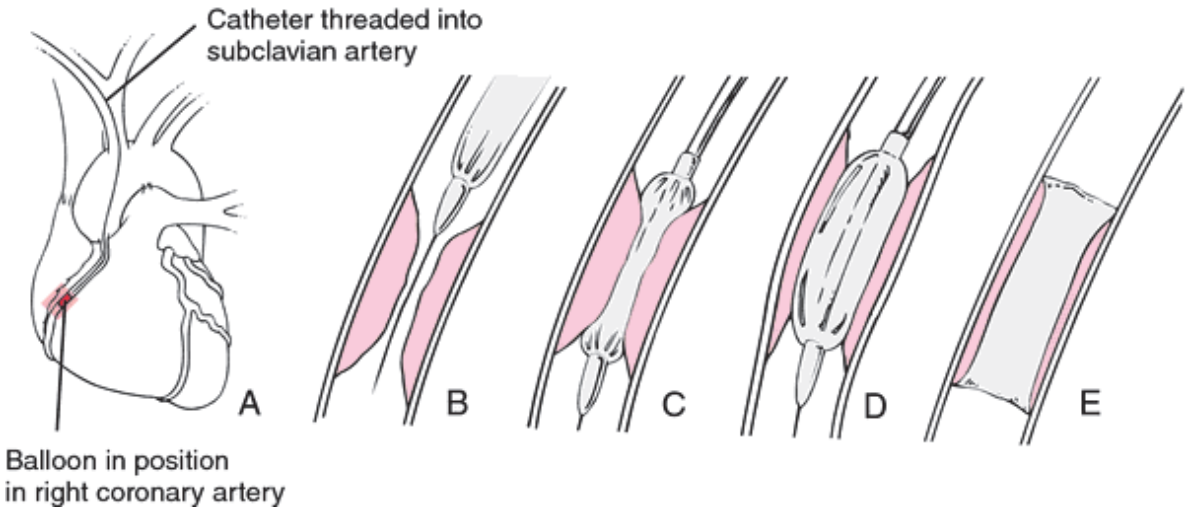

3D

- CT Scan (Computed Tomography, or Computer Axial Tomography (CAT))
- MRI (with/without contrast, typically varying paramagnetism)
- Dynamic Spatial Reconstructor (Mayo Clinic)
  - 14 image intensified X-ray tubes

Photons (EM waves)

Media to make human body semi-opaque

- Visible light (3800 Å- 7600Å) human body is opaque
- $400 \sim 800$ THz
- $1.6 \sim 3.28$ eV
- Recall:

$$E = h\nu = \frac{hc}{\lambda} \quad \text{(v is frequency)} \tag{1}$$

$$h = 6.626 \times 10^{-34} J \cdot s = 4.14 \times 10^{-15} eV \cdot s \tag{2}$$

$$c = 3 \times 10^{8} m/s (speedoflight) \tag{3}$$

$$E(eV) = \frac{1.24 \times 10^{-6}}{\lambda(m)} eV \tag{4}$$

$$\frac{1.24 \times 10^{-6}}{\lambda(m)} = \frac{1240}{\lambda(nm)} eV \tag{5}$$

THINK BIG WE DO™

Photons (EM waves) (cont.)

- Recall human body is opaque to visible light
- Cosmic Rays (10^{-11} to 10^{-16}Å) human body is transparent
  - Energy is $10^{15} - 10^{20}$ eV
  - 1 eV $= 1.6 \times 10^{-12} erg = 1.6 \times 10^{-19} joules$
  - Charge on an electron is $1.6 \times 10^{-19} C$
- X-rays (energy 0.1 $\sim$ 123 keV, λ 0.1$\sim$ 100 Å) human body is semi-opaque
  - Trade-off between X-ray dose and SNR
  - radioactive isotope (Tc - 140 keV, Ga - 511 keV after positron electron annihilation)

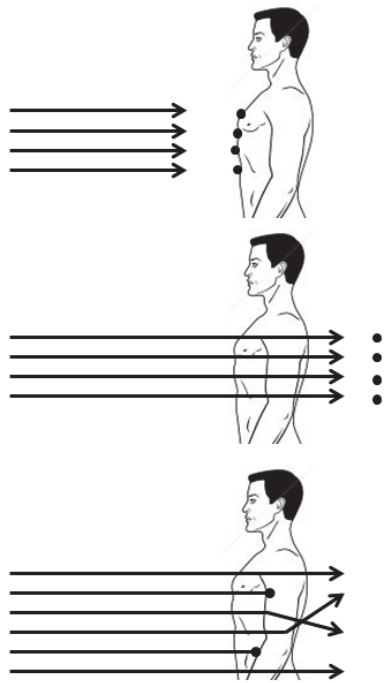

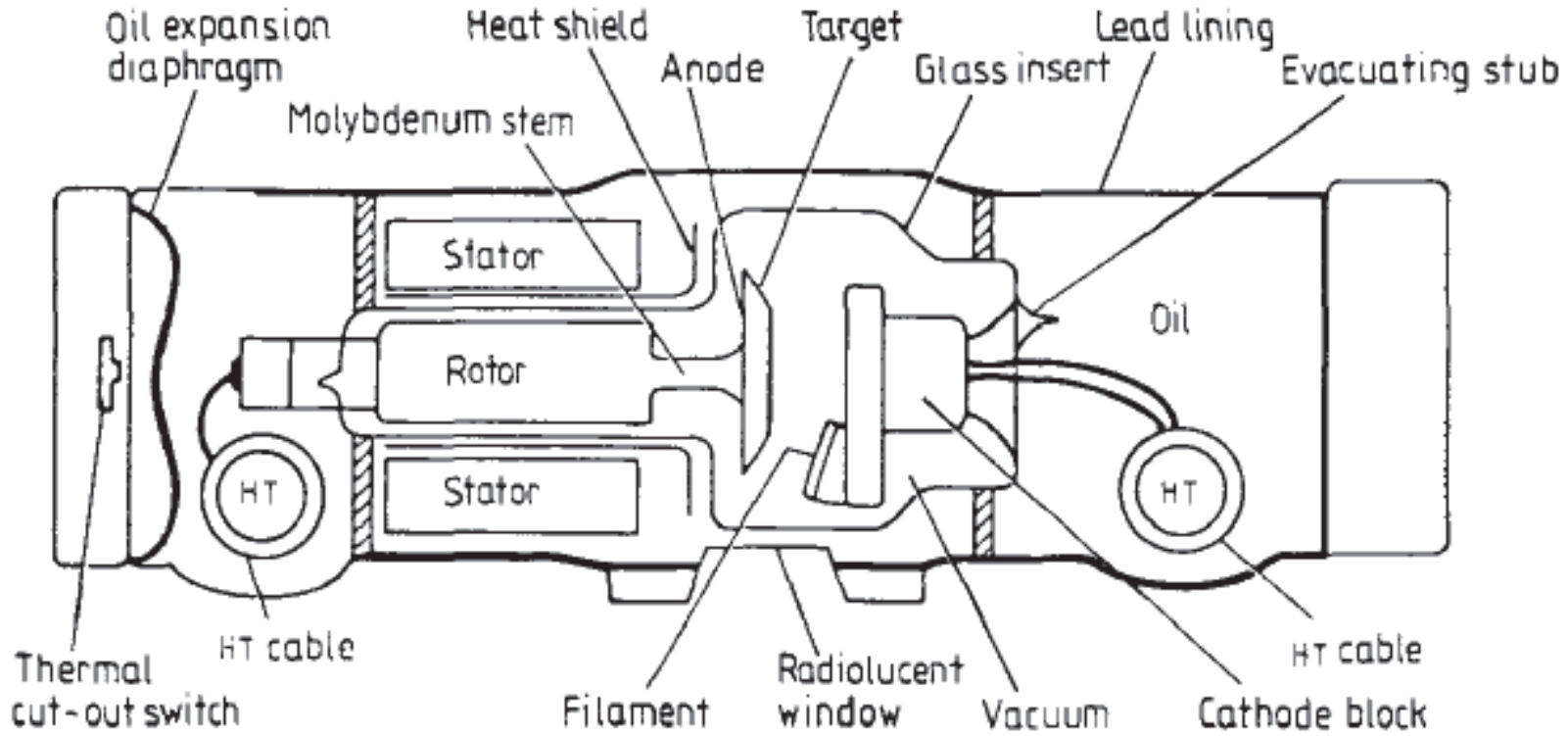

Figure 2.8 The construction of a rotating-anode x-ray tube. (Reproduced with permission of MTP Press Ltd from Forster (1985).)

Three Types of Interactions Between X-ray and Tissue

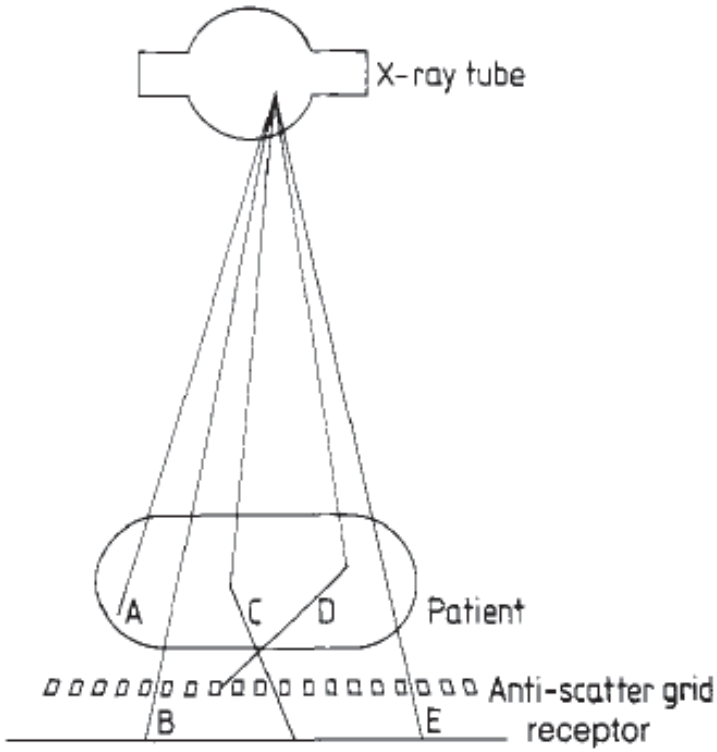

Figure 2.1 The components of the x-ray imaging system and the formation of the radiographic image. B and E represent photons that have passed through the patient without interacting. C and D are scattered photons. D has been stopped by an anti-scatter grid. Photon A has been absorbed.

THINK BIG WE DO™

Three Types of Interactions Between X-ray and Tissue

Photoelectric interaction - "ionization" effect (photoionization)

- Transmitted - passes through unaffected (Primary)
- Scattered - interacts with tissue or bone and passes through (Secondary)
- Absorbed - this is the delivery dose and is responsible for the damage
  - The characteristic x-ray may not always be absorbed but the ionized electron almost always will be
  - Mean free path of electron in water is 0.03 cm

THINK BIG WE DO™

Dose Versus Contrast Trade-off

- Low Energy Photons - Only a few get through
  - Good contrast but to get enough photons to the detector, HIGH DOSE
  - In case you're not sure, high dose is BAD
- High Energy Photons - Most get through
  - Poor contrast
  - Good news is low dose to patient
  - Bad news is unusable image - colossal waste of time
- X-ray energy determined by
  - X-ray target material, W(high), Mo(low)
  - X-ray tube potential (how much voltage is supplied)
  - Filtration (screening) - typically Al or Cu, with Al preferred for medical imaging (lower atomic number, control with thickness)

Dose Versus Contrast Trade-off

- For CT scan, can take advantage of redundant information
- Image processing can "filter" low contrast images
- Image at right current GE algorithm developed at Purdue University
  - Left, filtered back projection (we will cover)
  - Right, Veo™ iterative reconstruction (we will not cover)

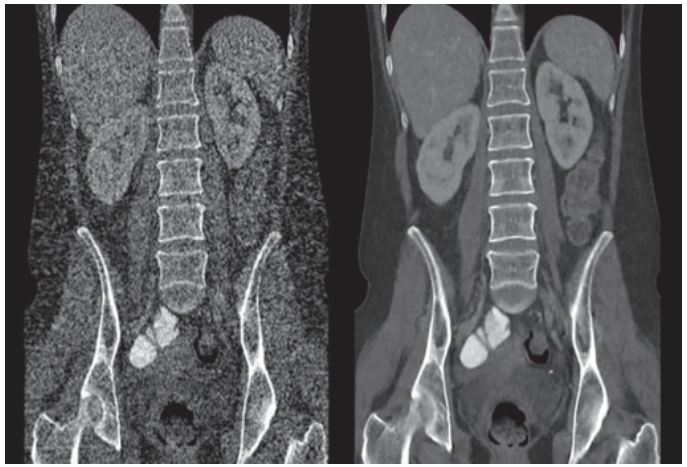

THINK BIG WE DO™

Image Receptors

- Film, though much less now than historical use
- Screen film (copper, aluminum, etc)
- Xeroradiogram
- Image intensifier tube (IIT) and Photomultipliers (PMT)
- Charge-Coupled Device (CCD - often used with IIT)

Other receptors include ionography chamber and stimulable phosphor, though the prevalence of other modalities (CT, PET, MRI, etc.) have made the development of these modalities somewhat moot

THINK BIG WE DO™

Film

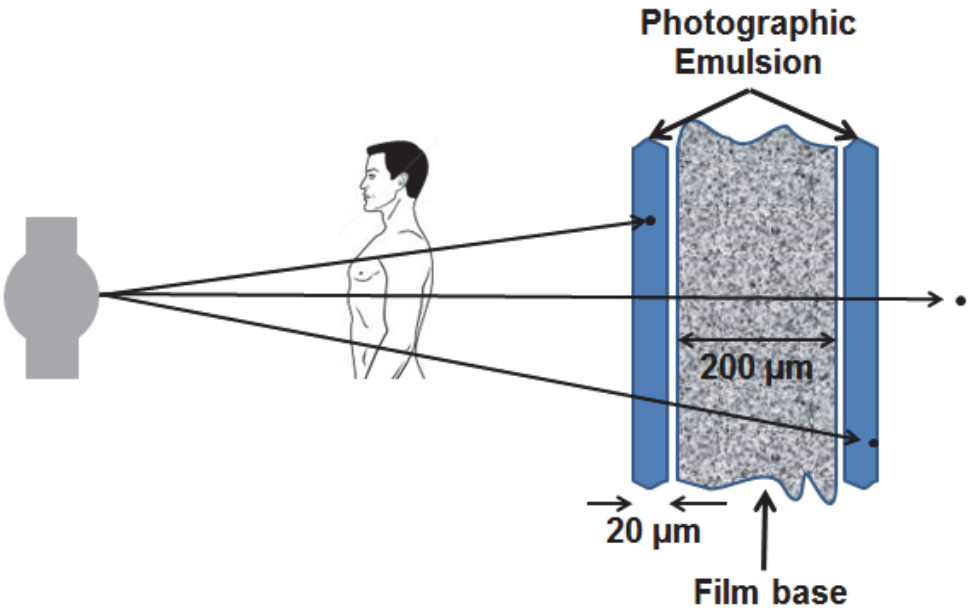

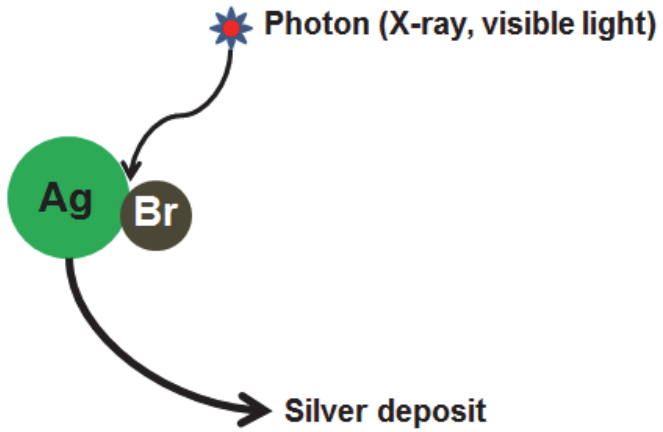

- Speed: Low
- Dose: High
- Resolution: High
- Photographic emulsion is AgBr suspended in gelatin (lime, I think)

Expose-Develop-Fix-Stop-Wash

Δ sensitized grains $\propto$ Δ incident photons and the # unsensitized grains

$$dg = (G - g)bdN, \text{ where}$$

- G: # grains of AgBr per unit area
- b: cross-sectional area of a single AgBr grain
- g: # sensitized grains per unit area
- N: # photons(i.e. the dose)

Boundary condition: N = 0, g = 0 (G is a constant)

$$g = G(1 - e^{(-bN)}) + g_0$$

g is now the optical density (sort of, more later), N is the exposure, and g_0 is the fog level

Optical Density (Darkening)

$$D = \log_{10} \frac{I_0}{I}$$

- I_0: incident light intensity
- I: exit light intensity

Near the maximum contrast point

THINK BIG WE DO™

Graphical Representation of Scatter at I(x,y)

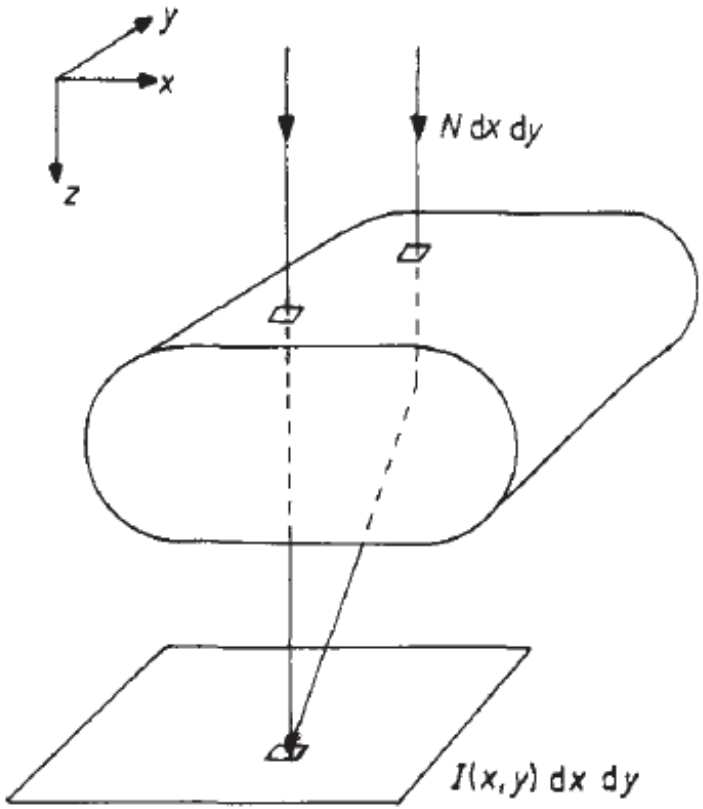

Figure 2.2 Simple model of the formation of the radiographic image showing both a primary and a secondary photon.

Lambert-Beer Law of Photon Absorption

$$I(x,y) = N\mathcal{E}(E,0)Ee^{-\int \mu(x,y,z)dz} + \int \mathcal{E}(E_s,\theta)E_s S(x,y,E_s,\Omega)d\Omega dE_s \quad (6)$$

I(x,y):	image at the receptor
N:	# of incident x-ray photons per unit area (assumed single energy E)
$\mu(x,y,z)$:	attenuation coefficient (i.e. YOU)
$S(x,y,E_s,\Omega)$:	# scatter photons arrived at (x,y) from solid angle (i.e. $d\Omega = \sin\theta\, d\theta\, d\phi$) with energy range dE_s
$\mathcal{E}(E,\theta)$:	energy absorption coefficient for energy E, solid angle Ω

Lambert-Beer Law of Photon Absorption

$$I(x,y) \approx N\mathcal{E}(E,0)Ee^{-\int \mu(x,y,z)dz} + \bar{S}\bar{\mathcal{E}}(E)E = N\mathcal{E}(E,0)Ee^{-\int \mu(x,y,z)dz}(1+R) \tag{7}$$

R: Scattered to primary ratio

If we now make the substitution

$$C = \frac{I_1 - I_2}{I_1} \tag{8}$$

where C is the contrast, we have

$$I_1 = N\mathcal{E}(E,0)Ee^{-\mu_1 t_1} + \bar{S}\bar{\mathcal{E}}(E)E \tag{9}$$

$$I_2 = N\mathcal{E}(E,0)Ee^{[-\mu_1(t_1-t_2)-\mu_2 t_2]} + \bar{S}\bar{\mathcal{E}}(E)E \tag{10}$$

$$C = \frac{e^{-\mu_1 t_1} - e^{[-\mu_1(t_1-t_2)-\mu_2 t_2]}}{e^{-\mu_1 t_1}(1+R)} \tag{11}$$

$$= \frac{1 - e^{-(\mu_2-\mu_1)t_2}}{1+R} \tag{12}$$

THINK BIG WE DO™

Contrast Integral

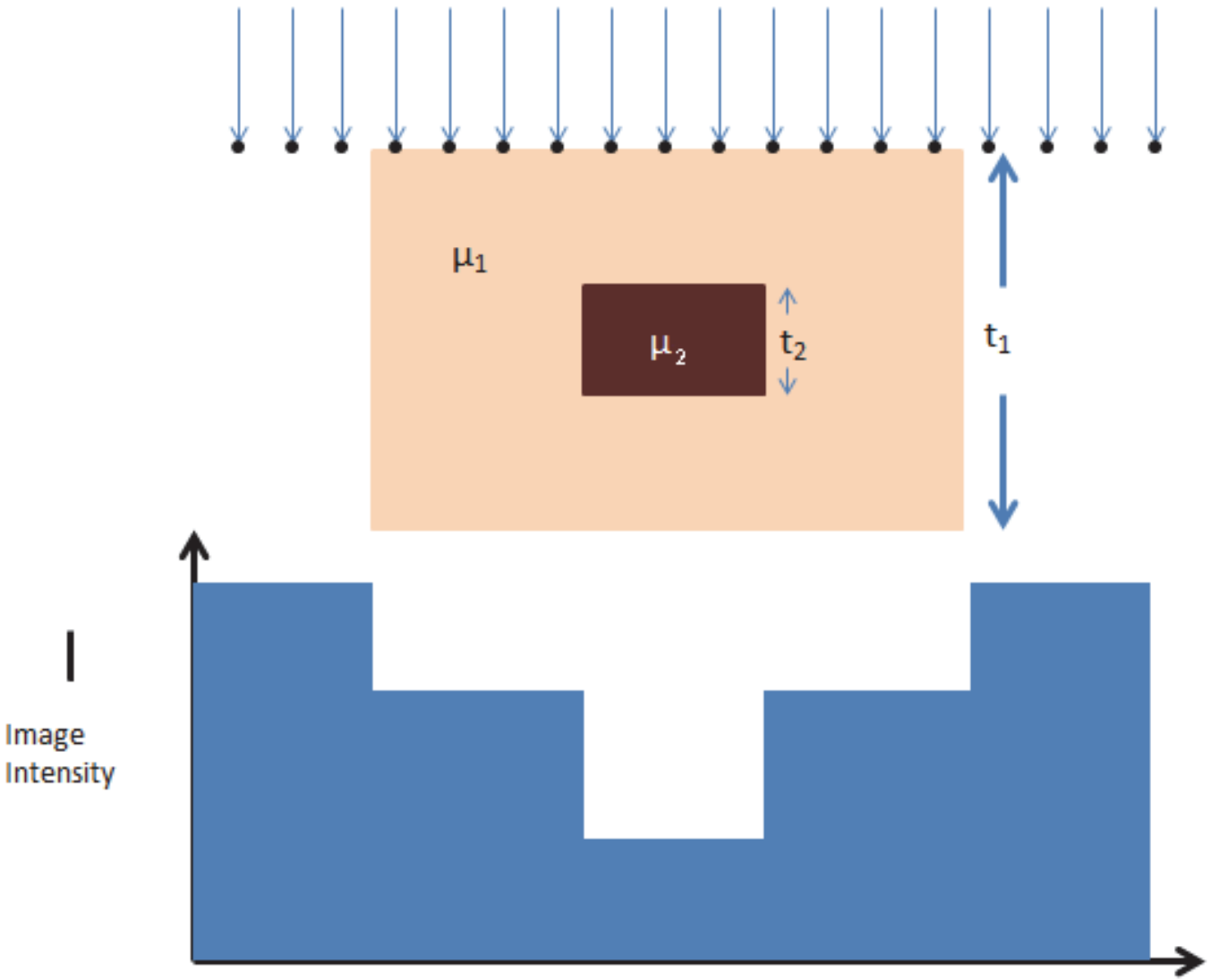

Contrast and SNR

So, when scatter $\uparrow \Rightarrow R \uparrow \Rightarrow C \downarrow$

The change in intensity between two regions is given by $\Delta I = I_1 - I_2 = CI_1$ So, the signal over area $A = \Delta I \cdot A = I_1 \cdot C \cdot A$

$$Signal_{area} = C \cdot A \cdot N \cdot \mathcal{E} \cdot E \cdot e^{\mu_1 t_1}(1 + R) \tag{13}$$

But what is the noise over the adjacent area?

Assume $\mathcal{E}$ is the same for primary and secondary photons and a Poisson process for X-Ray photon arrival at area A.

$$Noise_{area} = E\sqrt{\frac{I_1 A}{E}} = E\sqrt{N\mathcal{E}Ae^{-\mu_1 t_1}(1 + R)} \tag{14}$$

So

$$SNR_{area} = C\sqrt{N\mathcal{E}Ae^{-\mu_1 t_1}(1 + R)} = [1 - e^{-(\mu_2 - \mu_1)t_2}]\sqrt{\frac{N\mathcal{E}Ae^{-\mu_1 t_1}}{1 + R}} \tag{15}$$

THINK BIG WE DO™

Dose

Given the minimal acceptable SNR (typically 5 (units are dB but more on this later)), what is the required dose to see a cube of $t_2 \times t_2 \times t_2$? The required # of incident X-Ray photons is derived from

$$SNR = k = [1 - e^{-(\mu_2 - \mu_1)t_2}]\sqrt{\frac{N\mathcal{E}Ae^{-\mu_1 t_1}}{1+R}} \tag{16}$$

which is approximately equal to

$$SNR = k = [1 - [1 - (\mu_2 - \mu_1)t_2]]\sqrt{\frac{N\mathcal{E}Ae^{-\mu_1 t_1}}{1+R}} \tag{17}$$

Dose

Rearrange terms and clear the radical

$$(1+R)k^2(\mu_2-\mu_1)^{-2} = N\mathcal{E}At_2^2e^{-\mu_1 t_1} \quad (18)$$

$$N = \frac{k^2(1+R)e^{-\mu_1 t_1}}{\mathcal{E}(\mu_2-\mu_1)^2 t_2^4} \quad (19)$$

This is the number of photons per unit area (that's why the A went away). To get surface dose, we have

$$Dose_{surf} = N(\frac{\mu_{EN}}{\rho})E = \frac{\mu_{EN}Ek^2(1+R)e^{\mu_1 t_1}}{\rho\mathcal{E}(\mu_2-\mu_1)^2 t_2^4} \quad (20)$$

Where N is the number of incident photons per unit area, $\frac{\mu_{EN}}{\rho}$ is the mass energy absorption coefficient for tissue, and E is the photon energy.

THINK BIG WE DO™

Quantum Mottle

Exposure (X) due to **scatter** $\propto \sqrt{A\mathcal{E}N}$, but total exposure is $\propto A\mathcal{E}N \Rightarrow \frac{\Delta x}{x} = (A\mathcal{E}N)^{-\frac{1}{2}}$.

Recall, $\Delta D = 0.434\Gamma\frac{\Delta x}{x} \therefore \Delta D_Q = 0.434\Gamma(A\mathcal{E}N)^{-\frac{1}{2}}$, which is the optical density due to quantum mottle (*proportional to film gamma)

Film Granularity

Recall, $\Delta D_G = 0.434\frac{\sqrt{gA}\sigma}{A}$, where σ is the cross-sectional area of a silver speck resulting from a sensitized AgBr grain.

Nutting's Law gives $D = 0.434g\sigma \therefore \Delta D_G = \sqrt{\frac{0.434D\sigma}{A}}$

(*proportional to $\sqrt{D}$)

THINK BIG WE DO™

Film Granularity

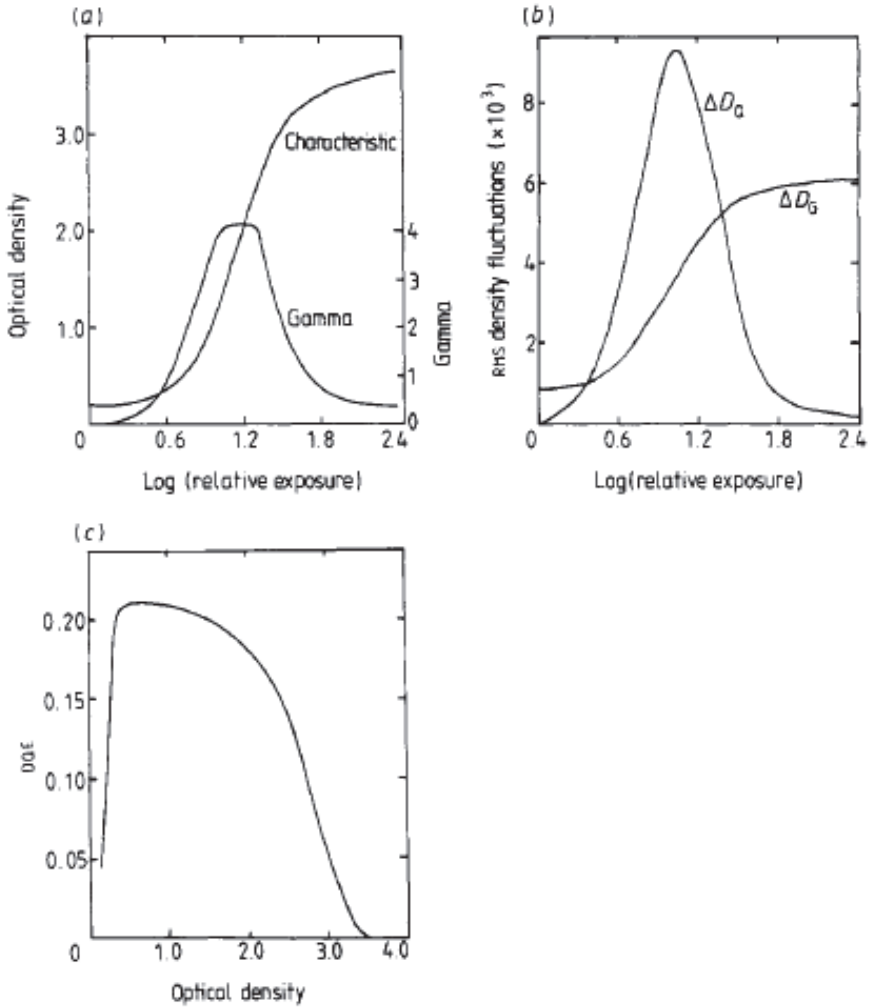

Figure 2.26 Measurements and calculations for the DuPont Cronex HiPlus/Kodak X-Omatic RP screen–film combination. (*a*) Film characteristic and gamma. (*b*) Calculations of the variation of quantum mottle and film granularity with exposure. (*c*) Calculations of the variation of DQE with optical density. Noise estimates are for a circular sampling area of diameter 0.5 mm. (After Barnes (1982).)

THINK BIG WE DO™

Detective Quantum Efficiency

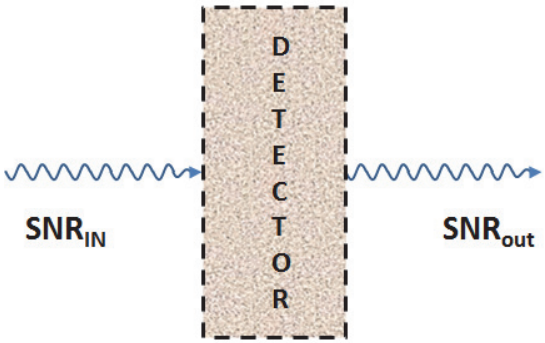

$$DQE = \left(\frac{SNR_{out}}{SNR_{in}}\right)^2$$

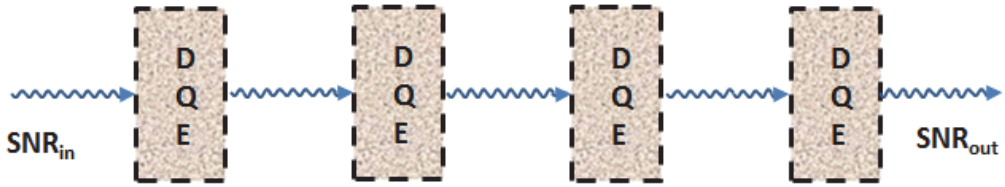

$$DQE_{total} = DQE_1 \cdot DQE_2 \ldots DQE_n$$

In other words, the total DQE is the product of each individual DQE

Geometric Unsharpness

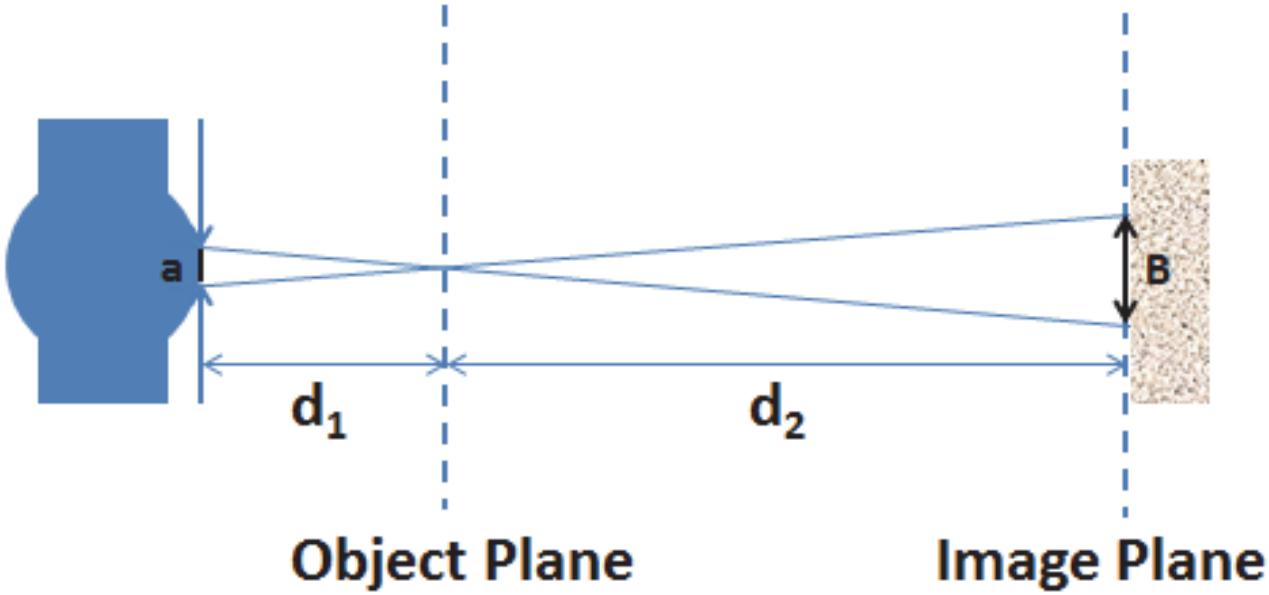

Image blurring $B = \frac{ad_2}{d_1} = a(m-1)$, where m is the image magnification, i.e. $m = \frac{d_1+d_2}{d_1}$ (divide both sides by m)

$$U_g = \frac{B}{m} = a(1 - \frac{1}{m}) \tag{21}$$

Directly proportional to focal spot size, a, i.e. $m \uparrow \Rightarrow U_g \uparrow$.

Receptor Unsharpness

Caused by lateral spread of photons. Let F be the intrinsic receptor unsharpness, i.e. the thickness of the image of an object which has NO thickness. Imagine a photograph. The reason you can hold it is because the paper and the ink have thickness - the image has zero thickness. The receptor has thickness, but the image does not.

$$U_r = \frac{F}{m} \tag{22}$$

Inversely proportional to magnification, m, i.e. $m \uparrow \Rightarrow U_r \downarrow$.

Total Unsharpness

Ignore motion unsharpness (patient movement), making total unsharpness the geometric mean of U_g and U_r

$$U = \sqrt{U_g^2 + U_r^2} \tag{23}$$

General Radiography

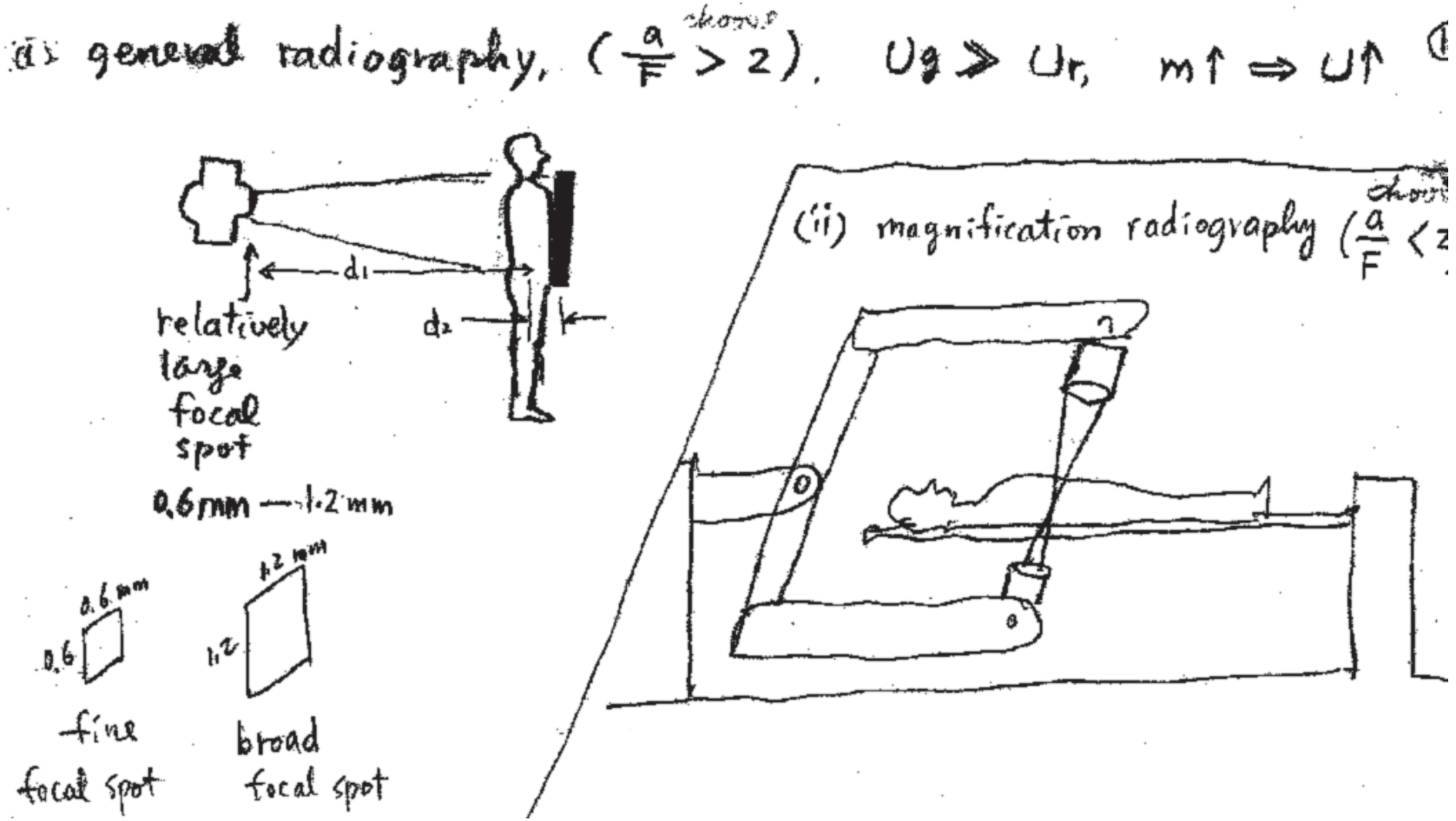

THINK BIG WE DO™

Xeroradiogram

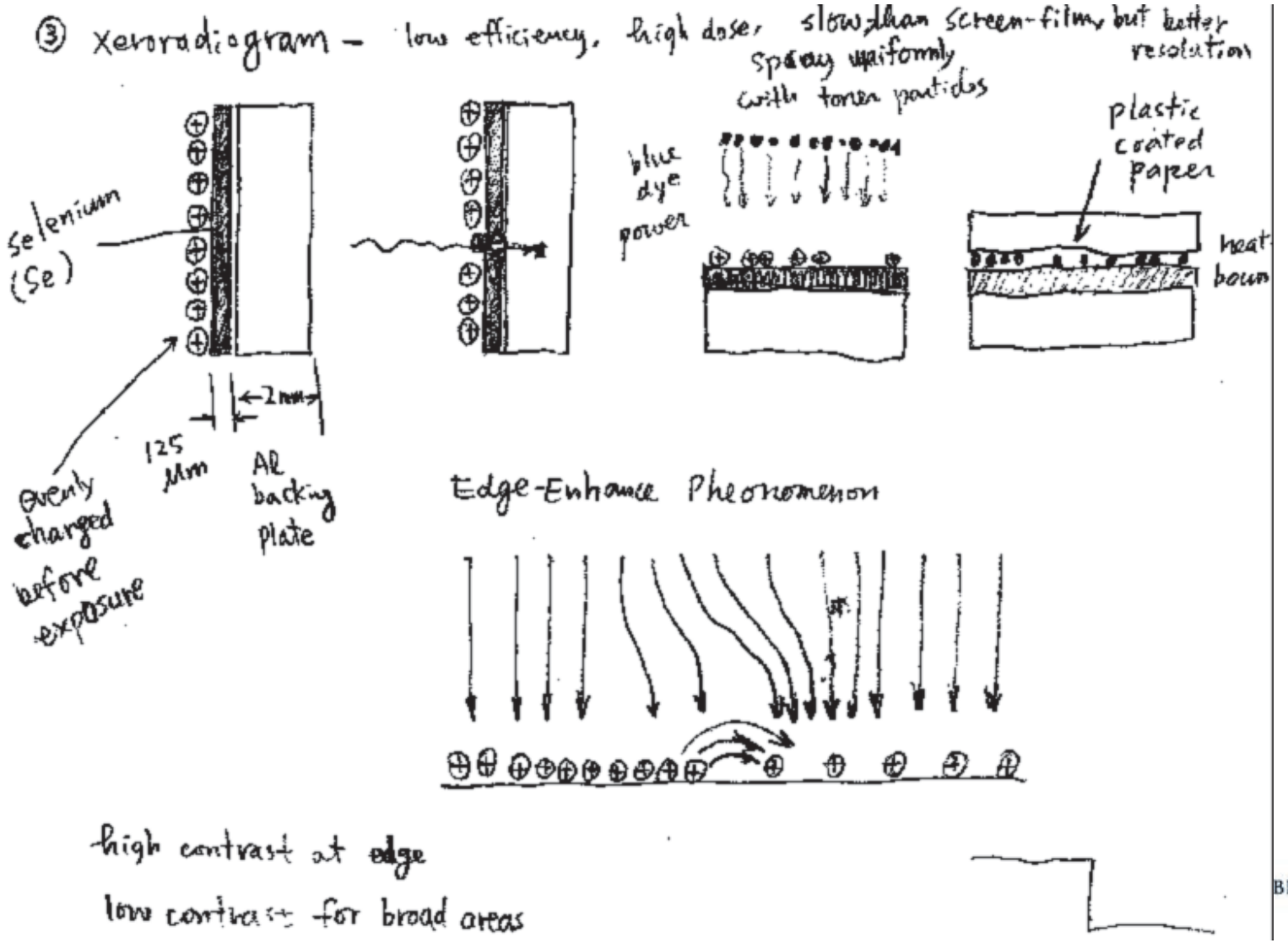

Image Intensifier

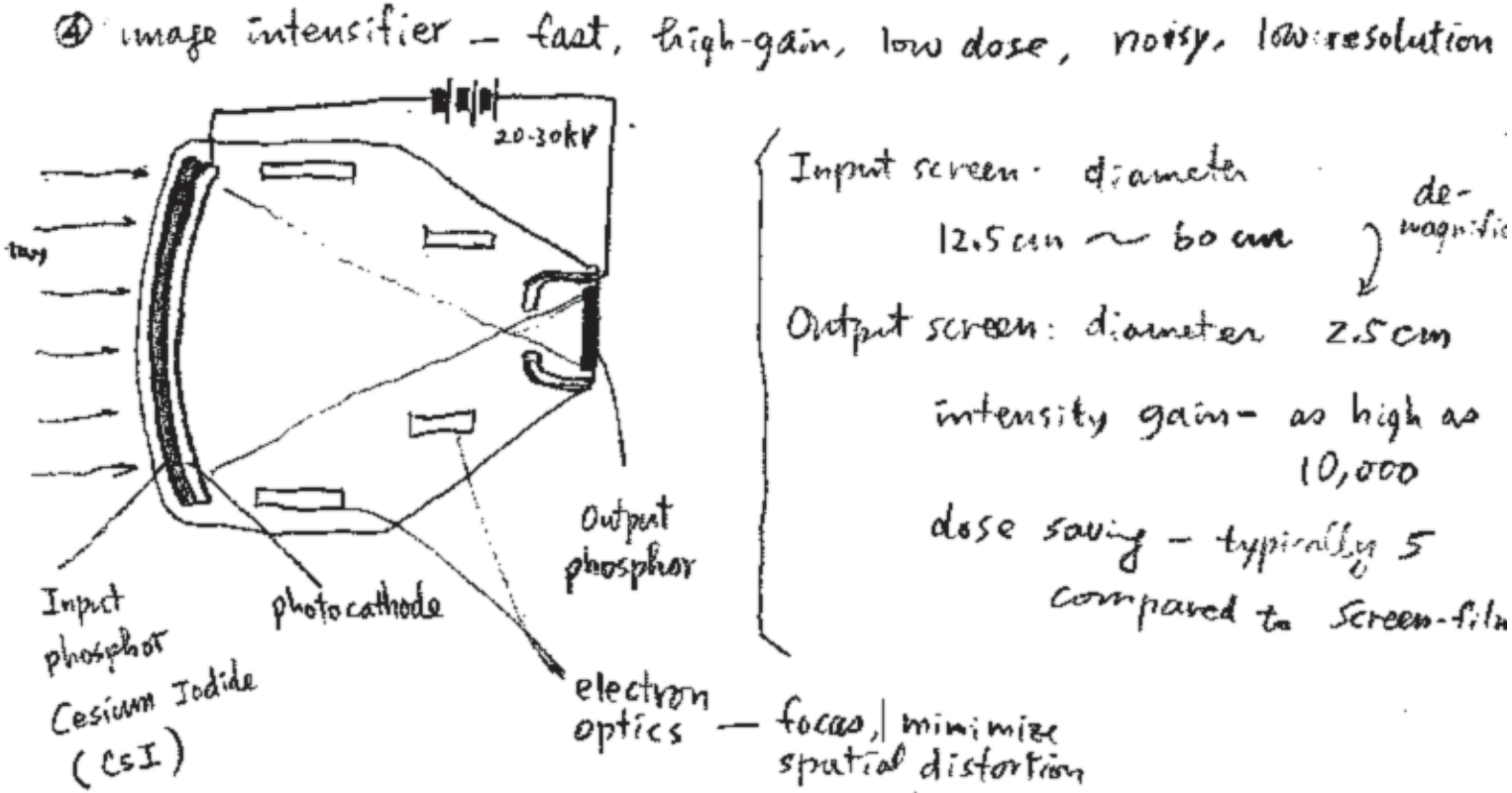

THINK BIG WE DO™

Photo Multiplier Tube

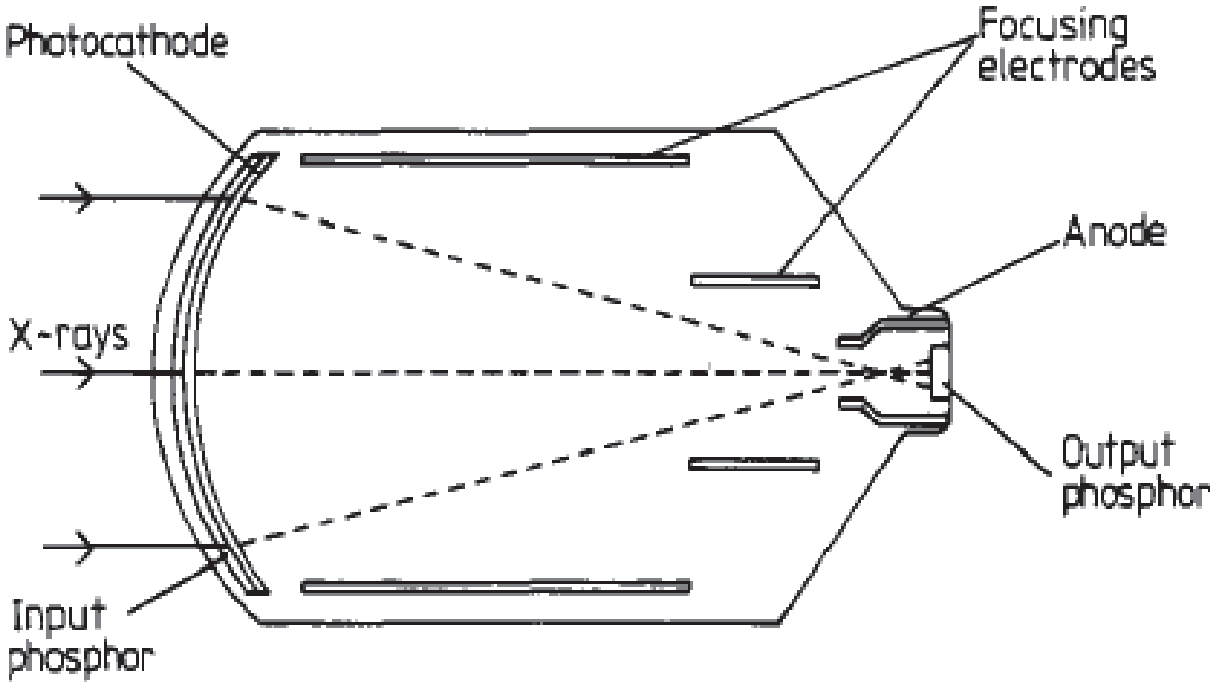

Figure 2.27 Construction of the image intensifier.

Digital Angiography

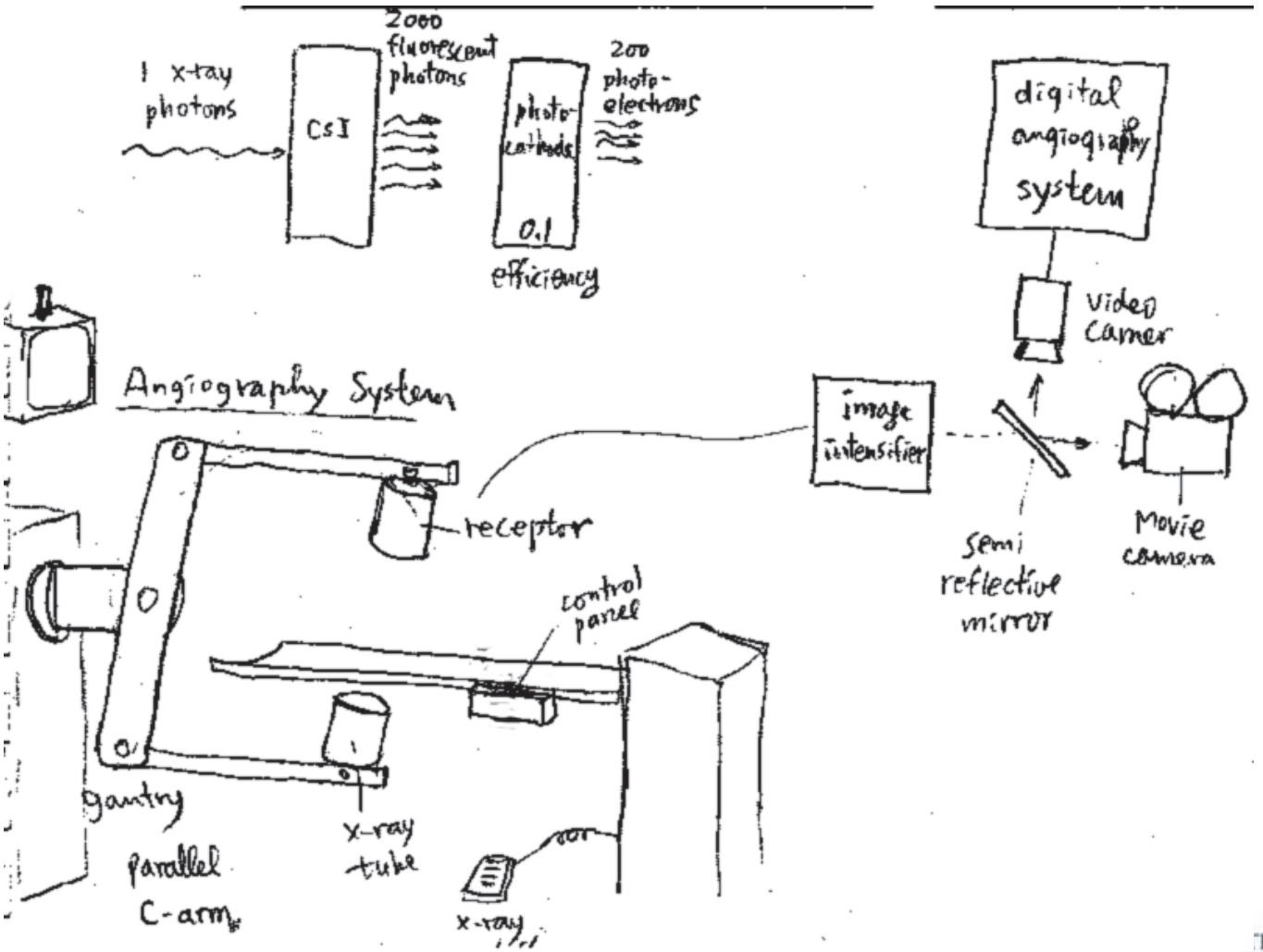

THINK BIG WE DO™

Digital Angiography

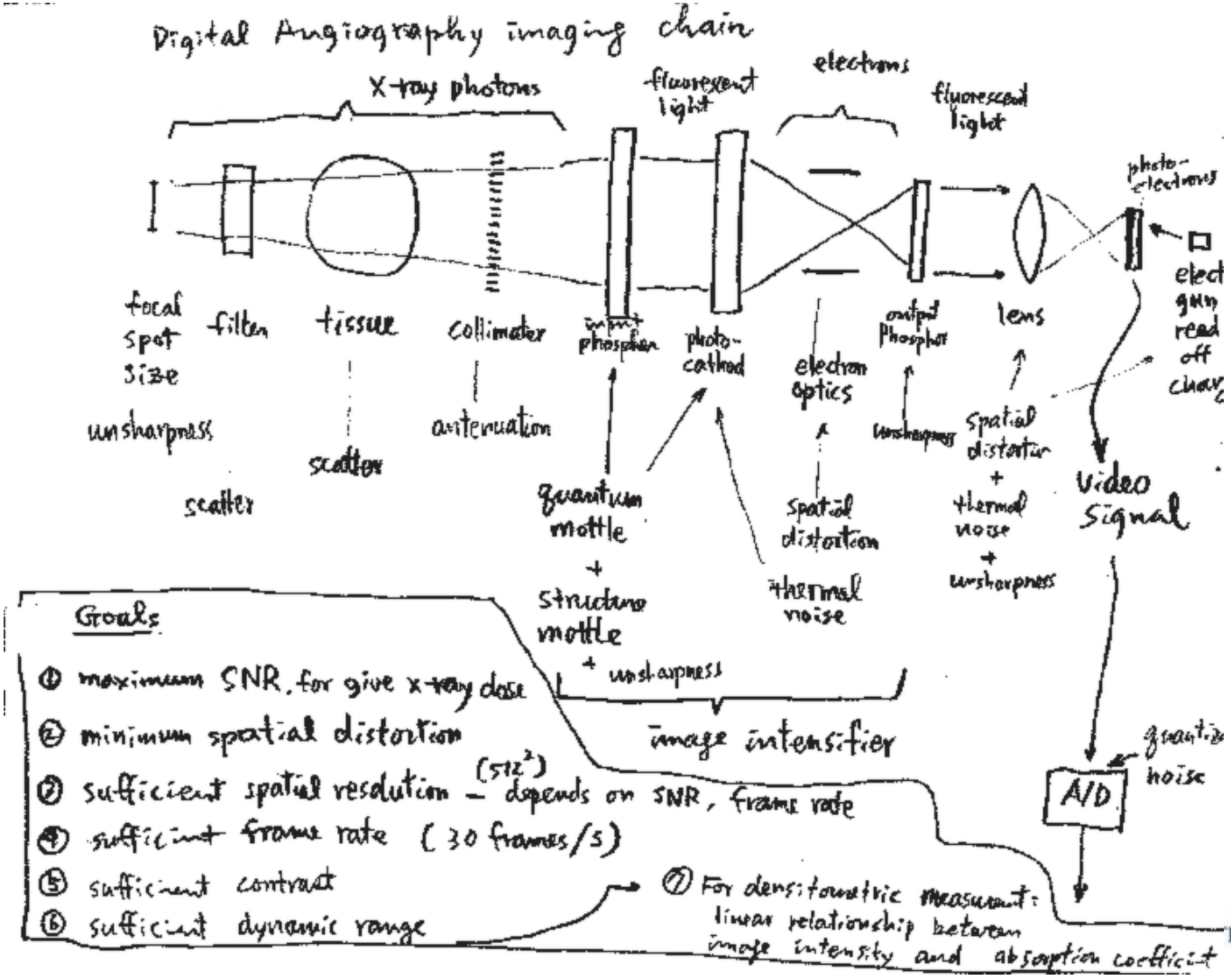

THINK BIG WE DO™

Four Generations of CT

- Actually 5, though the fifth is just a derivative of the fourth
- All modern CT scans can be traced to the first 1973 model

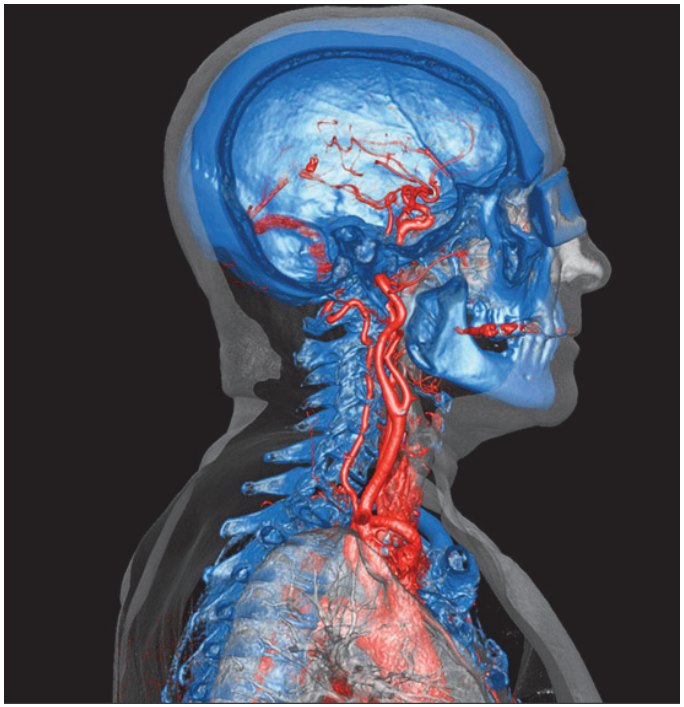

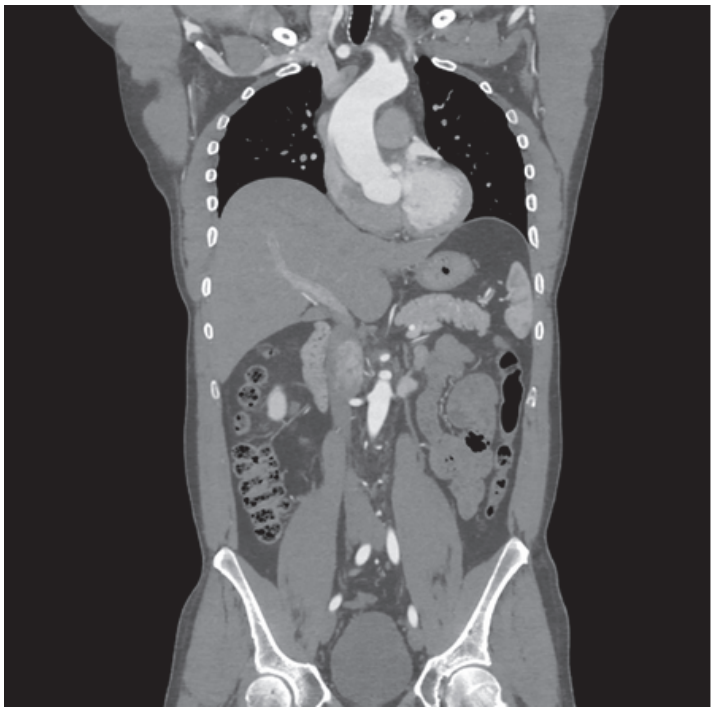

THINK BIG WE DO™

First Generation CT

- Single X-Ray source, single detector (180° rotate and shift)
- Parallel beam
- 4 minutes per slice

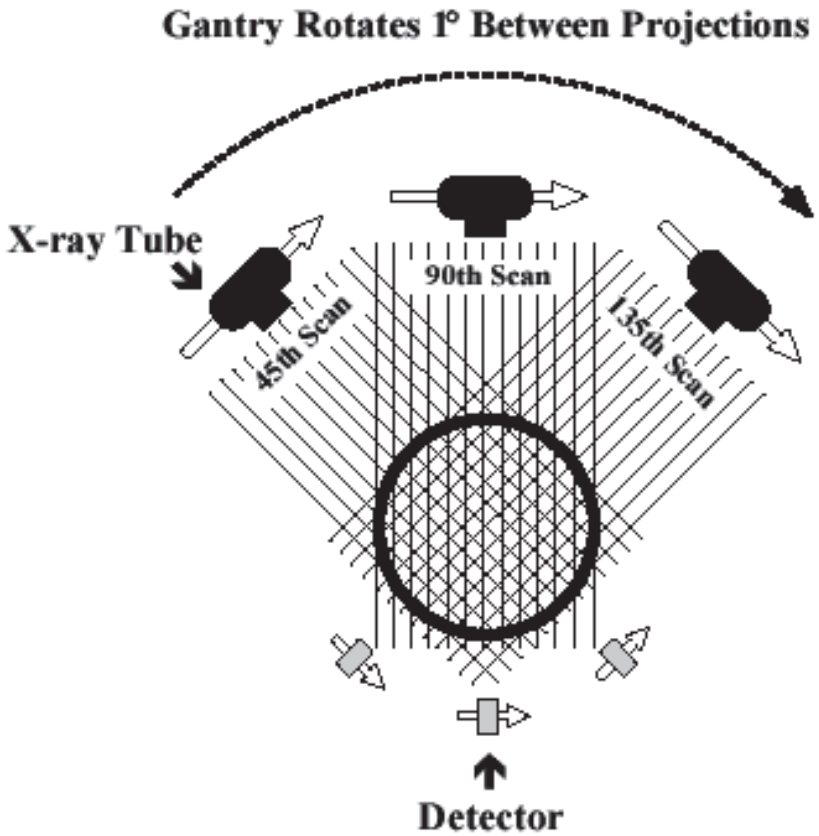

Second Generation CT

- Single X-Ray source, multiple (3-60) detectors (180° rotate and shift)
- Small angle fan beam (10°)
- 20 seconds per slice (240 seconds per slice/average 12 detectors)
- Wedge size determines the efficiency of the slice

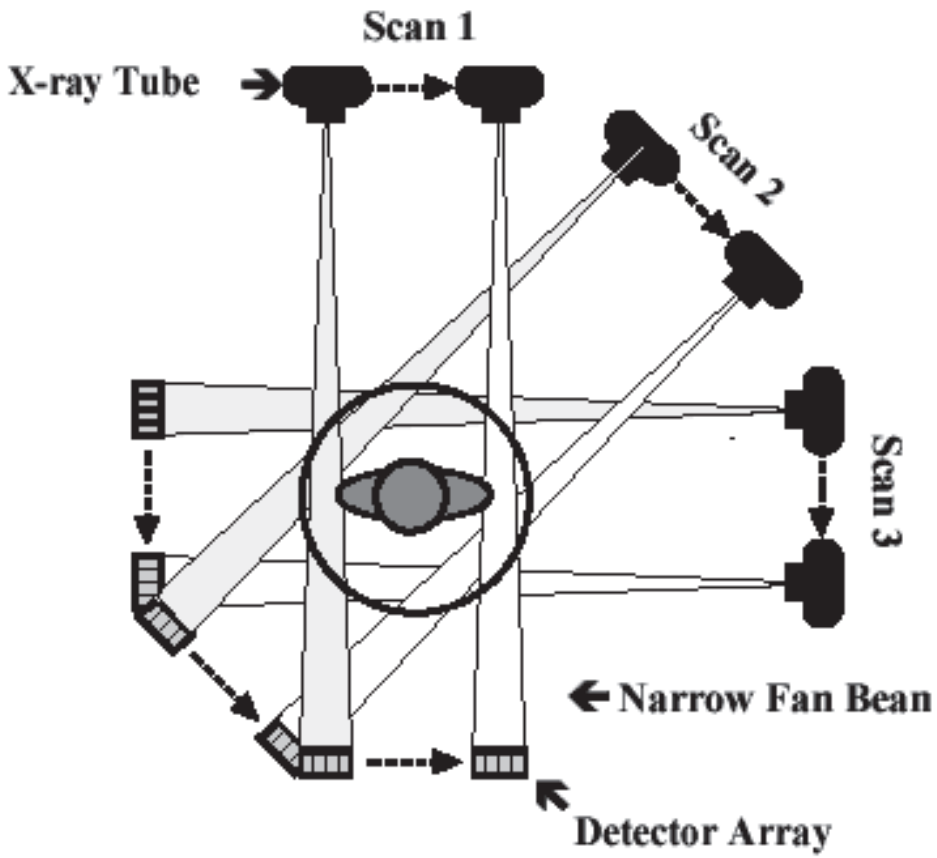

Third Generation CT (Fan beam reconstruction)

- Single X-Ray source, multiple (128-600) detectors (360° rotation only)
- Wide angle fan beam (pulsed)
- 5 seconds per slice (240 seconds per slice/average 48 detectors)
- Zenon gas detector

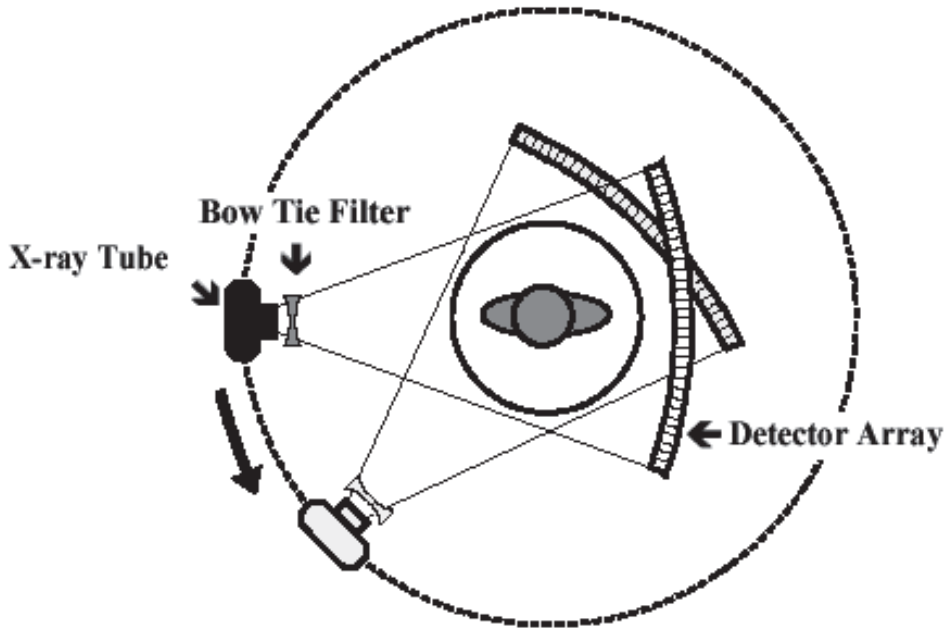

Fourth Generation CT

- Single X-Ray source, multiple ($\sim$ 1000) detectors (360° rotation only)
- Wide angle fan beam (continuous)
- 2 seconds per slice (240 seconds per slice/average 120 detectors)
- Zenon gas detector

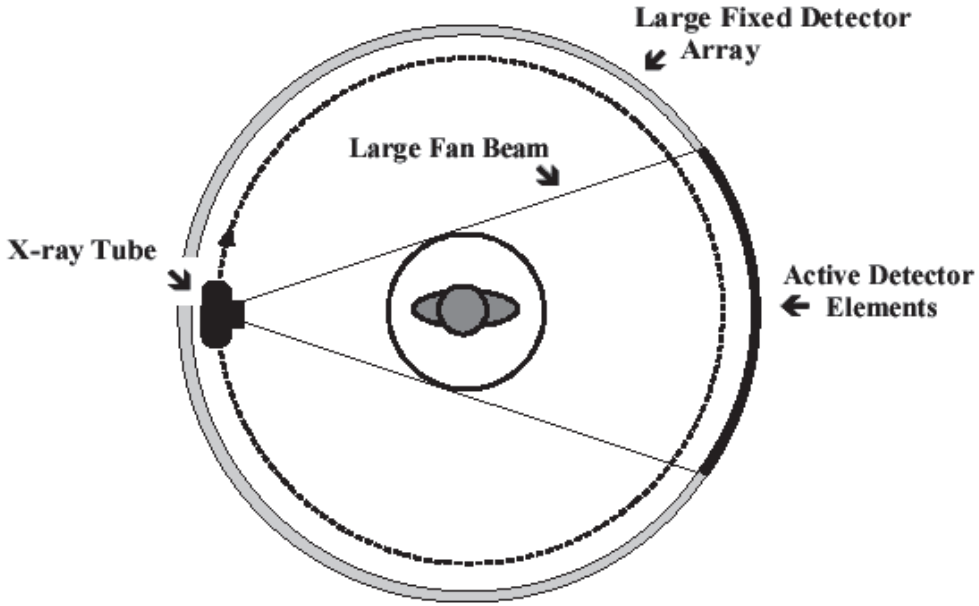

THINK BIG WE DO™

Fifth Generation

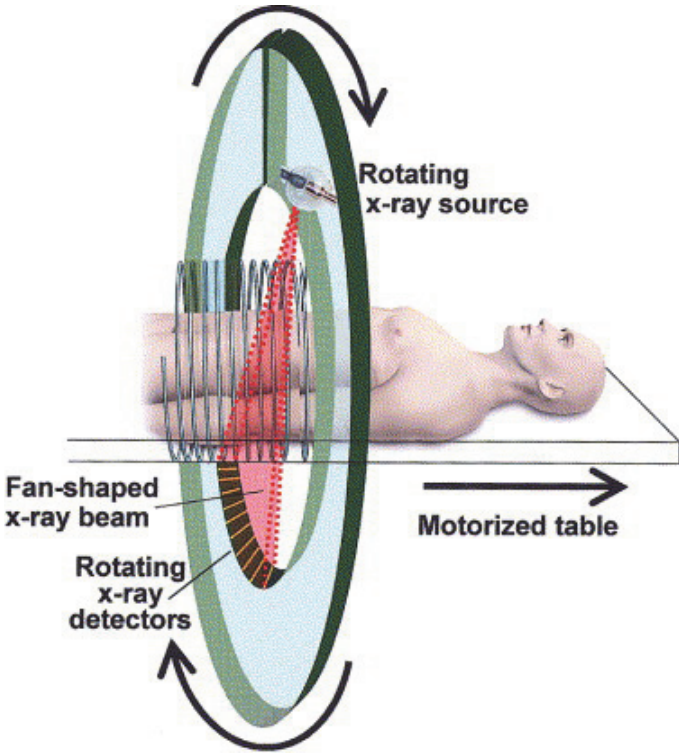

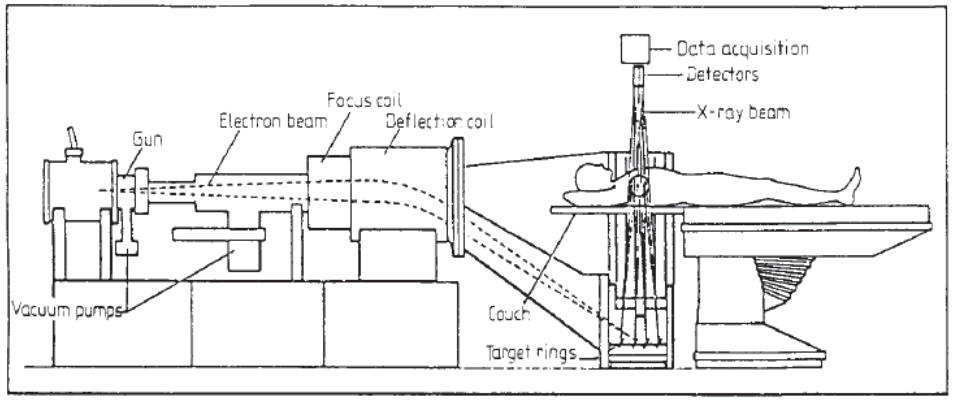

Figure 4.9 Imatron CT-100 ciné CT scanner; longitudinal view. Note the use of four target rings for multislice examination. (Courtesy of Imatron.)

Classical Tomography

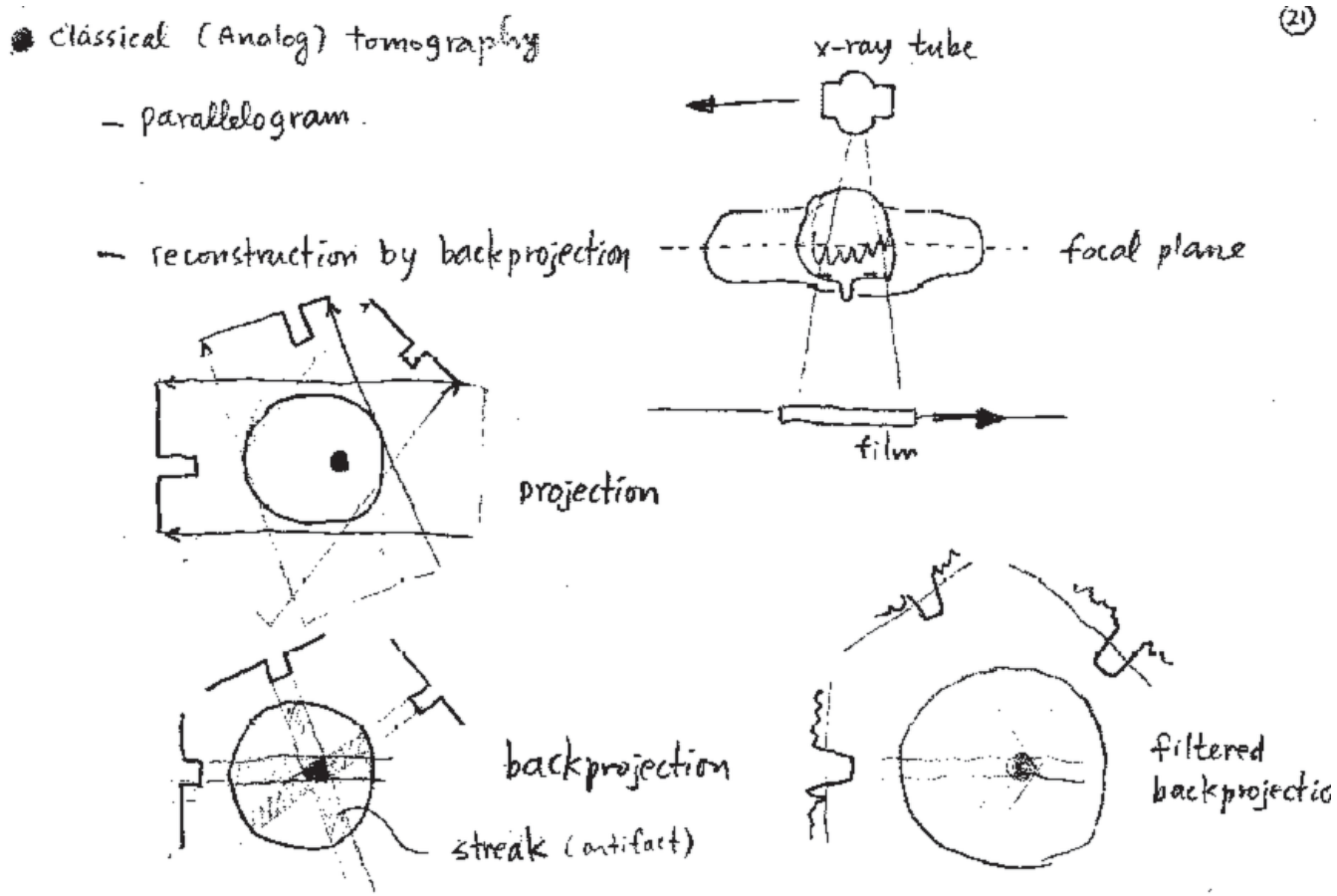

Computed Tomography

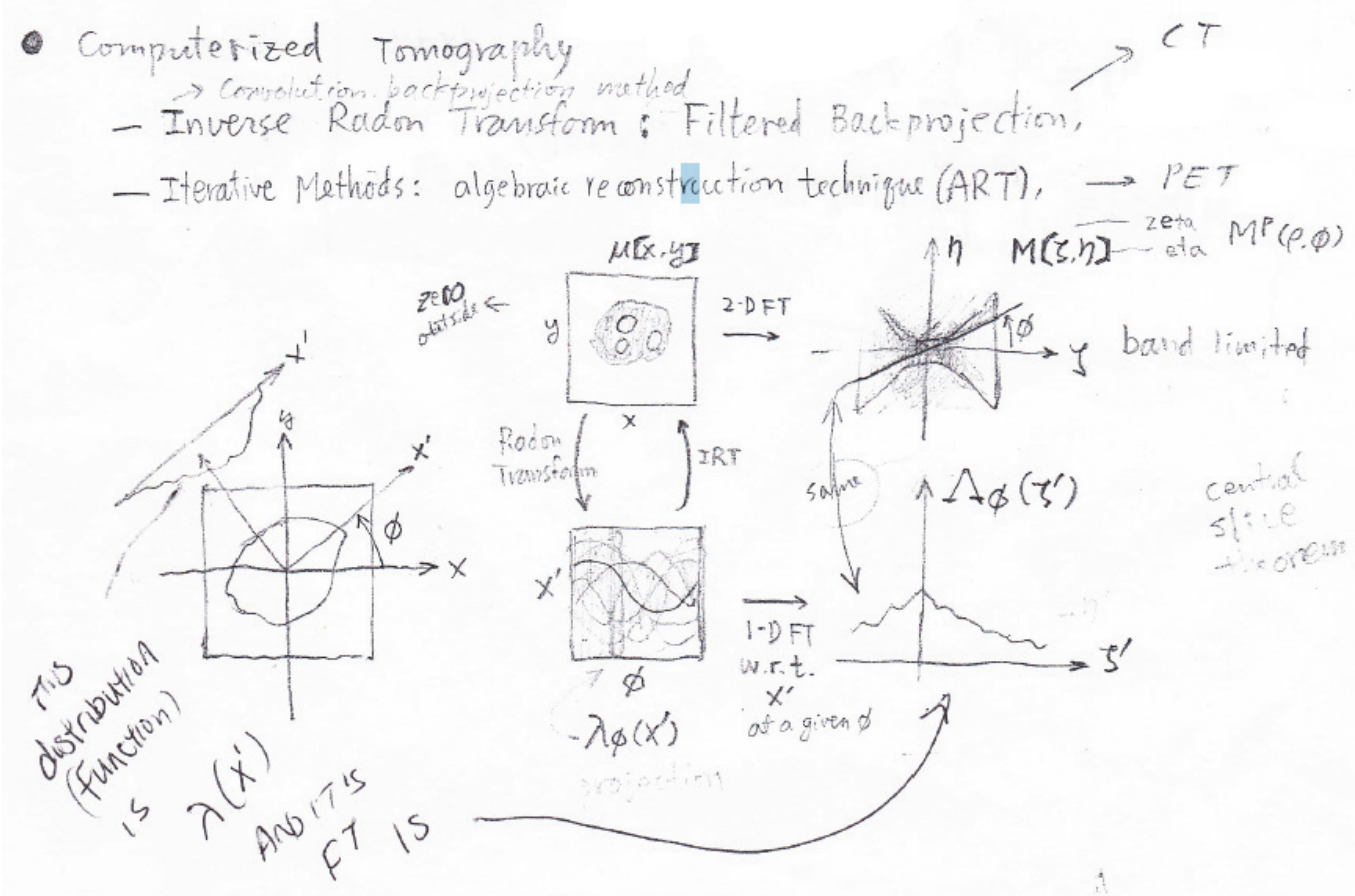

Computed Tomography

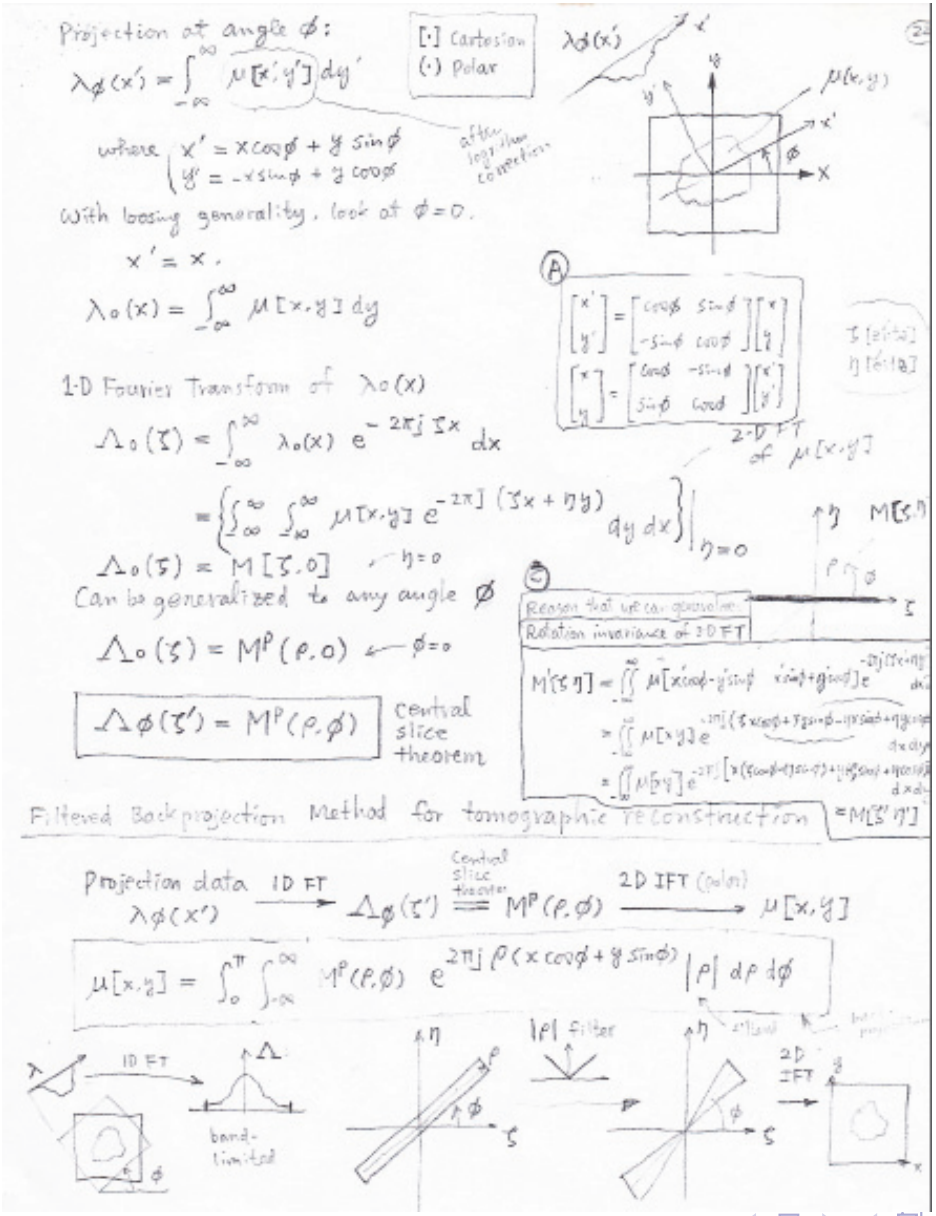

THINK BIG WE DO™

Projection

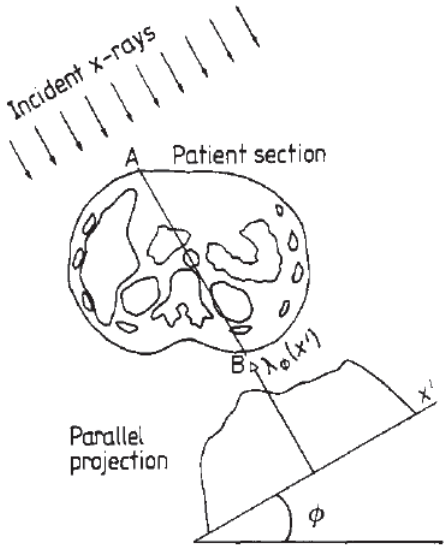

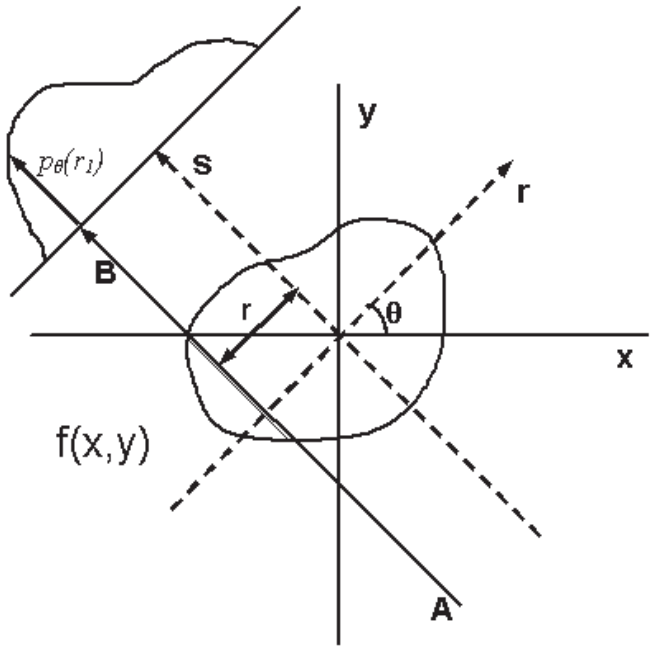

Figure 4.10 Projections are defined as the negative logarithm of the fractional x-ray transmittance of the object, $\lambda_\phi(x') = -\ln[I_\phi(x')/I_\phi^0(x')]$. ϕ is the angle at which the projection data are recorded.

THINK BIG WE DO™

Back Projection

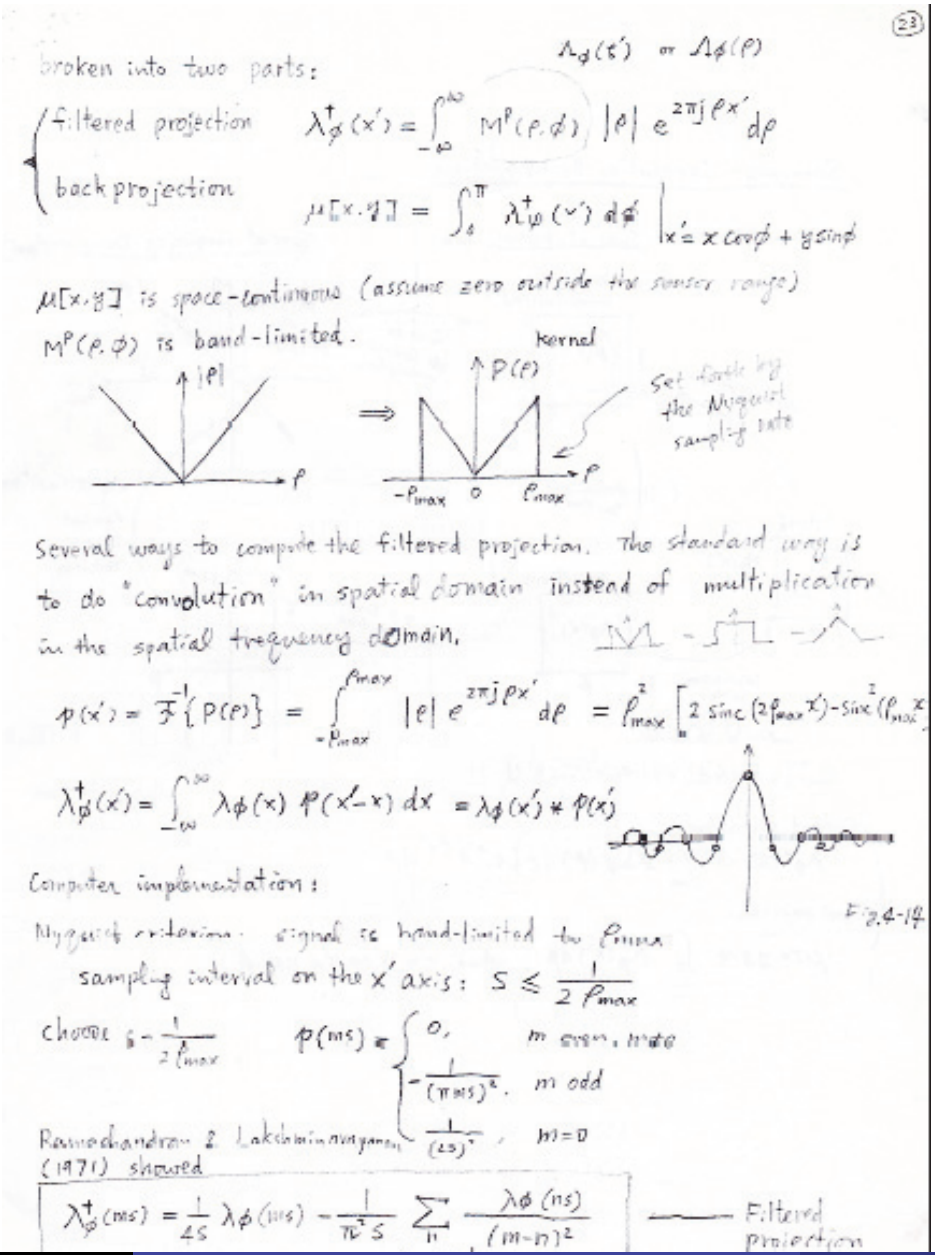

Back Projection

$$\mu_i = \sum_{n=1}^{N} \lambda^{\dagger}_{\phi_n}(m^* s)$$

backprojection for the ith pixel in the image

n : nth projection along angle ϕ_n

m^* : interpolated point within m

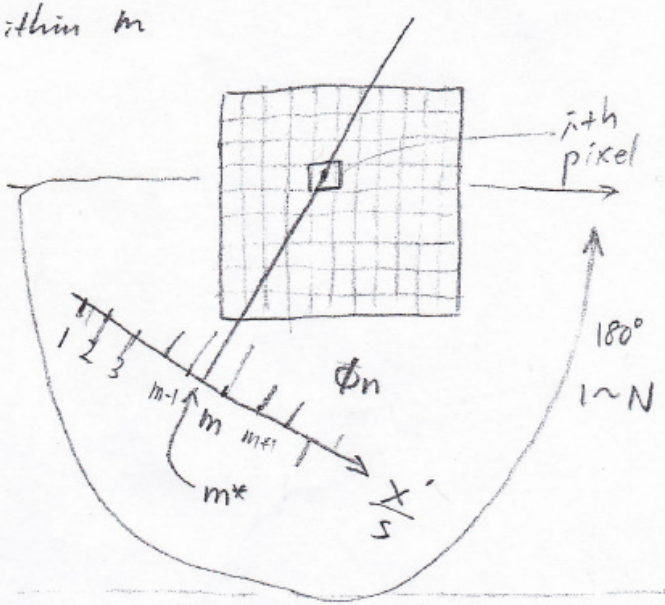

Fig 4.16

25 lines Fortran program to perform filtered backprojection

Algebraic Reconstruction Technique

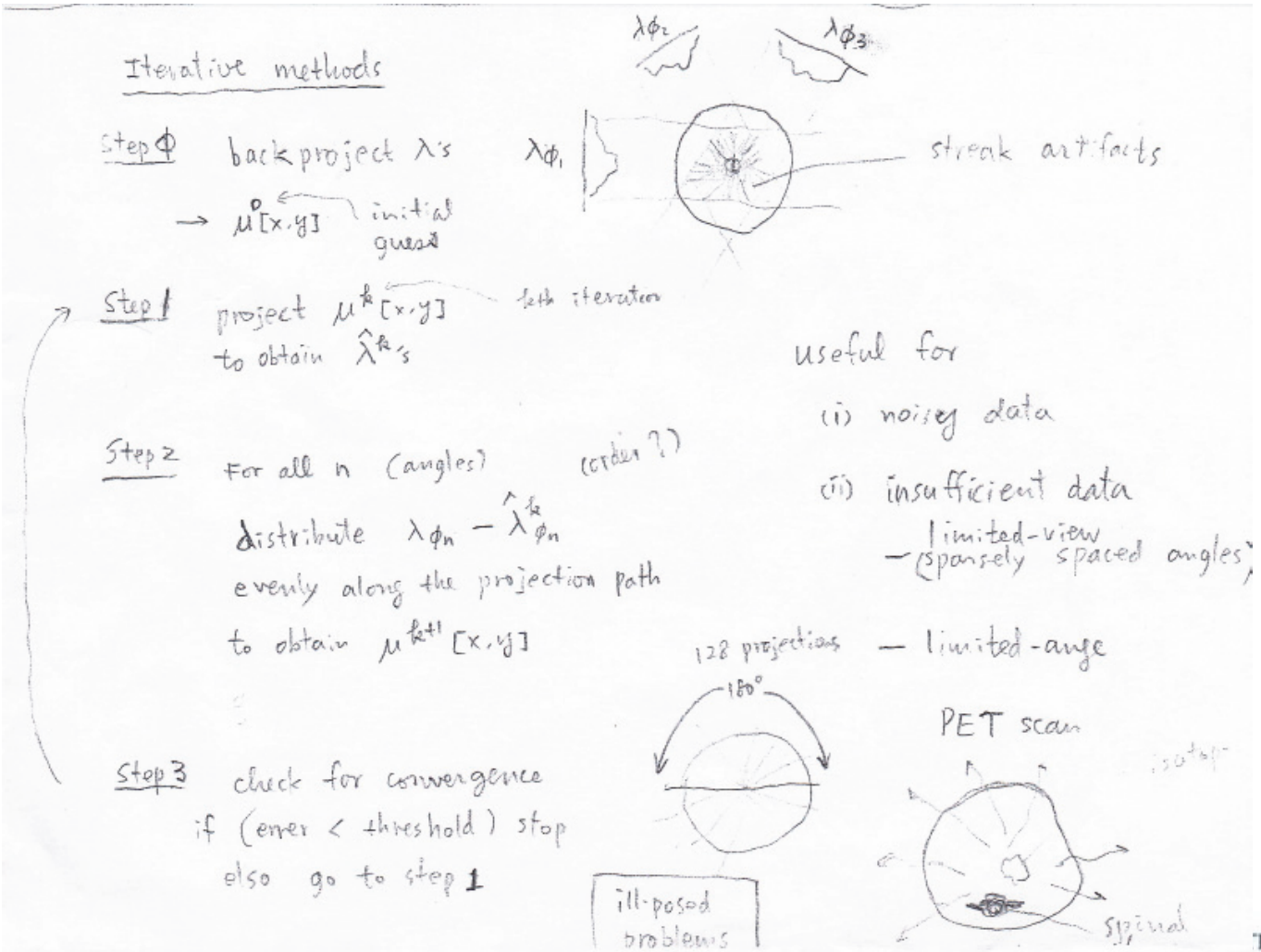

THINK BIG WE DO™

Convolution, Backprojection, and Radon Transform

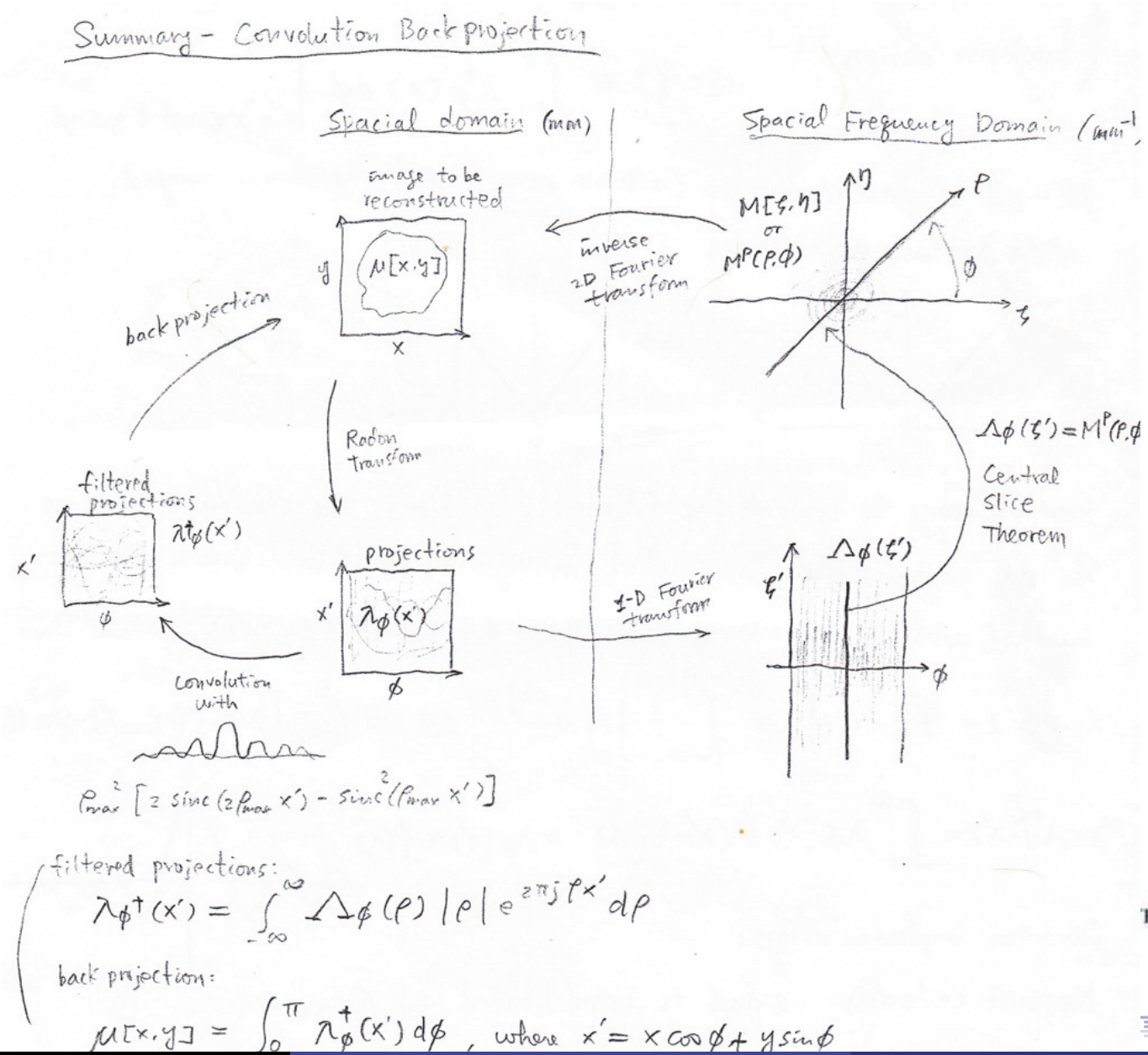

Dose vs. Resolution

Recall $N = \frac{SNR^2(1+R)e^{\mu_1 t}}{\epsilon(\mu_2-\mu_1)t_2^4}$ Now $\eta\upsilon = \frac{k_1(SNR)^2}{t^3(k_2 t)}$, where

- η: DQE
- υ: x-ray dose (related to N)
- k_1: constant related to E
- t: dimension of the smallest object visible
- $k_2 t$: thickness of the slice ($k_2 = 2 \sim 5 \times t$)

$$\text{dose} \propto \frac{1}{(spatial\ \ resolution)^4}$$

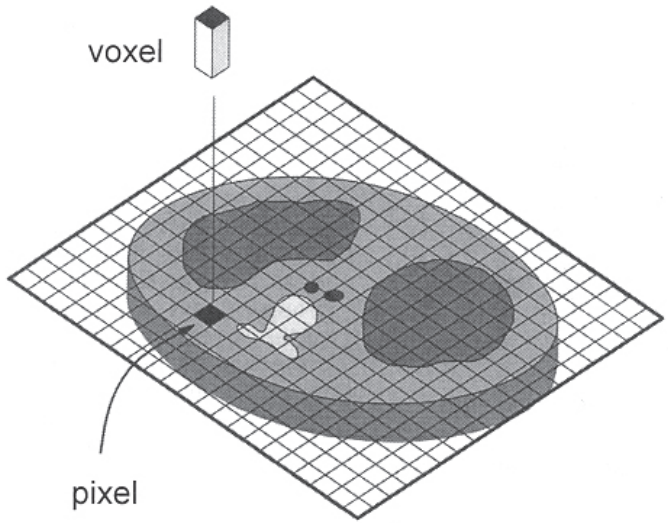

Values for diagnostic CT

- resolution: less than 1 mm
- discrimination: 1% in image density (related to SNR)
- dose: $10 \sim 100 mGy$ (compare to 1 mGy for mammogram)

Beam Hardening

Low energy x-rays are attenuated first

Diagnostic radiology with x-rays

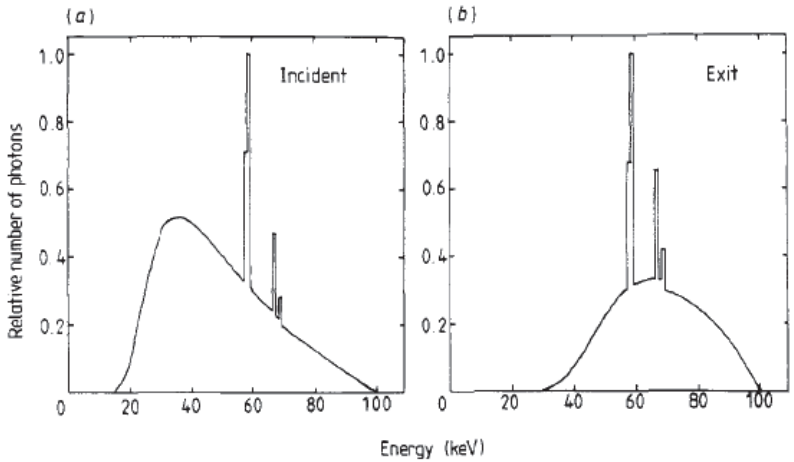

Figure 2.11 X-ray spectra for an x-ray tube with a tungsten target; 100 kV constant potential with 2.5 mm aluminium added. The spectra are shown both before and after attenuation by 18.5 cm soft tissue plus 1.5 cm bone. (The spectra are based on the work of Birch *et al* (1979).)

4.5.4 Beam-hardening artefacts

As the x-ray beam passes through tissue, the lower-energy components are attenuated more rapidly than the higher-energy components. The average photon energy increases; the beam becomes *harder*. As a result, the exponential law of attenuation no longer holds.

With no absorber in the beam, the detector output is

$$I_0 = k_3 \int_0^{E_{max}} S(E)\, dE \tag{4.31}$$

where the source spectrum $S(E)$ is defined such that $S(E)\,dE$ is the energy fluence in the energy range E to $E + dE$.

With an object in the beam, Beer's law must be weighted by the energy spectrum and integrated, to give

$$I = k_3 \int_0^{E_{max}} S(E) \exp\left(-\int_{AB} \mu_E[x, y]\, dy'\right) dE \tag{4.32}$$

and the projection λ is thus

$$\lambda = -\ln\left(\frac{\int_0^{E_{max}} S(E) \exp(-\int_{AB} \mu_E[x, y]\, dy')\, dE}{\int_0^{E_{max}} S(E)\, dE}\right). \tag{4.33}$$

THINK BIG WE DO™

Radioisotope Imaging

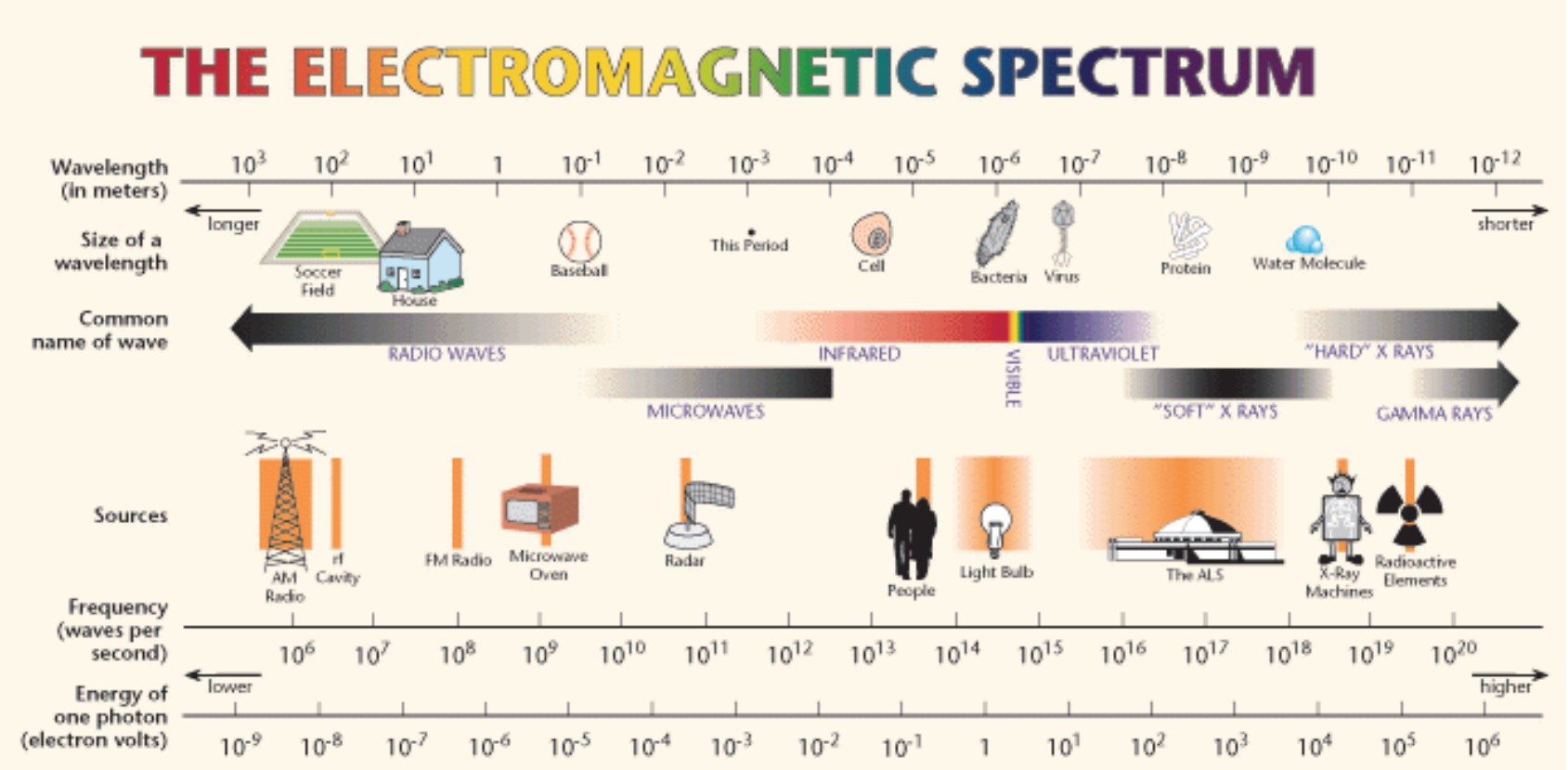

THINK BIG WE DO™

Ways to Detect γ-rays

- Scintillation Crystal
  - NaI (Tl doping)
  - γ-ray$\rightarrow$ visible light$\rightarrow$ voltage (NaI PMT)
- Gas-filled, multi-wire chamber
  - Xe
  - γ-ray$\rightarrow$ charge$\rightarrow$ voltage (wires)
- Semiconductor
  - Si, Ge with doping (HPGe, CdTe, HgI_2
  - γ-ray$\rightarrow$ charge$\rightarrow$ voltage

THINK BIG WE DO™

Radioisotope Imaging

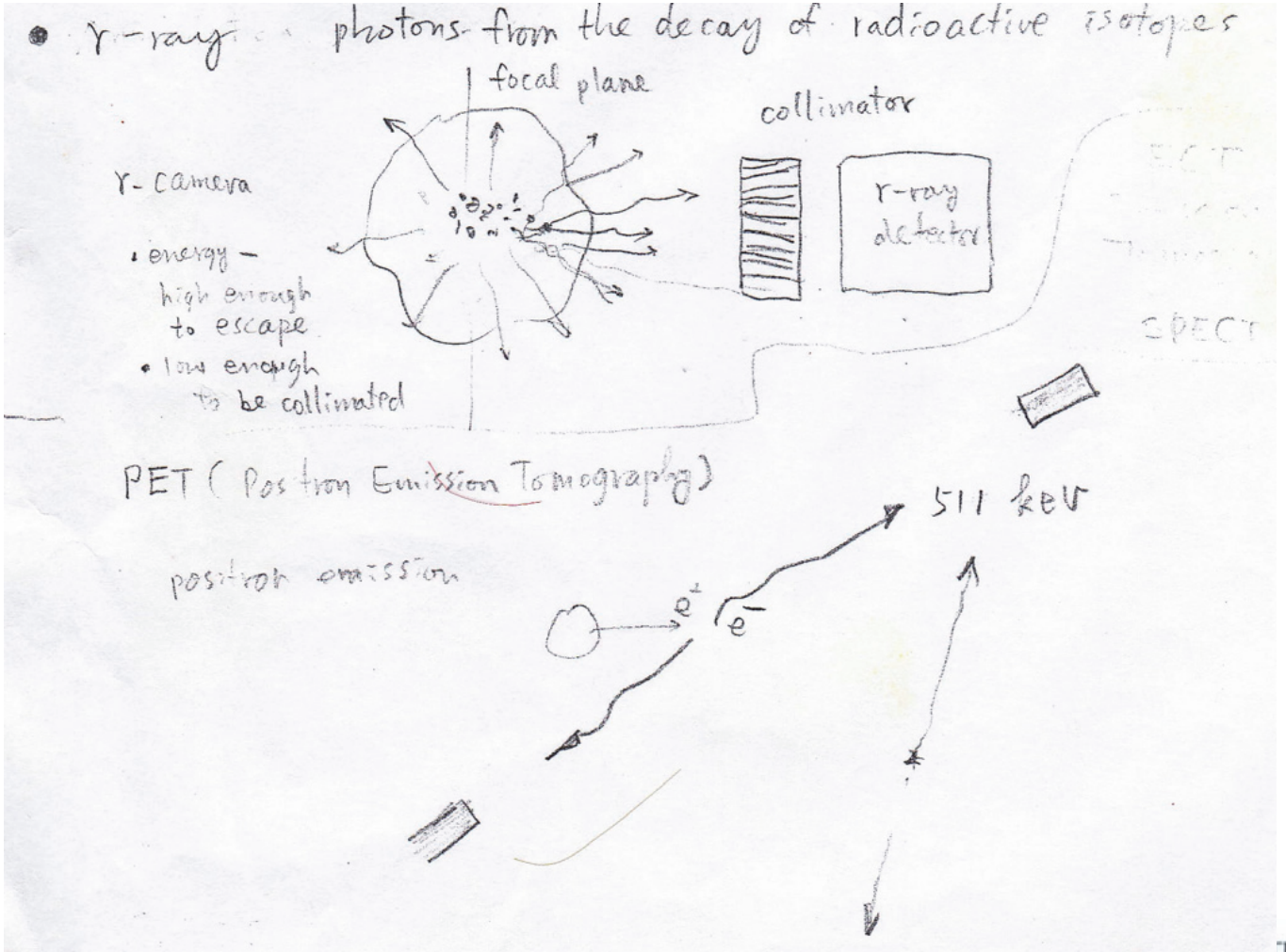

Gamma Camera

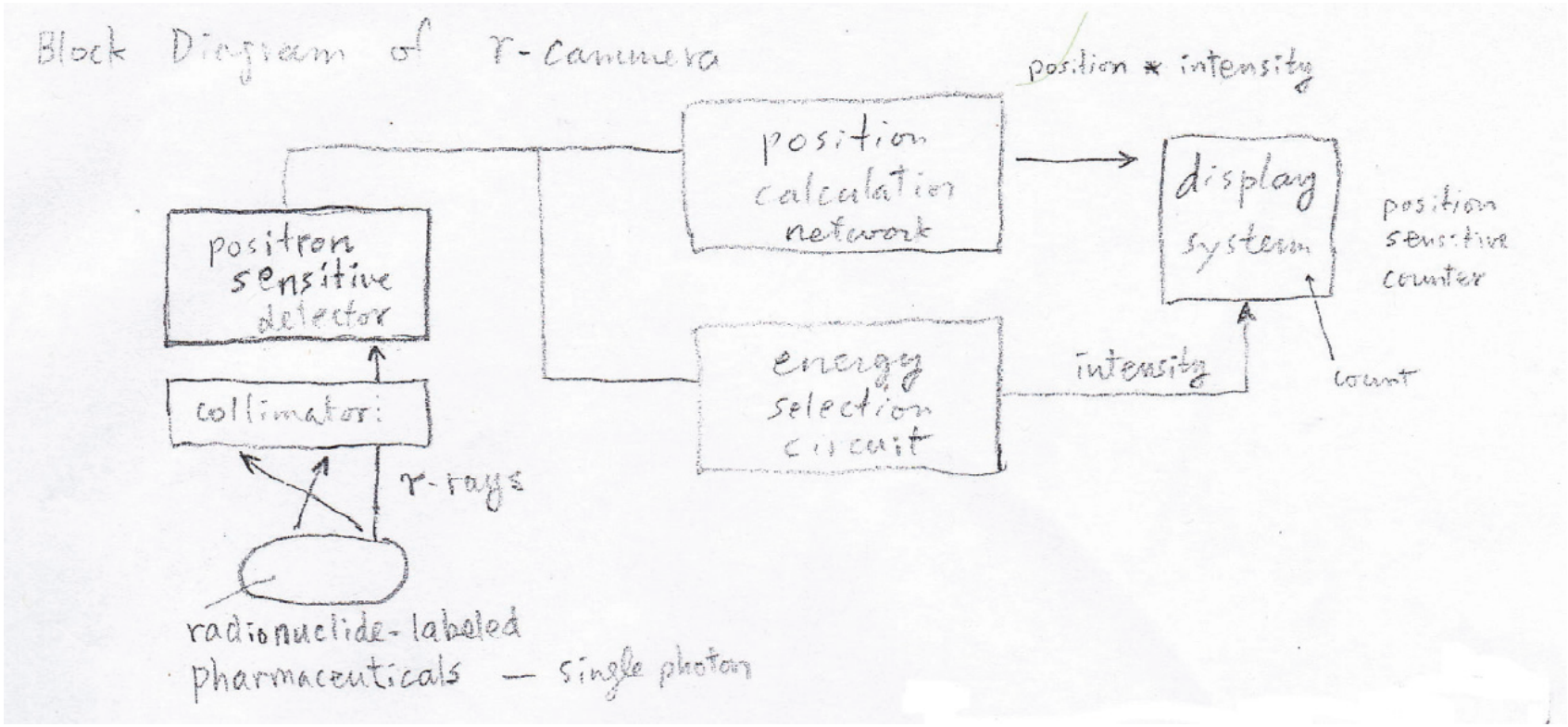

Gamma Camera

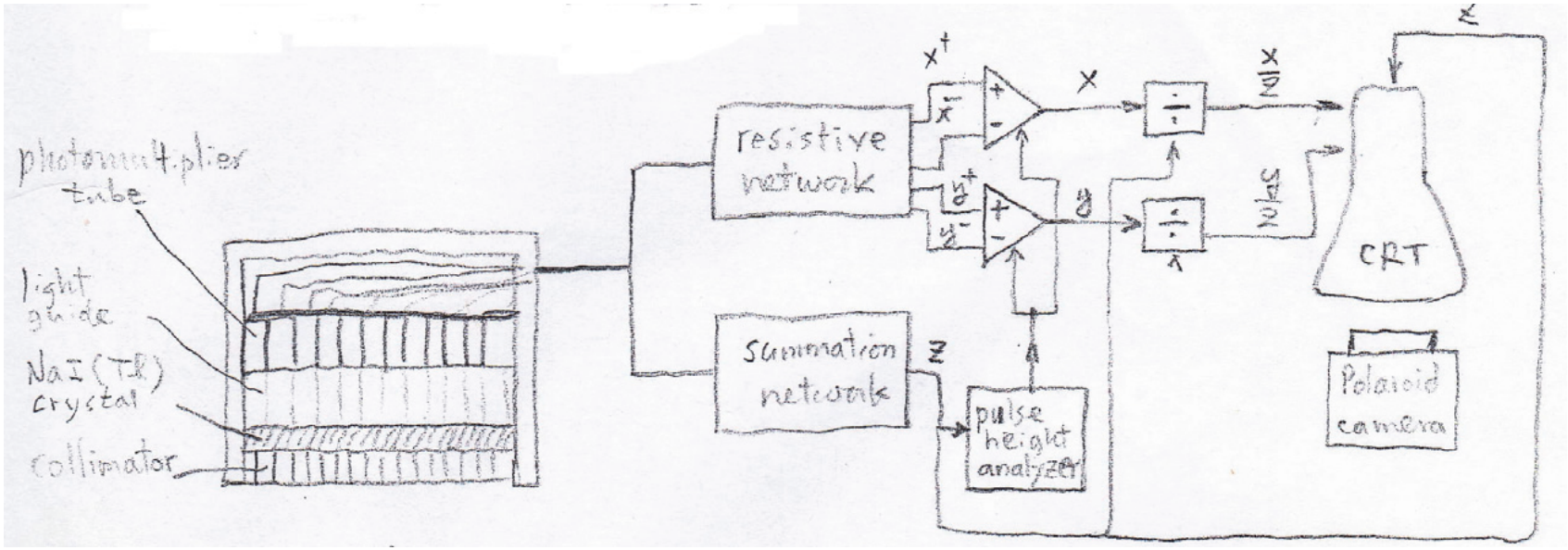

THINK BIG WE DO™

Position Determination

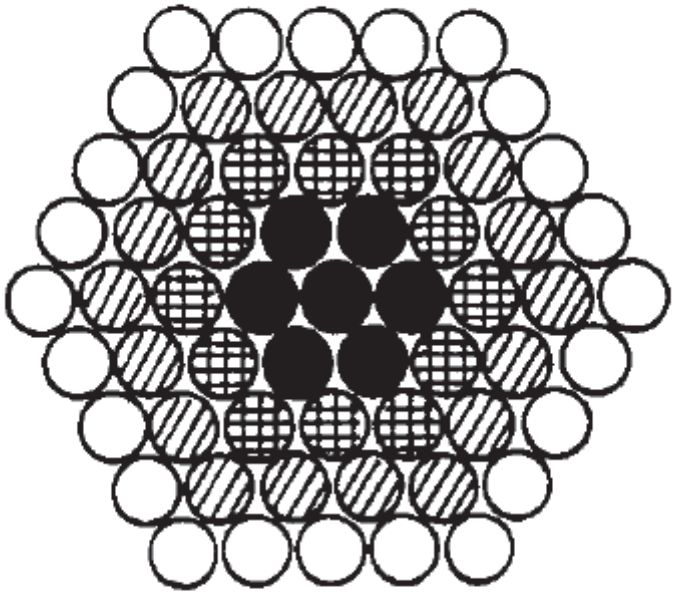

Figure 6.31 The arrangement of photomultiplier tube arrays on the crystal of a gamma camera containing 7, 19, 37 and 61 photomultiplier tubes.

THINK BIG WE DO™

Spatial Resolution

- Geometric Unsharpness: determined by the γ-ray energy and the collimator design ($R_c < 10$mm)
- Intrinsic Unsharpness: determined by the thickness of the NaI crystal, the number of PMTs and the position calculation network ($R_i < 4$mm)
- Total Unsharpness (Spatial Resolution): $R = \sqrt{R_c^2 + R_i^2}$ ($R < 10$mm)

At least an order of magnitude LESS than other modalities (CT, MRI) Advantage of radioactive isotopes

- Functional Imaging: Not just anatomical but physiological information (metabolism)
- Strong signal from small amount of tracer (nanograms)

Production of Radionuclides

- Neutron Capture: Place target in a field of thermal neutrons (nuclear reactor)
  - $^{98}_{42}\text{Mo} + \text{n} \rightarrow {}^{99}_{42}\text{Mo} + \gamma$
- Nuclear Fission (nuclear reactor)
  - $^{235}_{92}\text{U} + \text{n} \rightarrow {}^{236}_{92}\text{U} \rightarrow {}^{99}_{42}\text{Mo} + {}^{133}_{50}\text{Sn} + \gamma$
- Charged Particle Bombardment: H^+ (p), H^-, D^+, He^+, $^3\text{He}^{++}$, $^4\text{He}^{++}$ (α) (Cyclotron)
  - $^{68}_{30}\text{Zn} + \text{p} \rightarrow {}^{67}_{31}\text{Ga} + \text{n}$
- Radioactive Decay: Metastable
  - $^{99}_{42}\text{Mo} \underset{\beta^-}{\rightarrow} {}^{99}_{43}\text{Tc} \underset{\textit{Isomeric Trans}}{\rightarrow} {}^{99}_{43}\text{Tc} + \gamma$ (140 keV)

THINK BIG WE DO™

Decay of Radionuclides

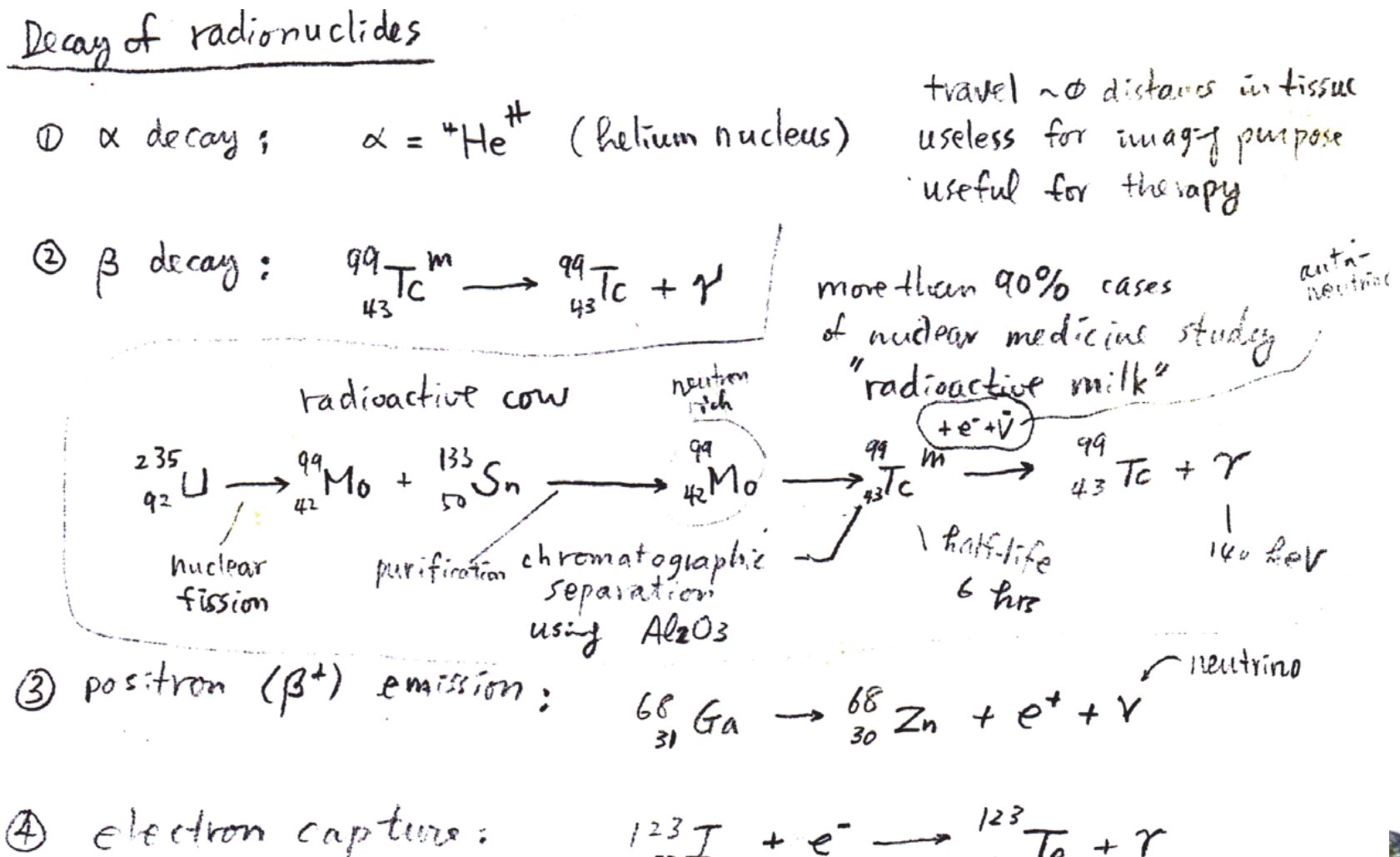

Two Most Used Decays

- Single Photon Emission
  - $(^{99}\mathrm{Mo} \underset{2.7\ day}{\rightarrow}) \ ^{99}_{43}\mathrm{Tc}^{m} \rightarrow \ ^{99}_{43}\mathrm{Tc} + \gamma$ (140 keV) (Technetium half-life 6.02 hours)
- Positron Emission
  - $(^{68}\mathrm{Ge} \underset{271\ day}{\rightarrow}) + \ ^{68}_{31}\mathrm{Ga} \rightarrow \ ^{68}_{30}\mathrm{Zn} + \mathrm{e}^{+} + \nu$ (Gallium half-life 68 minutes)
  - Annihilation produces two photons, each with energy 511 keV ($\mathrm{E} = \mathrm{mc}^2$)
  - Detect both, reduces scatter, increases spatial resolution (¡ 5 mm)

Compton γ-Camera Refraction

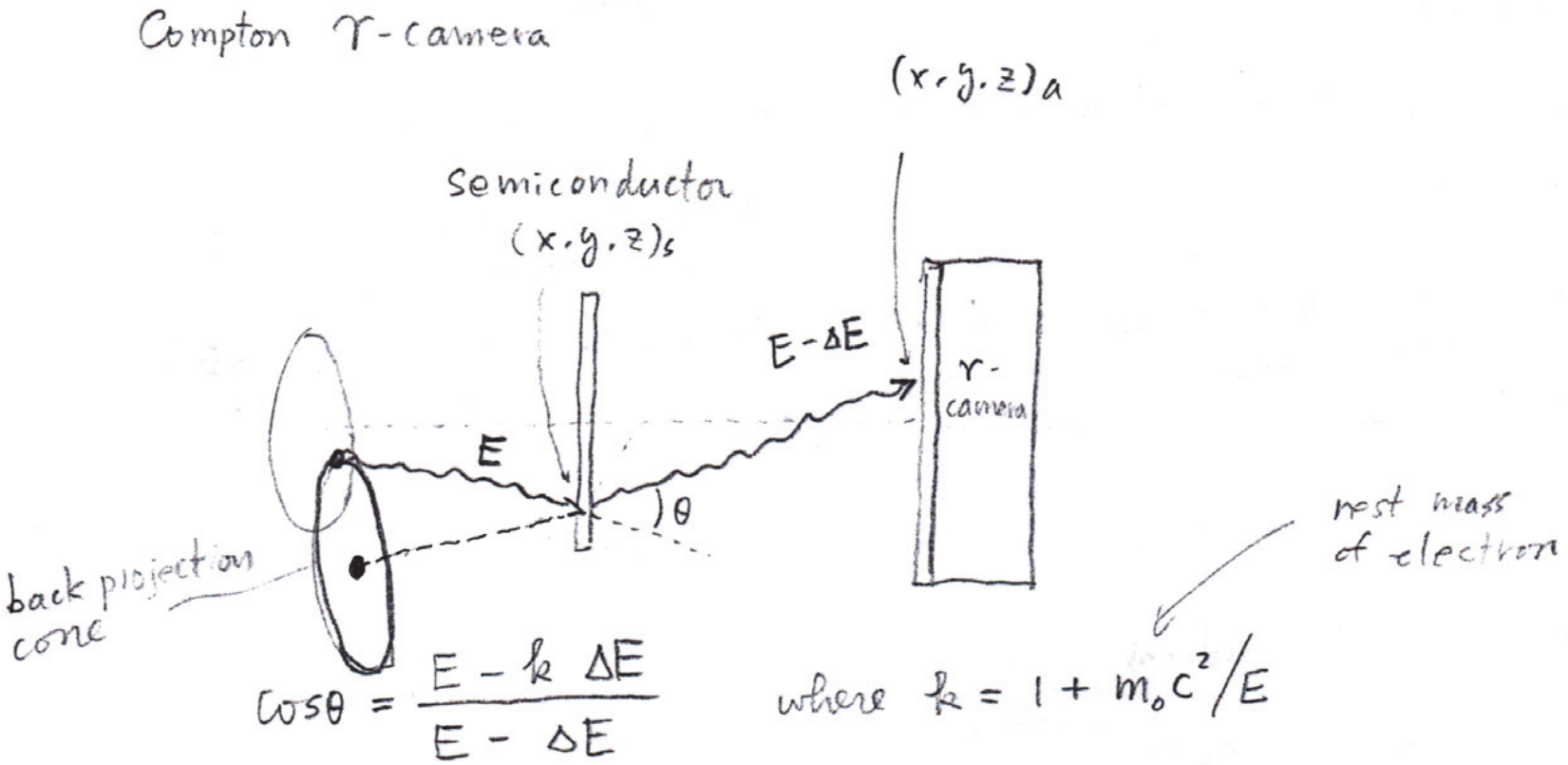

backprojection + iterative reconstruction

Compton γ-Camera Refraction

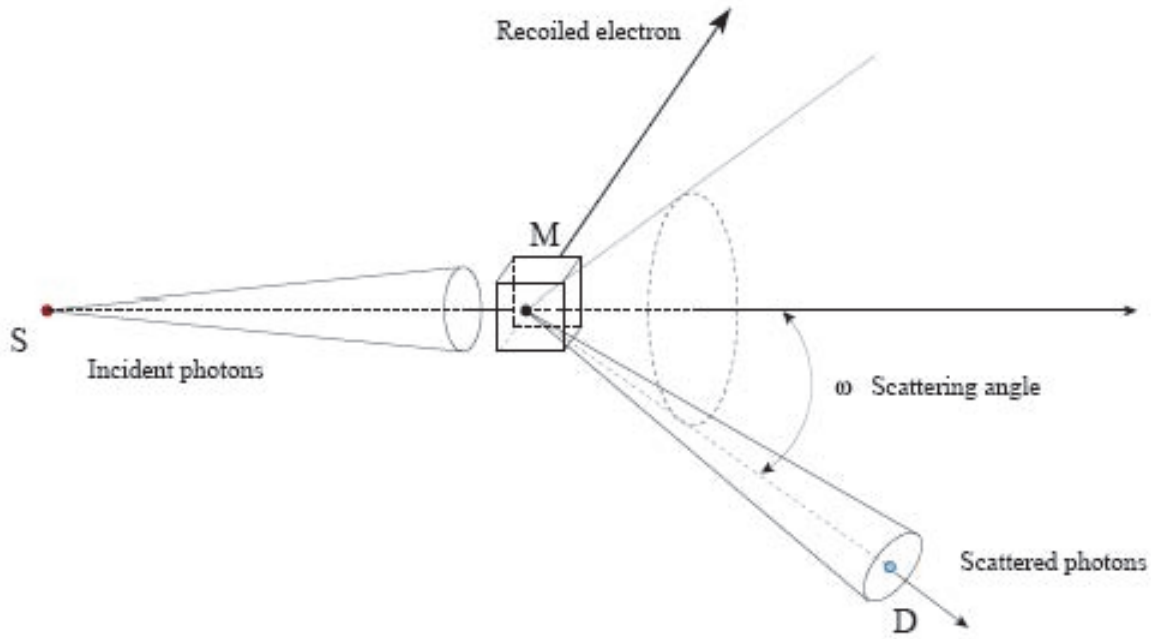

Compton γ-Camera Refraction

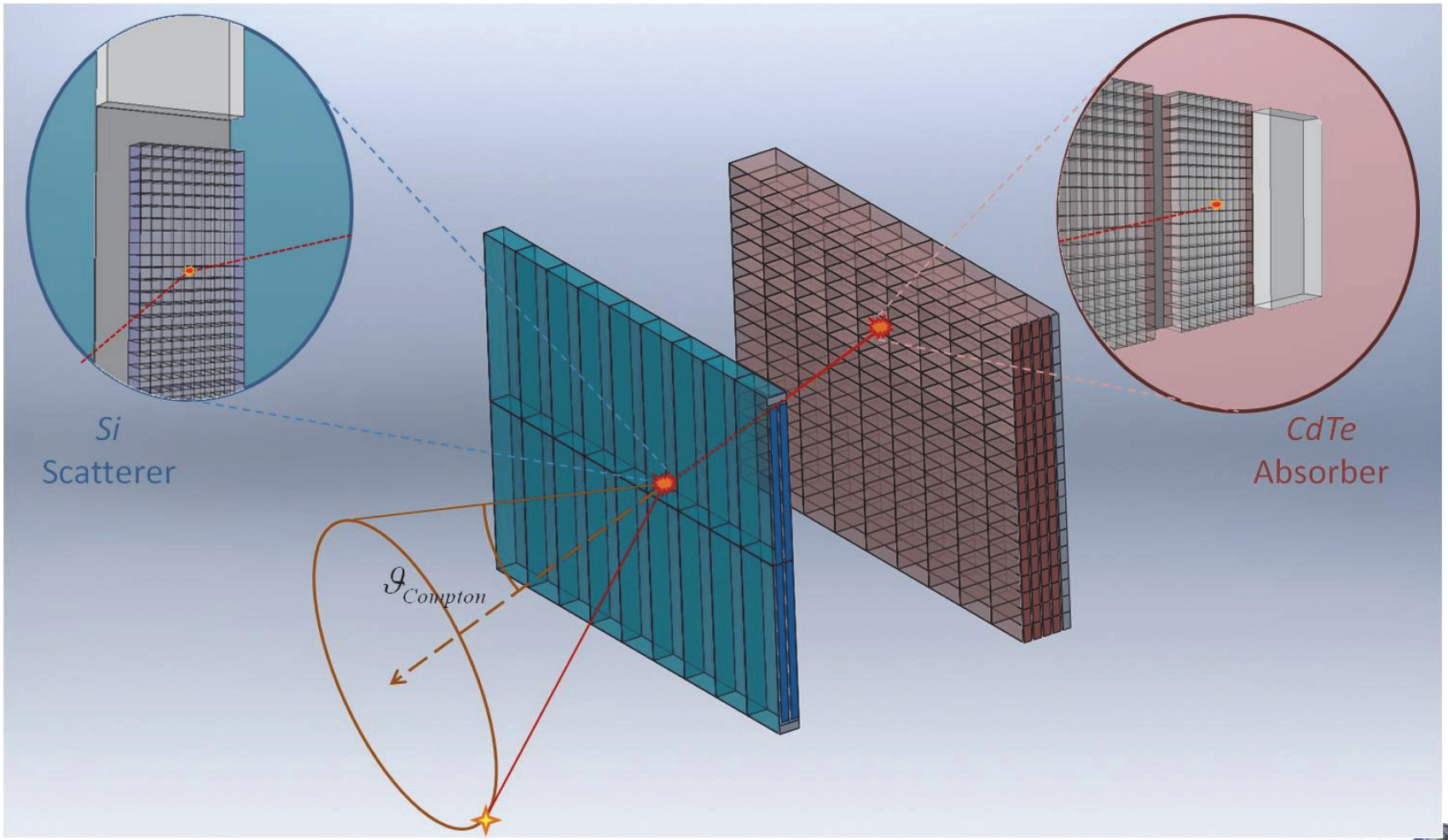

THINK BIG WE DO™

MUGA - Multiple Uptake Gate Acquisition

dynamic imaging

MUGA cardiac study (multiple uptake gated acquisition)

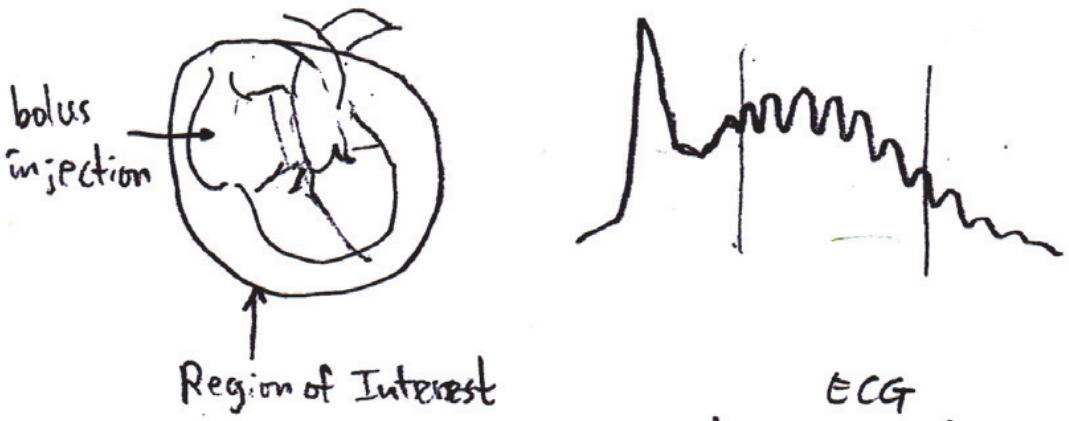

ECG-gated study

List-mode

Dodge's Area Length Formula

Dodge's area-length formula (Dodge 1960)

Biplane angiogram
Area planimetry

$$\text{Volume} = \frac{8 A_1 A_2}{3\pi \ \text{smaller}\{L_1, L_2\}}$$

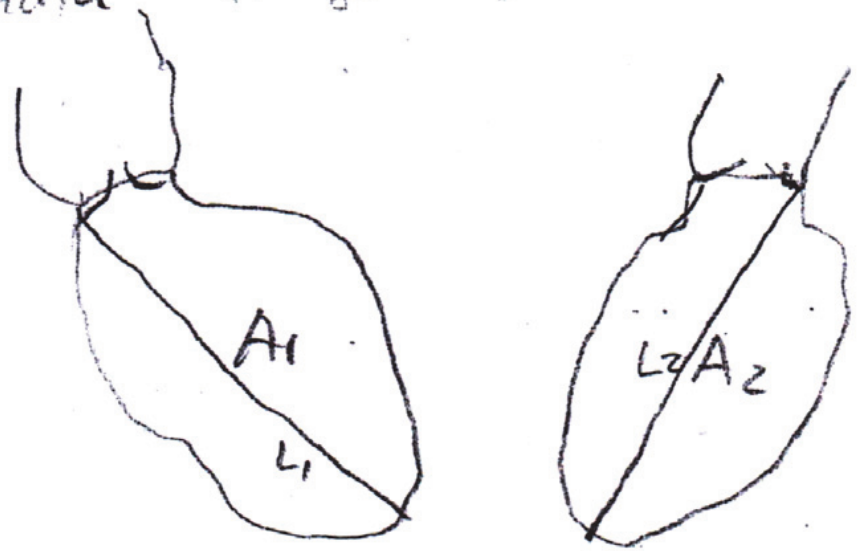

Single plane

$$\text{Volume} = \frac{8 A^2}{3\pi L}$$

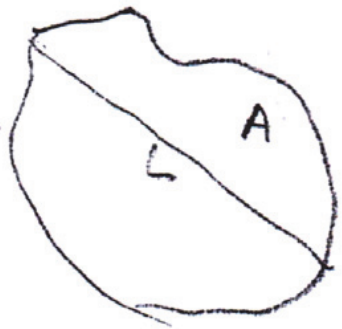

Pulse Echo Imaging

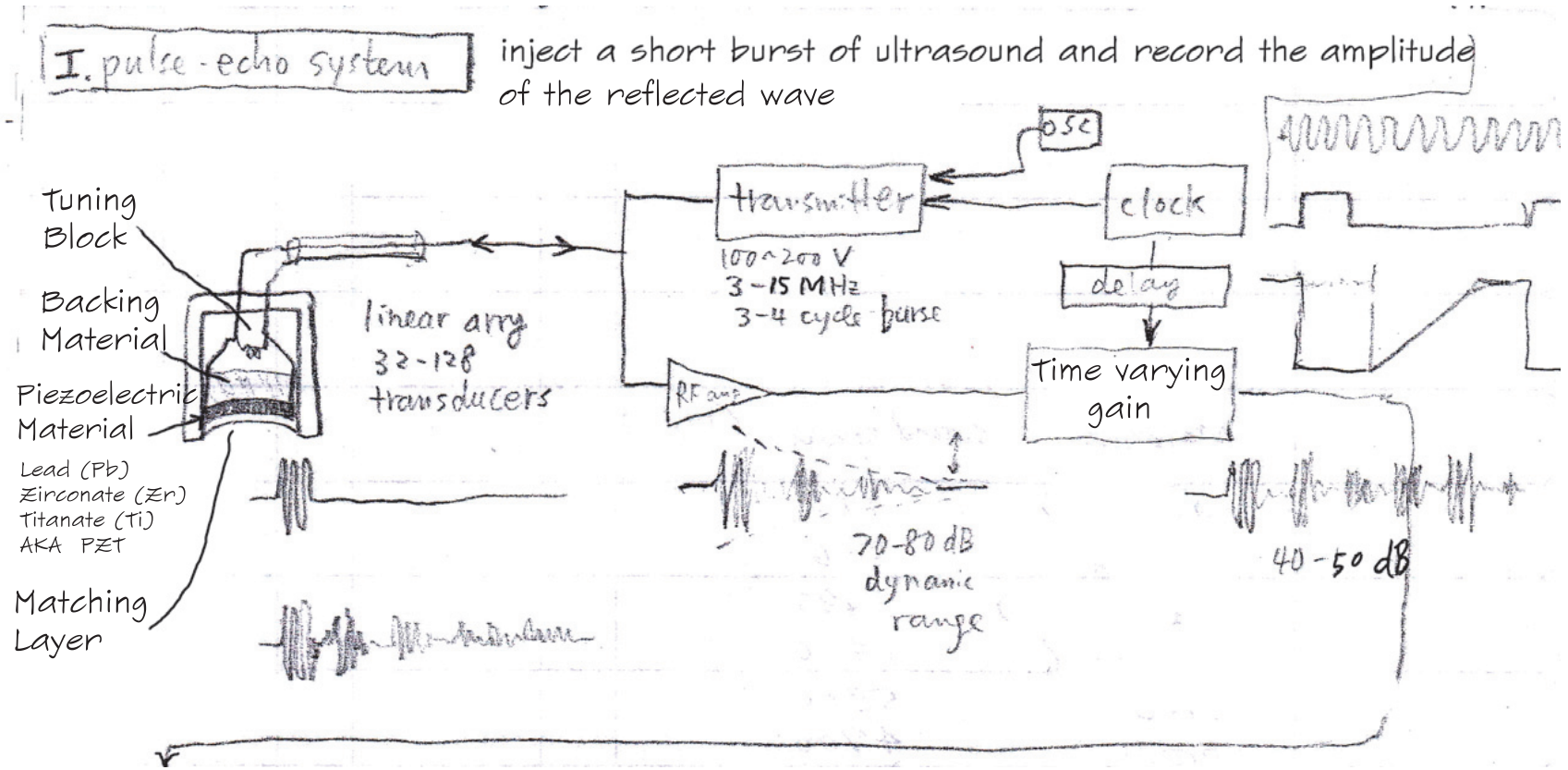

Diagnostic Ultrasound

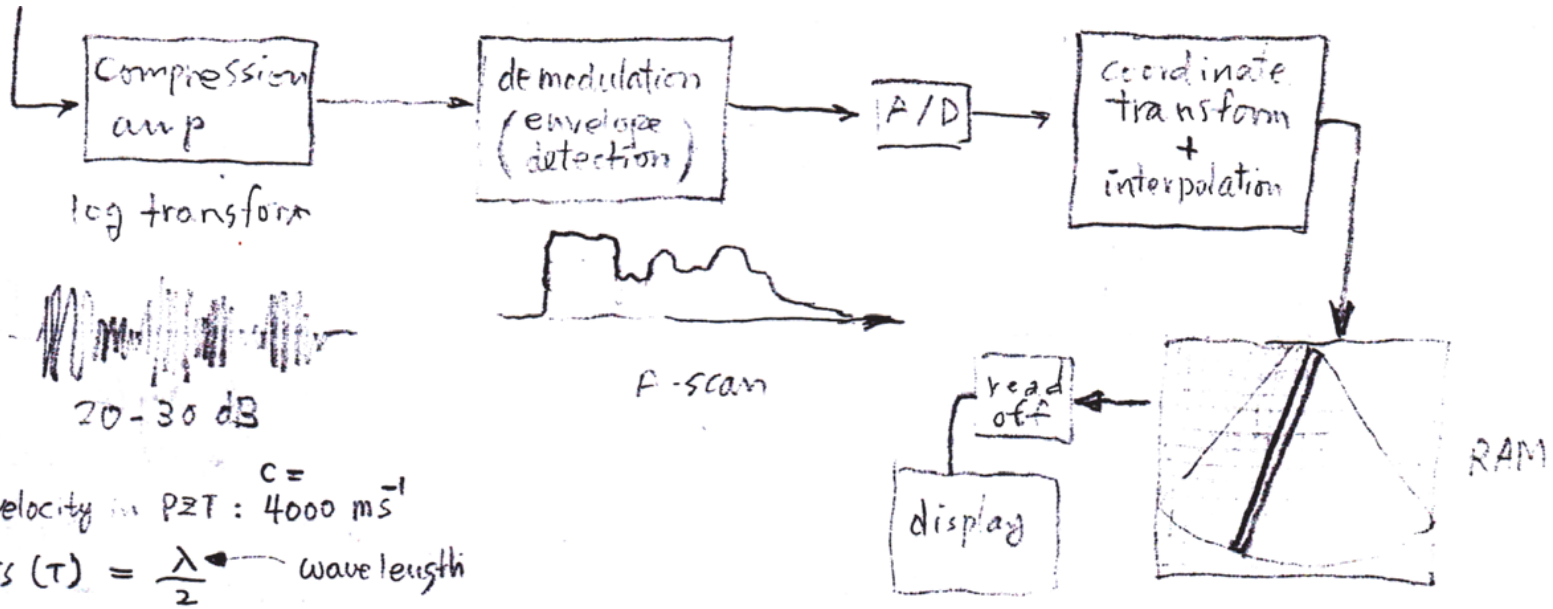

Sound velocity in PZT: $c = 4000\ ms^{-1}$

Thickness (T) $= \frac{\lambda}{2}$ ← wavelength

$\doteq \frac{c}{2f} = \frac{4000}{2f(Hz)}\ m$

$= \frac{2000}{f(Hz)}\ m = \frac{2}{f(MHz)}\ mm$

Ex: $f = 5\ MHz$

$T = \frac{2}{5} = 0.4\ mm$

Sound velocity: air → 340 m/s
tissue → 1500 m/s
PZT → 4000 m/s

(6 bits: $20 \log_{10} 64 = 36\ dB$
8 bits: $20 \log_{10} 256 = 48\ dB$ (overkill)

dynamic range: SNR

1 bit ≈ 6 dB amplitude
1 bit ≈ 3 dB power

Pulse Echo Display Modes

- pulse-echo display modes ((single-scan)

(1) A-mode : amplitude vs. time

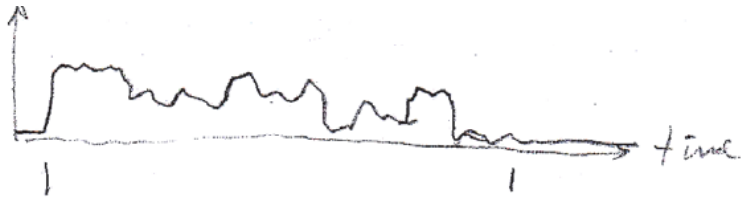

(2) M-mode : A-scan vs. time

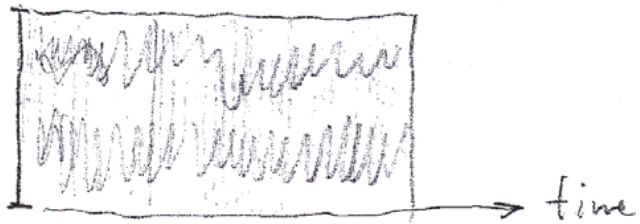

(3) B-mode :

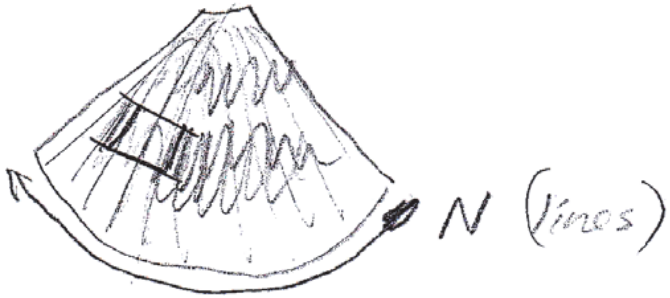

(4) C-mode contrast-depth scan, enhanced resolution

THINK BIG WE DO™

Sound Speed (velocity), Bulk Modulus, Density, and Impedance

- Sound Velocity (speed): $c = \sqrt{\frac{K}{\rho}}$
  - $\frac{K}{\rho} = \frac{dP}{d\rho} = \rho\frac{\frac{dP}{d\rho}}{\rho}$ (pressure per unit change of percent density)
- K: Bulk modulus $\frac{dyn}{cm^2} = \frac{g}{cm \cdot s^2}$, where $\frac{dyn}{cm^2}$ is pressure
  - $dyne = \frac{g \cdot cm}{s^2}$
- Elastance $= \frac{1}{\text{capacitance}}$
  - Recall Bulk modulus measures resistance to compression, related to elastic modulus
- Sound velocity (speed) in tissue: 1540 $\frac{m}{s}$
  - $\frac{K}{\rho} \rightarrow (g \cdot cm^{-1} \cdot s^{-1}) \cdot (g^{-1} cm^3) = \frac{cm^2}{s^2}$
  - $\sqrt{\frac{K}{\rho}} \rightarrow \frac{cm}{s}$, i.e. velocity
- Acoustic characteristic impedance: $z = \rho c = \sqrt{\rho K}$

Fluid Mechanical Analogue

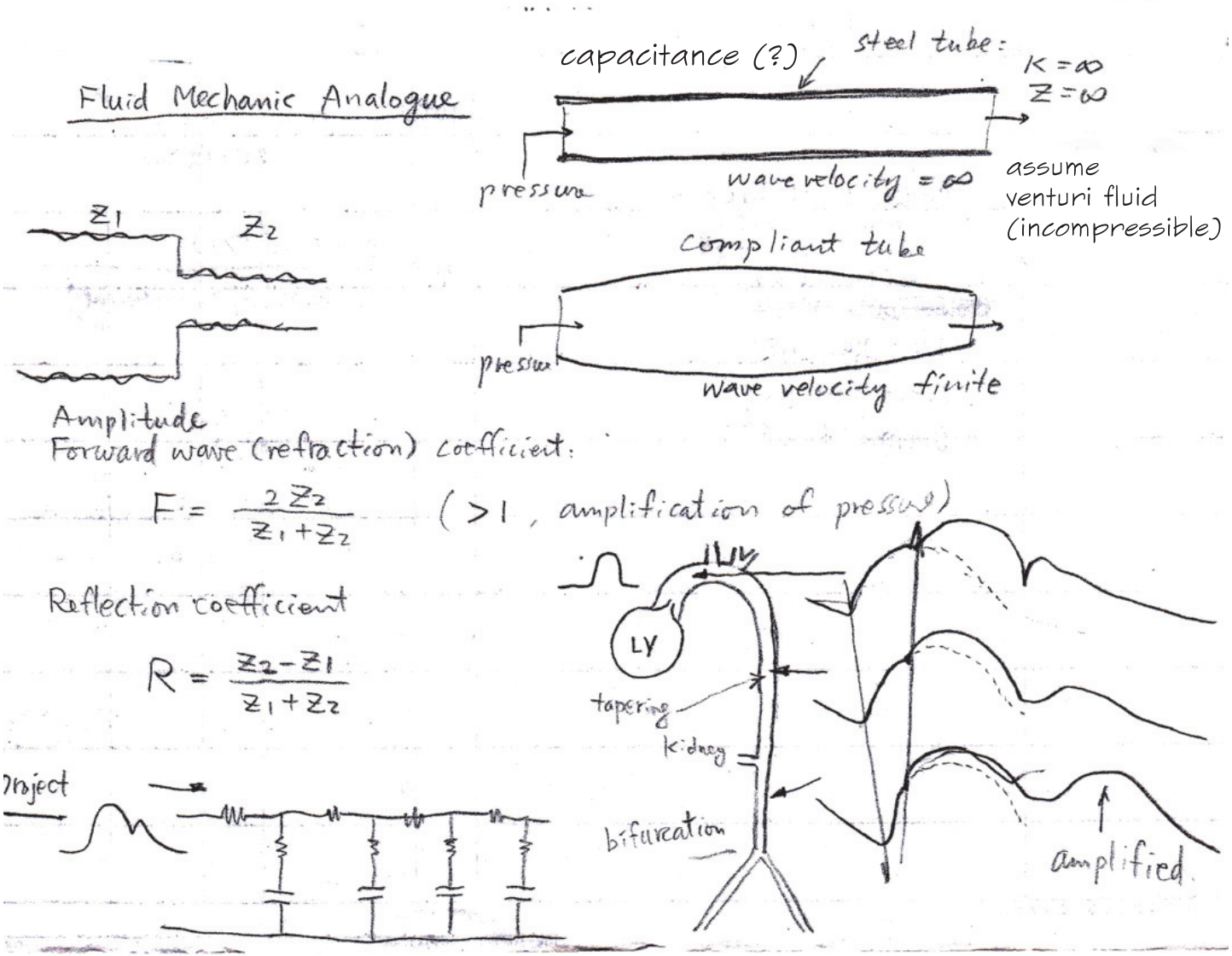

Reflection/Refraction of Sound Waves at Interface

Reflection / Refraction of sound wave at interface

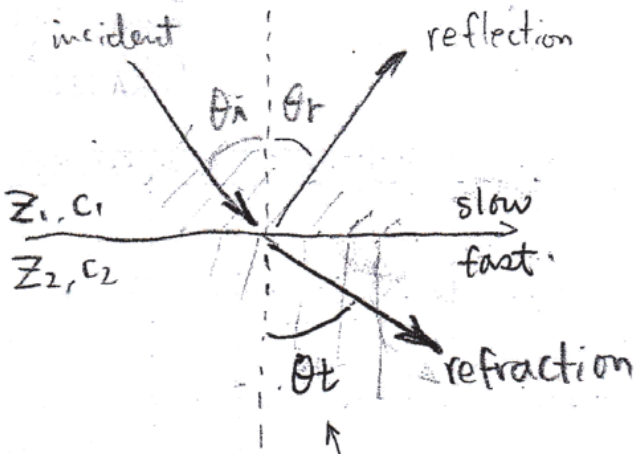

Snell's Law

$$\frac{c_1}{c_2} = \frac{\sin\theta_i}{\sin\theta_t}$$

Snell's law

$c_1 < c_2 \Rightarrow \theta_i < \theta_t$

$\theta_i = \theta_r$

~~intensity~~ reflection coefficient:

$$R = \left(\frac{Z_2\cos\theta_i - Z_1\cos\theta_t}{Z_2\cos\theta_i + Z_1\cos\theta_t}\right)^2$$

mistake in text book (Fig. 7-3 P.325)

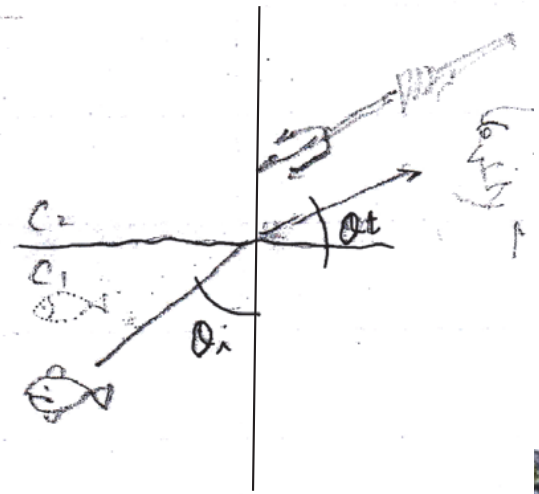

Doppler effect

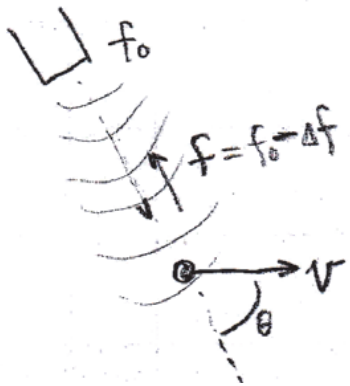

Doppler shift

$$\Delta f = \frac{\pm 2 f_0 v \cos\theta}{c}$$

R

Pulsed Doppler System

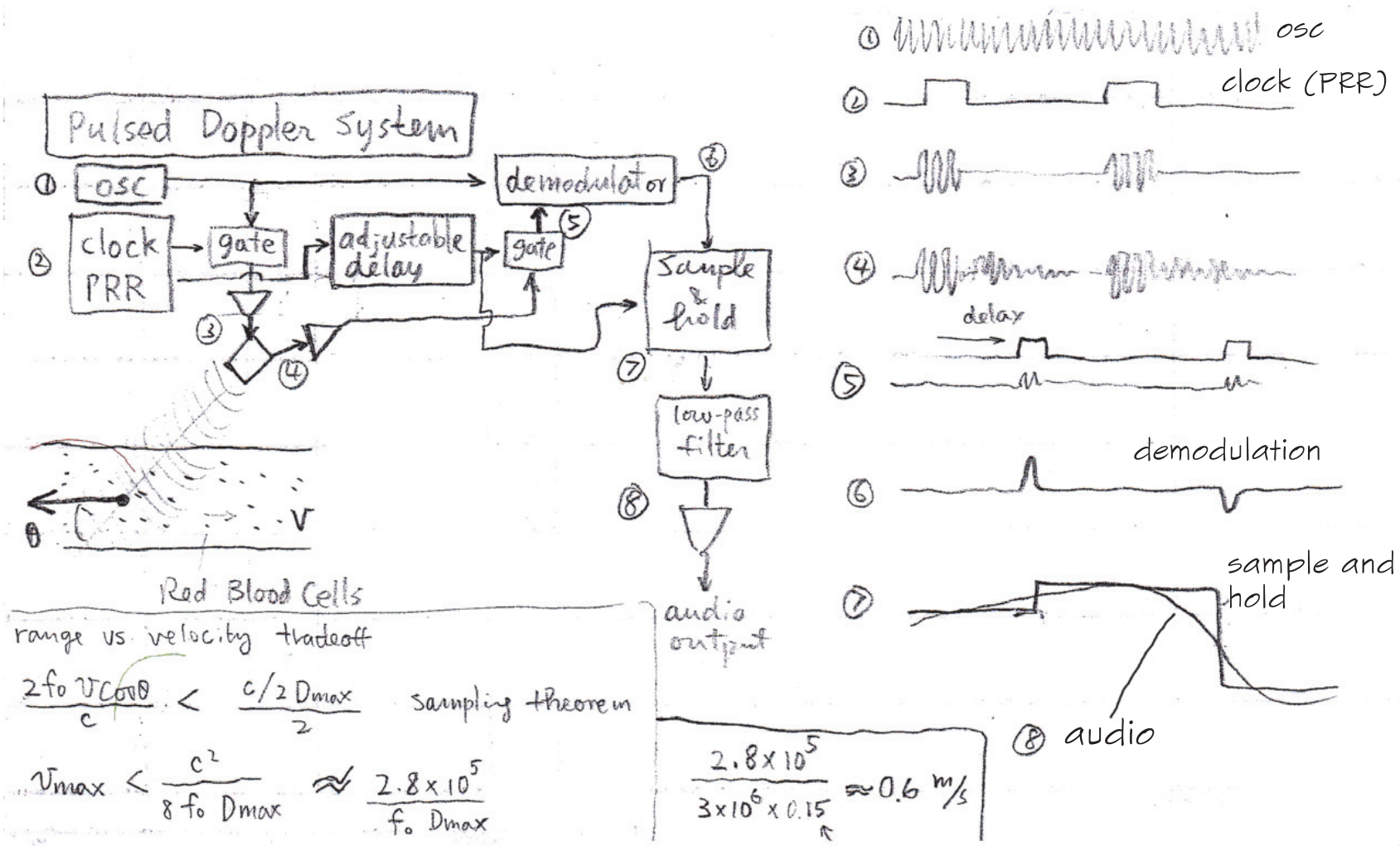

Beamforming, Dynamic and Geometric Focusing

- beam forming

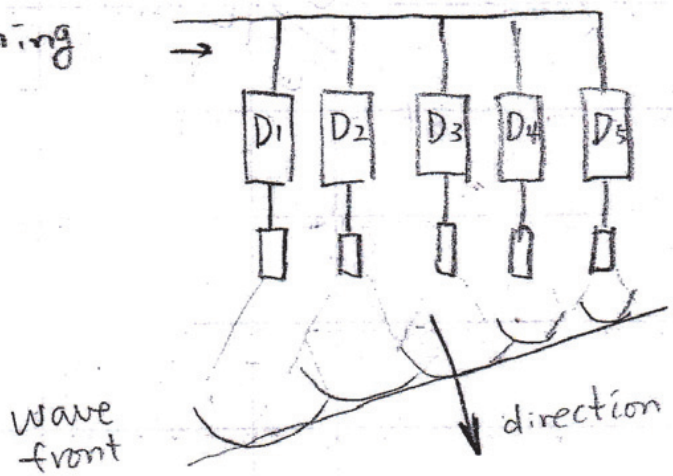

- electronic focusing

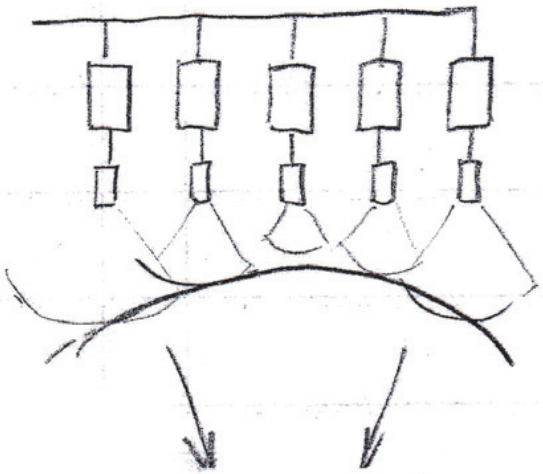

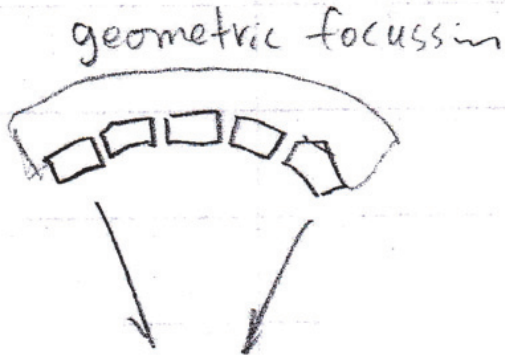

Duplex Scanning

- Duplex scanner — pulse-echo + color Doppler flow

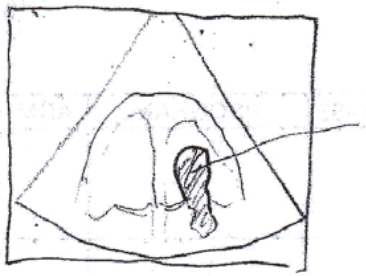

- endoscopic scanner — rotating transducer

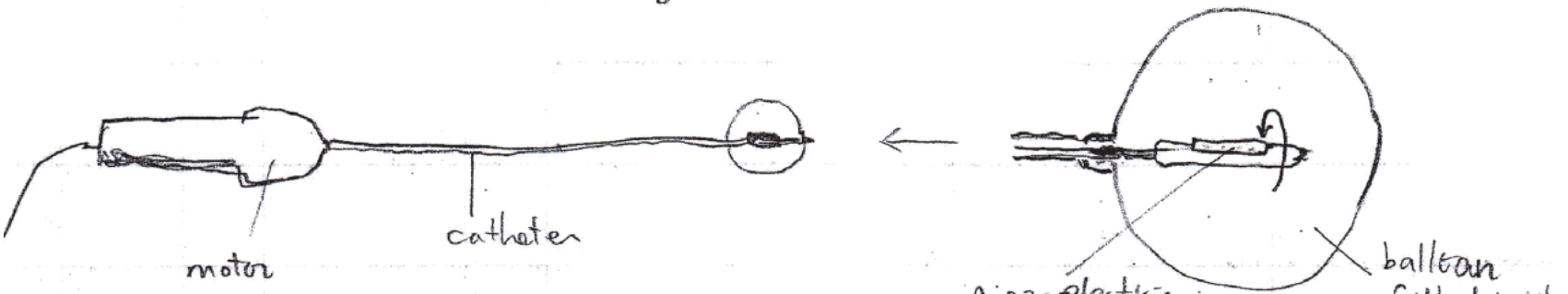

intravascular image

prostate, rectum, uterus, ovaries, bladder, stomach ...

The proximal isovelocity surface area (PISA)

PISA of a regurgitant color flow jet can be useful in the estimation of valvular insufficiency. PISA is based on the hemodynamic principles of flow through a small circular orifice in a flat plate. There is flow acceleration just proximal to the orifice. The flow converges on the orifice in hemispheric layers of equal velocity. The surface area of a hemisphere is calculated by the formula: two pi radius squared.

Color flow Doppler can be used to calculate the area of the hemisphere. This area in centimeters squared is then multiplied times the aliasing velocity in centimeters per second yielding cubic centimeters per second, which provides the volume of regurgitant blood flow. The principal theoretic limitation is that the usual regurgitant orifice is neither circular nor flat.

Furthermore, it is possible to calculate the effective regurgitant orifice area by dividing regurgitant flow volume by the velocity of the mitral insufficiency jet: ERO = Flow / Velocity

This is based on conservation of energy. The flow velocity "V" in a vessel will vary inversely with the area of the orifice. Since flow equals velocity times orifice area. Multiplying both sides of the equation: " Flow = Velocity times Area " V X A " by 1/V yields: " Area = Flow / Velocity ".

PISA

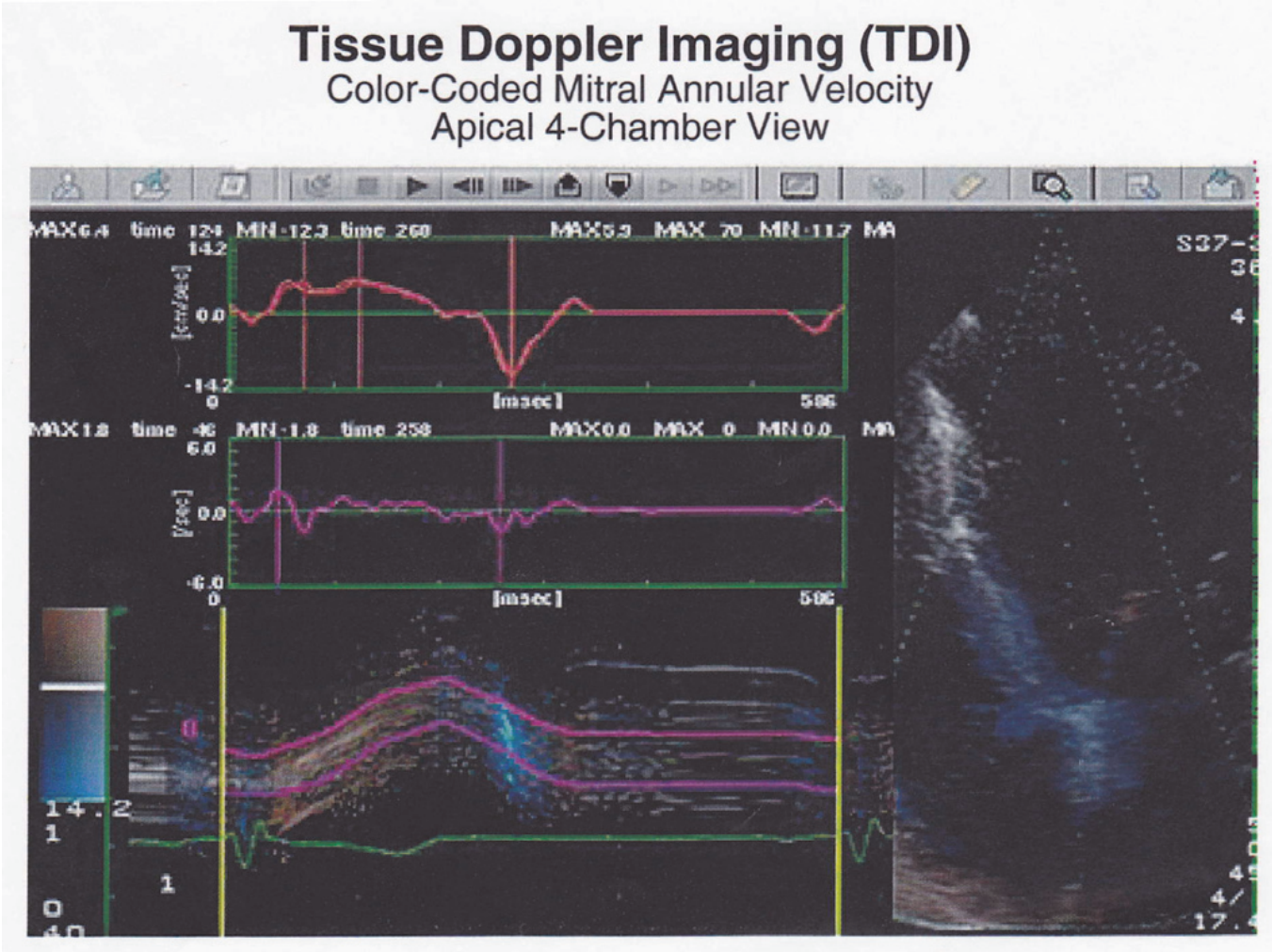

THINK BIG WE DO™

Pathology

- Mitral Valve Regurgitation (prolapse)
  - "Green Monstah"
- Mitral Valve Stenosis
- Aortic Valve Regurgitation
- Aortic Valve Stenosis

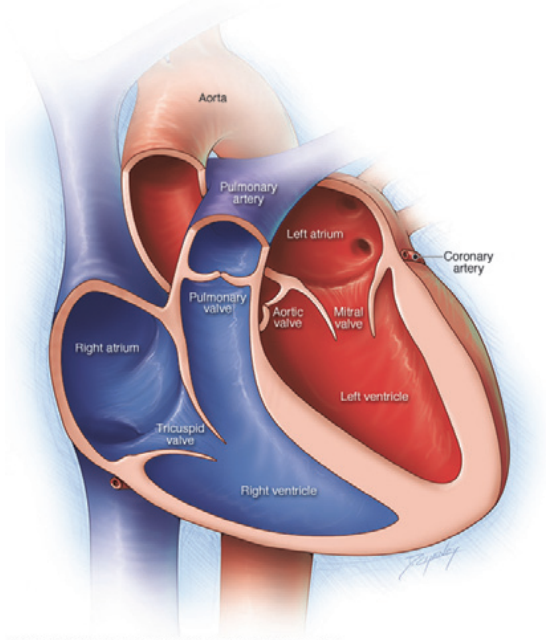

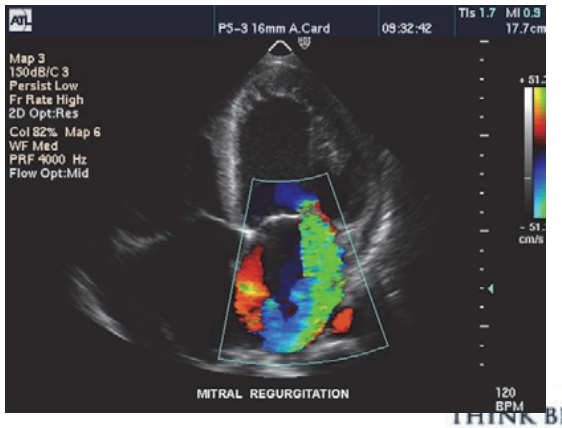

[1]

Future Directions

- Future directions
  - acoustic tomography (synthetic aperture)
  - tissue characterization (texture info. in the image)

TEE (Transesophageal Echocardiography)
TTE (Transthoracic Echocardiography)

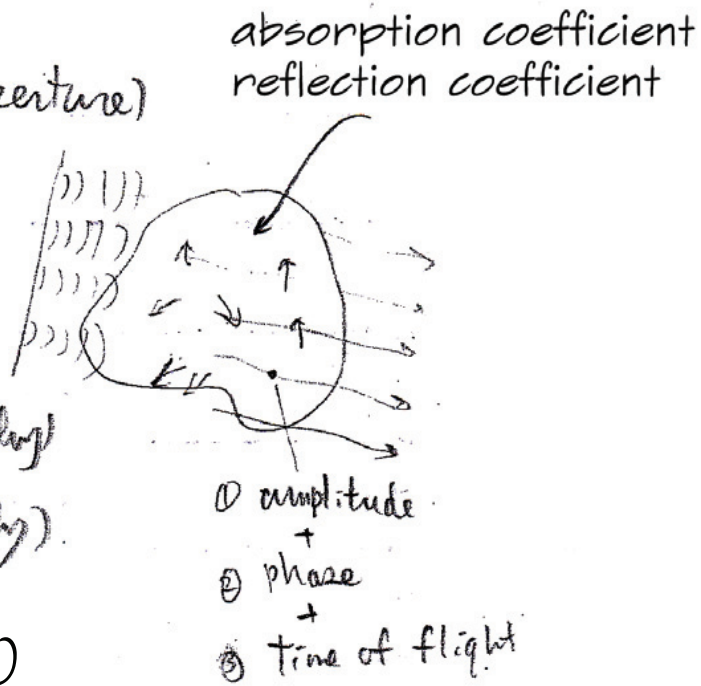

Photo acoustic tomography (PAT)

PAT

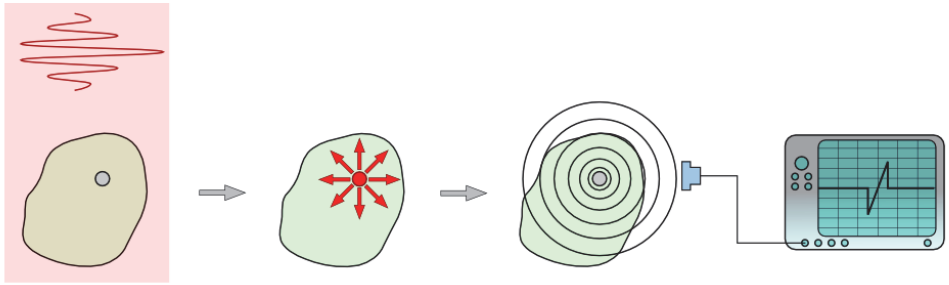

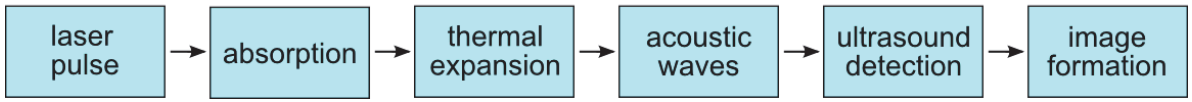

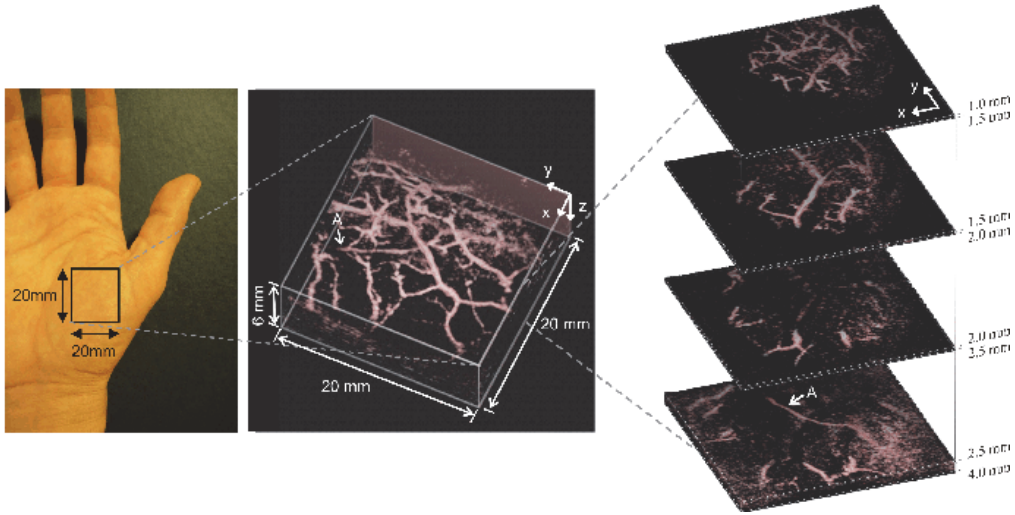

https://www.ucl.ac.uk/cabi/imaging/imaging_techniques/photoacoustics

Magnetic Resonance Imaging

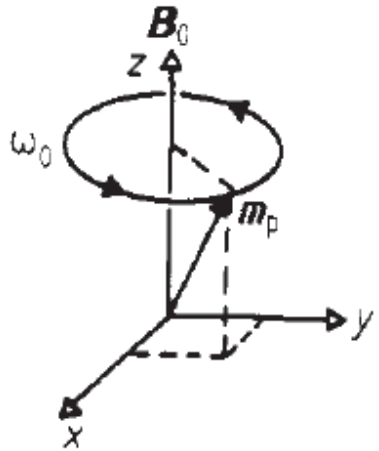

Figure 8.2 The interaction of a magnetic moment m_p with a magnetic flux density B_0 results in the magnetic moment experiencing a couple C which produces motion (precession) with angular velocity ω_0 about B_0.

THINK BIG WE DO™

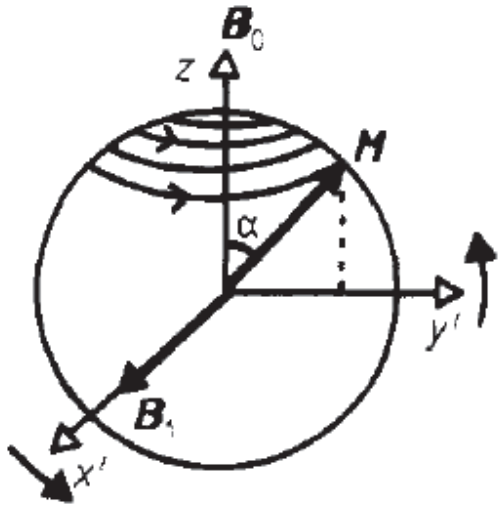

Figure 8.3 If a rotating magnetic flux density $\boldsymbol{B}_1$ is applied in the xy plane in the presence of a static field of flux density $\boldsymbol{B}_0$ orientated along the z axis, $\boldsymbol{M}$ will experience a torque $\boldsymbol{D}$ (in addition to the couple $\boldsymbol{C}$ which gives rise to precession about $\boldsymbol{B}_0$) moving $\boldsymbol{M}$ through an angle α from the z axis. (x' and y' are axes rotating at ω_0, the Larmor frequency (see §8.3.1.1).)

THINK BIG WE DO™

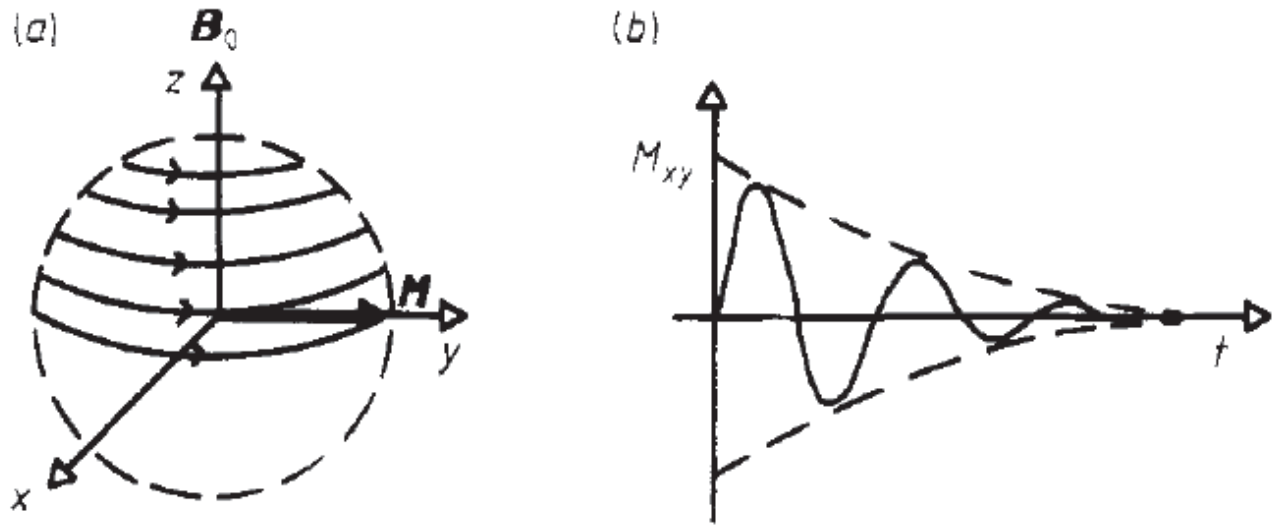

Figure 8.4 (*a*) The motion of $\boldsymbol{M}$ in the laboratory frame following a 90° RF pulse and (*b*) the resultant FID that can be measured from the *xy* component of the sample magnetisation.

Magnetic Resonance Imaging

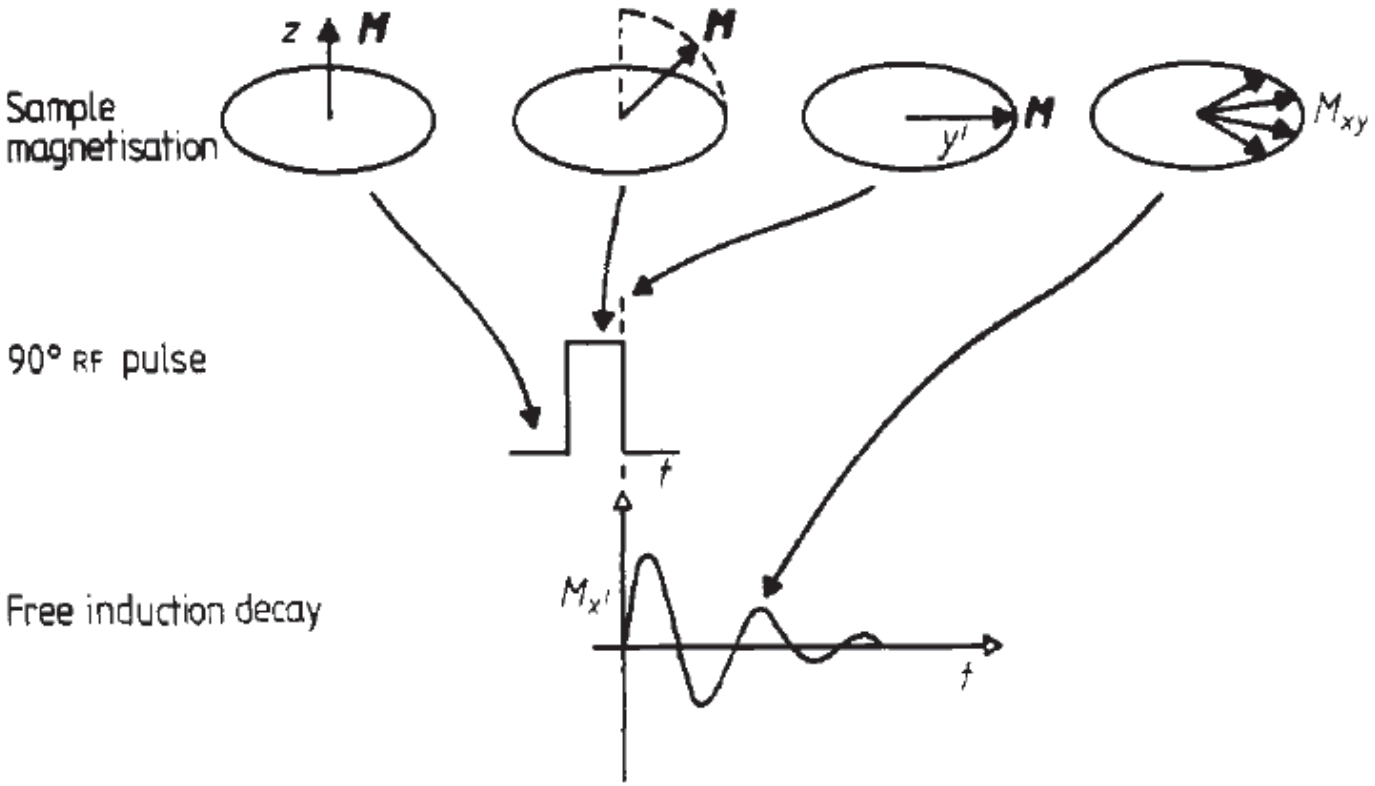

Figure 8.12 The effect of a 90° RF pulse on the sample magnetisation M, and the resultant FID showing loss of net magnetisation in the xy plane due to dephasing.

Magnet Demo

http://www.drcmr.dk/CompassMR/

MRI References

https://www.ncbi.nlm.nih.gov/pmc/articles/PMC1121941/

http://xrayphysics.com/sequences.html

Saturation Recovery

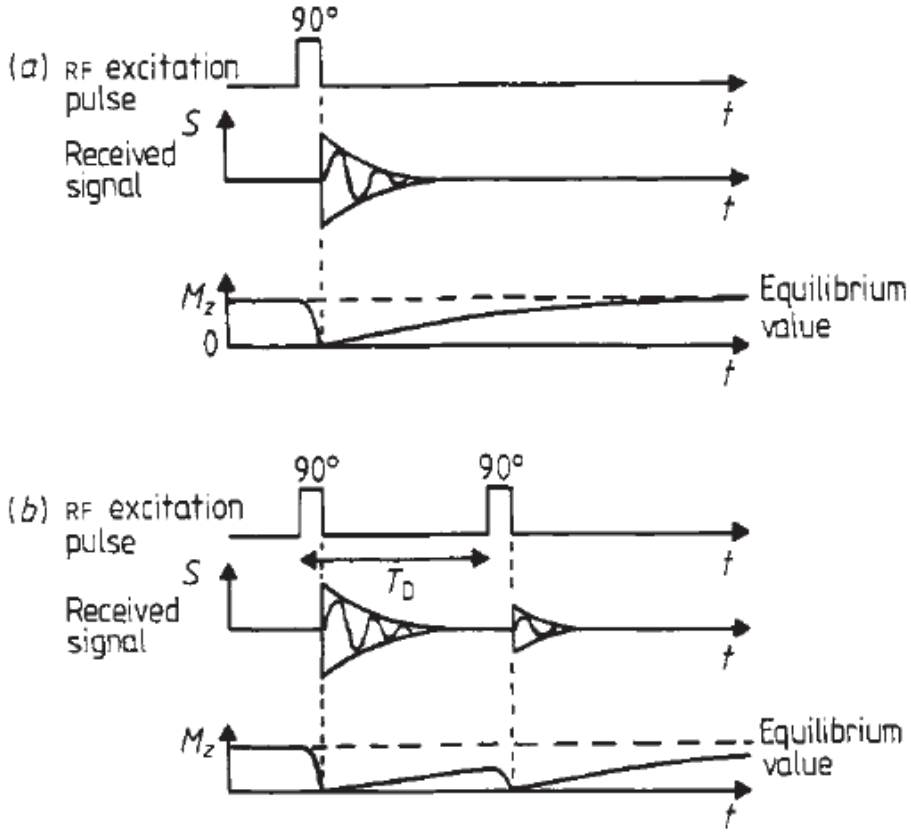

Figure 8.13 (*a*) The M_z component of magnetisation recovers to its equilibrium value following an initial 90° RF pulse of a saturation-recovery sequence; (*b*) the magnetisation M_z at time T_D can be monitored with a second 90° RF pulse in a saturation-recovery sequence.

THINK BIG WE DO™

Inversion Recovery

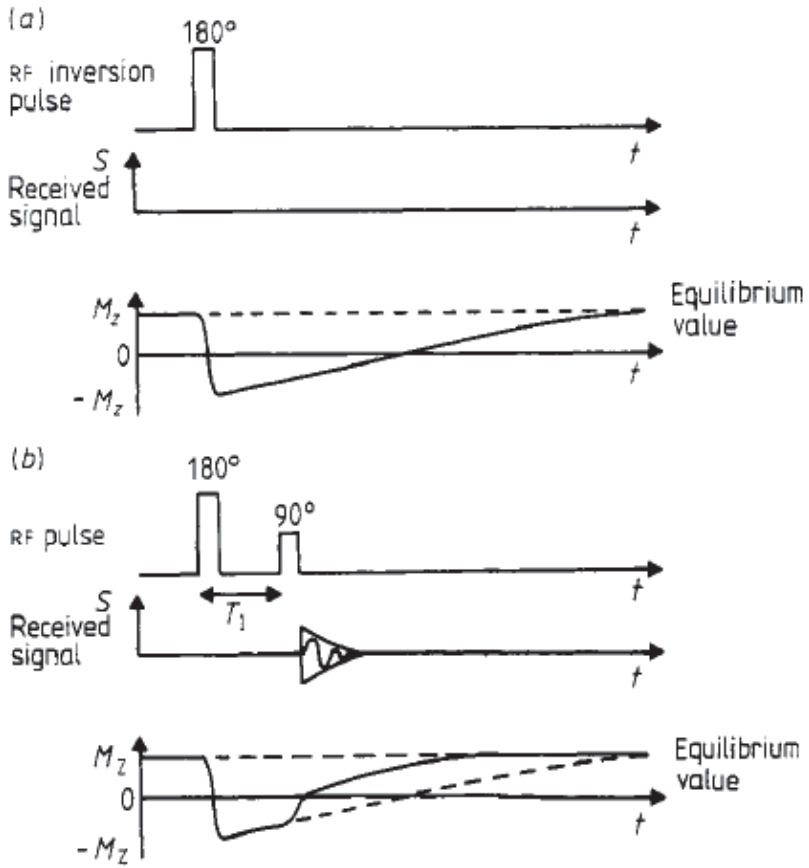

Figure 8.14 (*a*) Following a 180° RF pulse in an inversion-recovery sequence, the z component of magnetisation is inverted and subsequently returns to its equilibrium value; (*b*) by applying a second 90° RF pulse, the value of M_z at time T_I can be measured in a saturation-recovery sequence.

THINK BIG WE DO™

Spin Echo

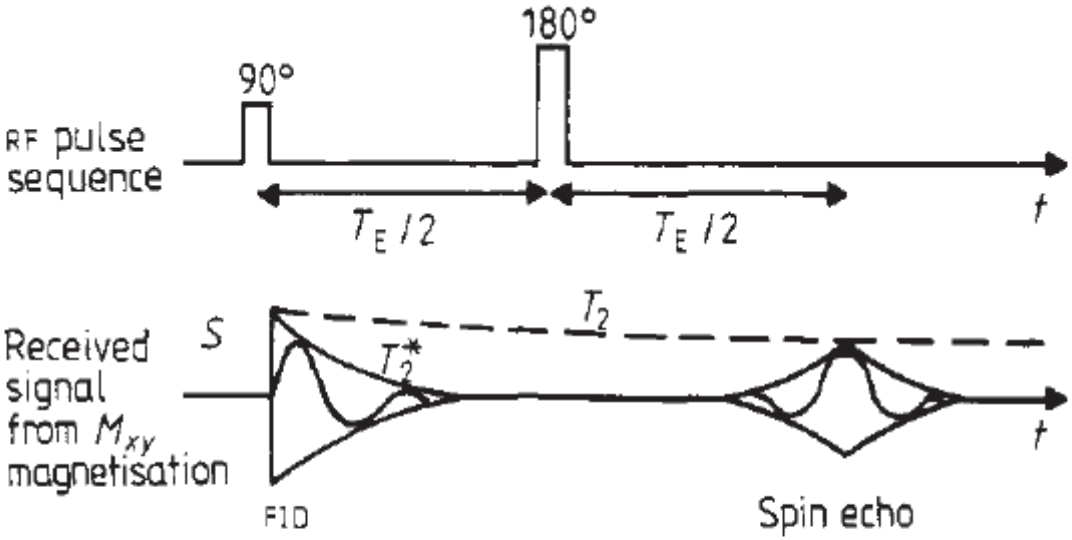

Figure 8.15 In a spin-echo sequence, a 90° RF pulse rotates M_z into the xy plane. Following the loss of coherence due to T_2^* relaxation, the M_{xy} magnetisation is refocused with a 180° RF pulse to produce an echo.

180 Rephasing

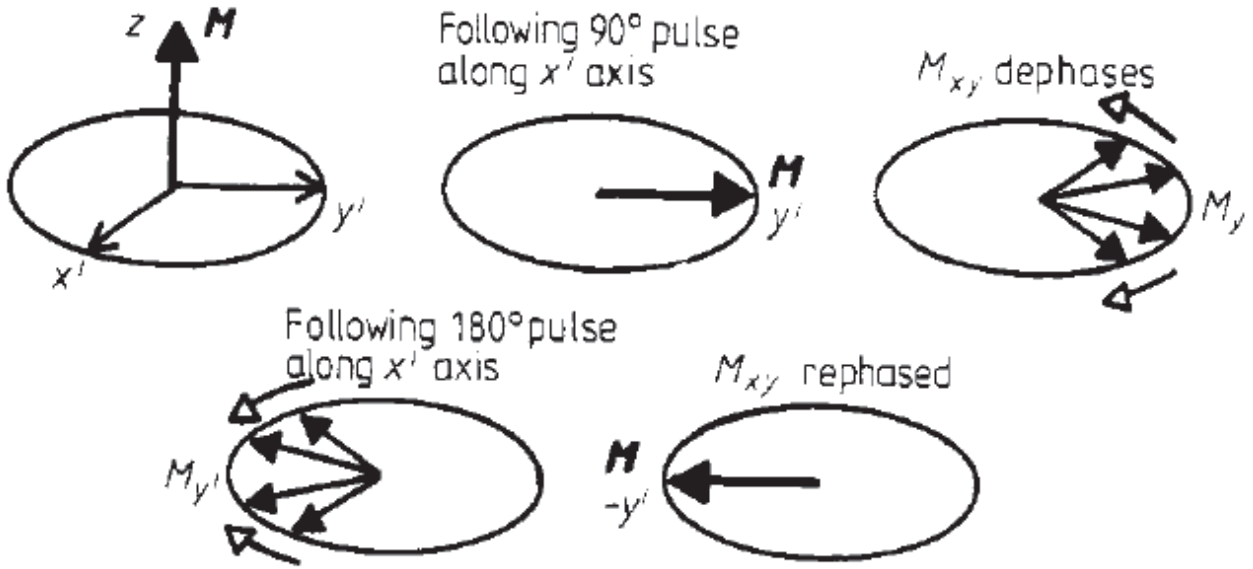

Figure 8.16 The M_{xy} component of magnetisation, produced following a 90° RF pulse oriented along the x' axis in the rotating frame, dephases due to B_0 inhomogeneity. A 180° RF pulse oriented along x' rotates the y' component of magnetisation through 180°, causing the spins to rephase.

RF Sequences

Carr-Purcell and Carr-Purcell-Meiboom-Gill

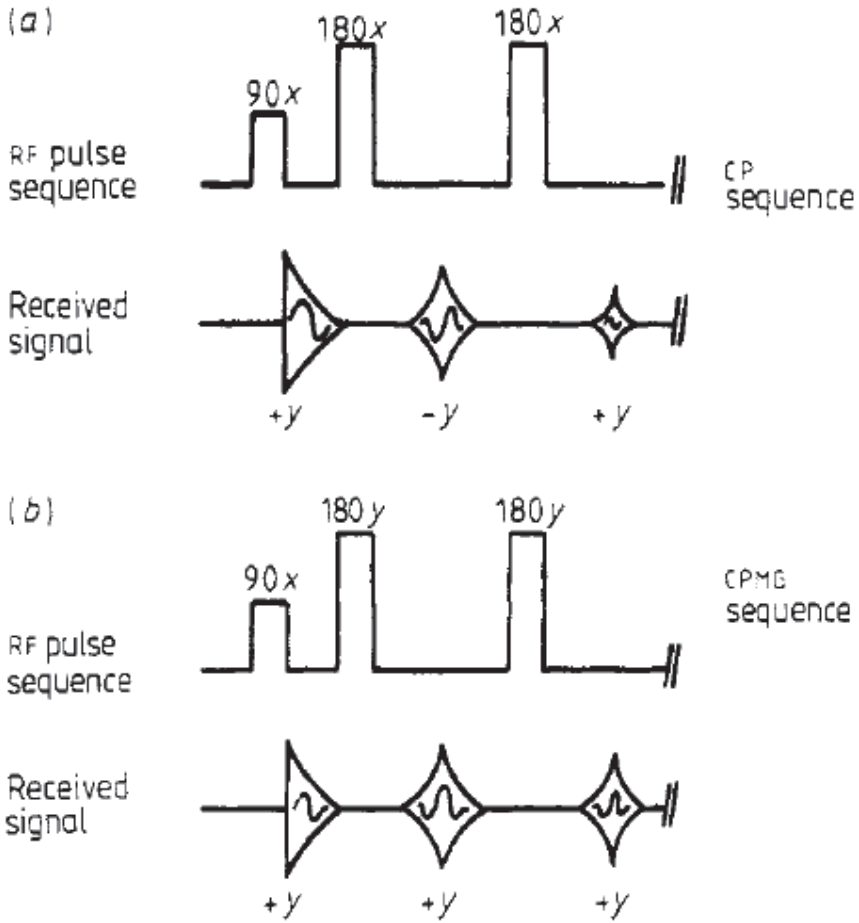

Figure 8.18 (*a*) The Carr–Purcell (CP) pulse sequence, and (*b*) the CP sequence as modified by Meiboom and Gill (CPMG).

T1 Longitudinal Time

Time constant measuring how quickly the precessing proton recovers to it's original state in the $\mathbf{B}_0$ field after being excited by the RF sequence.

T2 Latitudinal Time

Time constant measuring how quickly the proton spin dephases, which decreases the magnetic field coupling. When the RF pulse is applied, all the spinning protons (mostly the H in water) are in phase, creating a strong interaction with the $\mathbf{B}_0$ field. As they start spinning at different rates, the magnetic interaction decreases (think millions of tiny magnets, all aligned, acting on another magnet ... then slowly not aligned, decreasing the force of the interaction.) Note - pure water will exhibit identical T1 and T2 relaxation times.

T2* Latitudinal Time

A time constant due to the imperfections of the magnetic field, the RF, and the gradient detector. In a perfect world where there were no sensing imperfections and fields were uniform and well behaved, T2 and T2* would be identical.

Coils

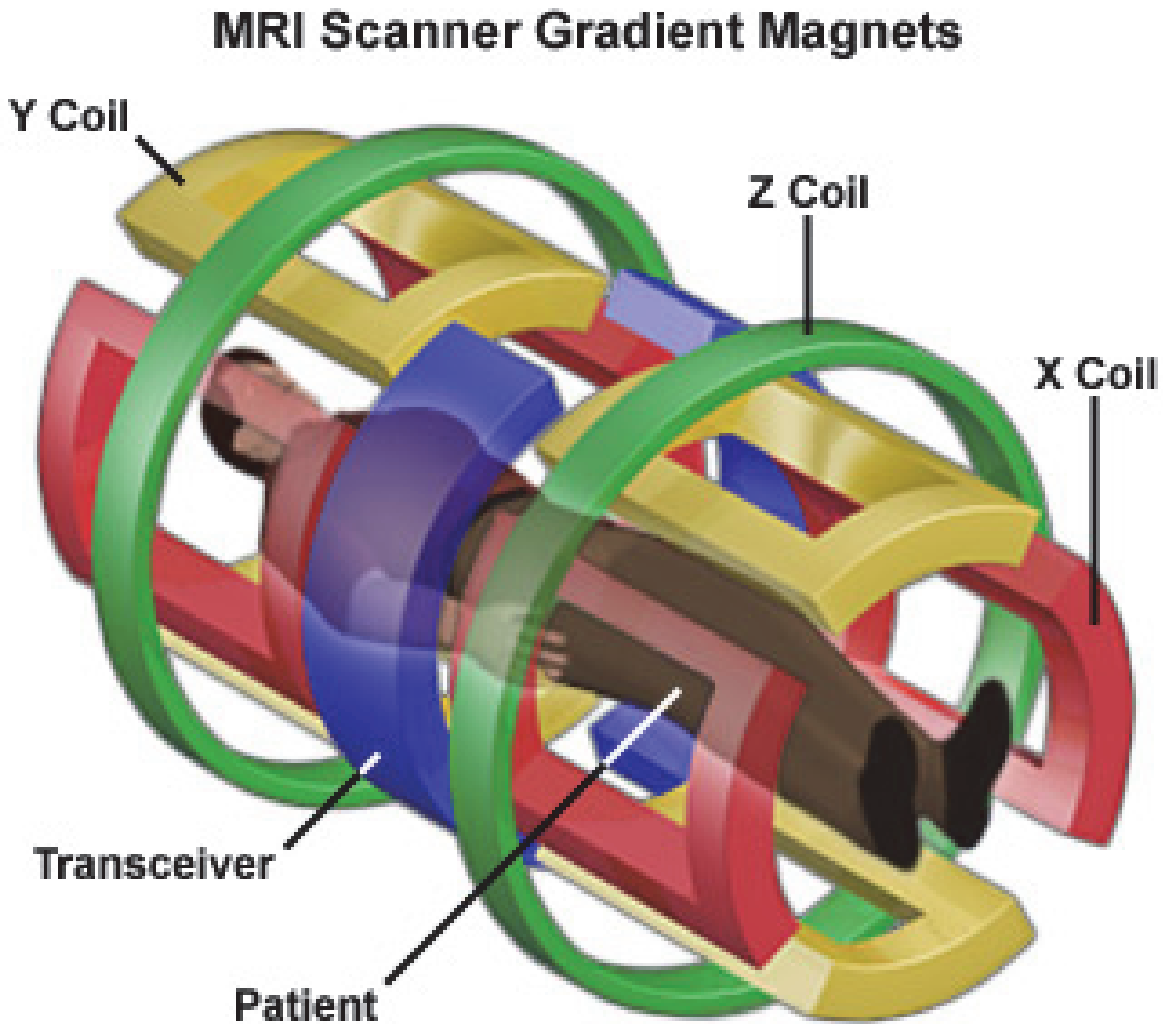

THINK BIG WE DO™

Coils

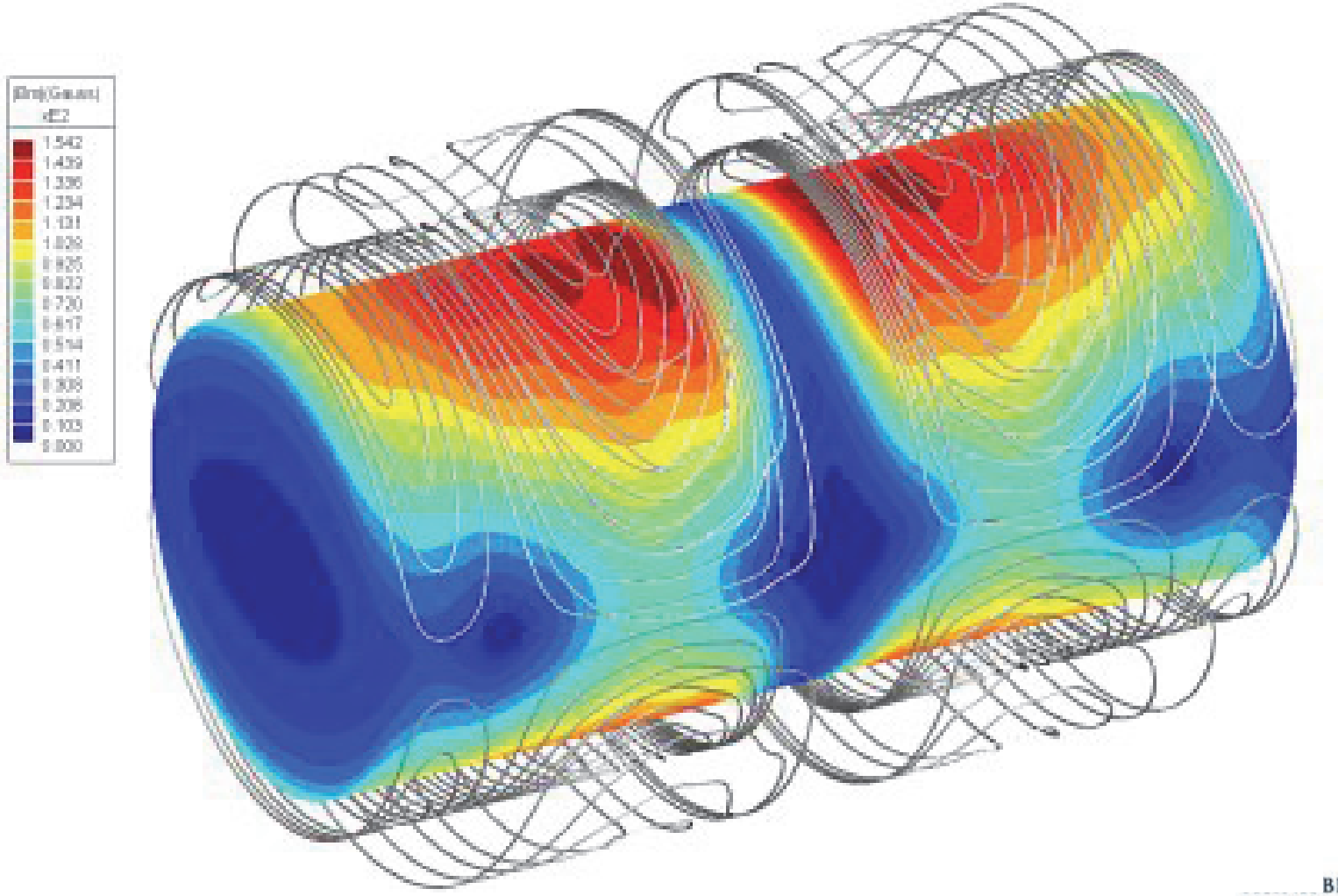
[Bmj](Gauss)
dE2
1.542
1.439
1.336
1.234
1.131
1.028
0.925
0.822
0.720
0.617
0.514
0.411
0.308
0.205
0.103
0.000

Coils

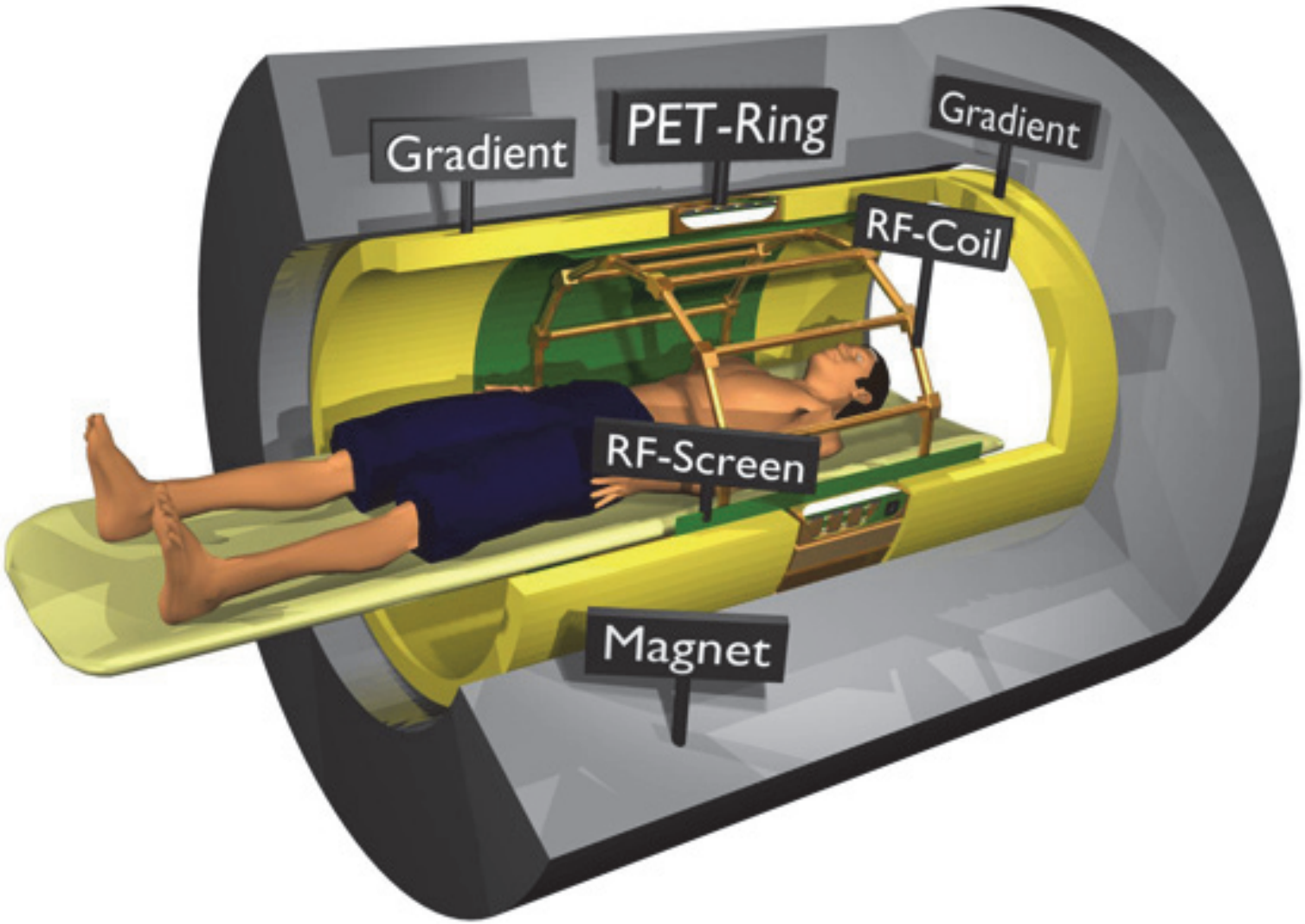

Some Math

Recall from physics that a dipole moment m_p for proton with charge $+e$ has an angular momentum I. The two quantities are related by

$$m_p = \gamma I \tag{24}$$

where γ is the gyromagnetic ratio

$$\gamma = e/(2m) \tag{25}$$

Some Math

Now, this magnetic moment when in the presence of a magnetic field, say B_0, produces a coupling force, i.e. a torque, given by

$$C = m_p \times B_0 \tag{26}$$
$$= dl/dt \tag{27}$$

Recall that force is the time derivative of momentum, i.e.

$$F = dp/dt \tag{28}$$

Substitutions

Make the substitution for I

$$d_m/dt = \gamma m_p \times B_0 \tag{29}$$

Above is the Larmor equation and gives rise to the Larmor frequency

$$\omega = \gamma B_0 \tag{30}$$

which is the frequency the dipole precesses about the z axis associated with the magnetic field B_0

Compressive Sensing

Original signal (image) **x** is observed as signal **y** through sampling such that

$$\mathbf{A}x = y \tag{31}$$

where is **A** is an observation matrix. Question, how do we recover x such that

$$\mathbf{x} = Ay \tag{32}$$

This leads to the other inevitable question, how do we construct A?

Compressive Sensing

- The original signal must be mathematically Sparse
  - Lots of zeros
- Turns out the best measurement matrix A is IID
- We need to minimize the error between what we measure and what is true

How do we do that? Did you ever hear of a little thing called Least Squares minimization?

That's OK because it's not that ... but it is related.

Least Squares $\|x\|_2$

```
1 line = (0:0.01:1);
2 line = line + randn(1,101);
3 A = [ones(101,1) (0:0.01:1)'];
4 LS = inv(A'*A)*A'*line';
5 plot(line)
6 hold on
7 plot(LS(2)*(0:0.01:1)+LS(1),'r')
```

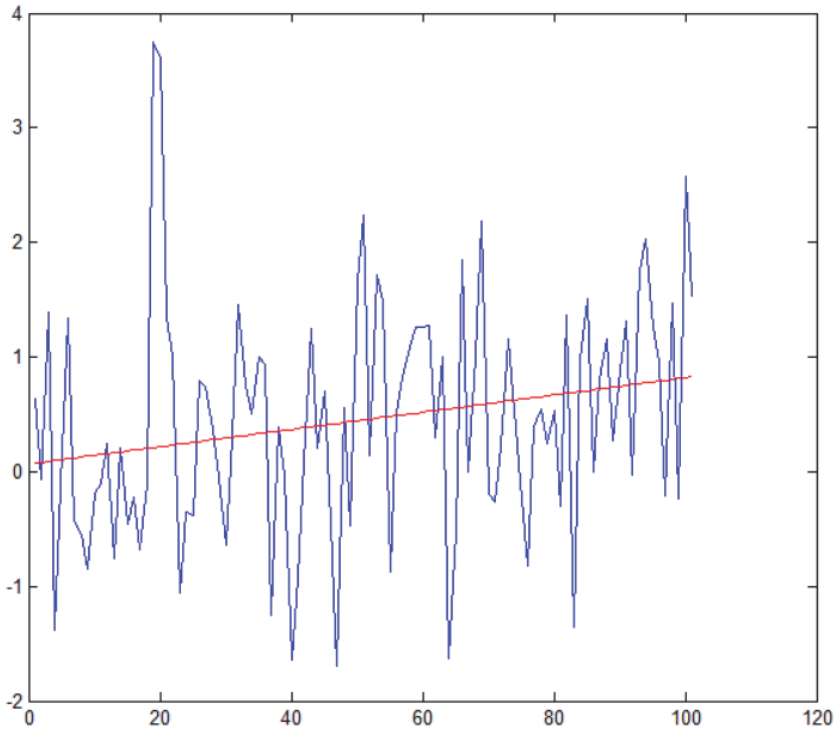

Need $\|x\|_0$, Settle for $\|x\|_1$

The $\|x\|_2$ norm is the Euclidean norm, i.e. find the distance between 2 vectors (i.e. points) in Euclidean space.

The $\|x\|_0$ norm, which technically isn't a norm at all, is a measure of finding the locations of all the zeros in a signal.

Turns out for large N number of samples, this is really hard - essential you have to check each point and determine it's value. This is what's called N-P hard (non-deterministic polynomial-time hard), which is not good.

But given the signal is KNOWN to be sparse, i.e. very few non-zero entries, there is a proof that shows that $\|x\|_1$ converges to $\|x\|_0$, or $\ell_1 \rightarrow \ell_0$.

The ℓ_1 norm is called the Taxi Cab or Manhattan norm, since it reduces to finding the distance between two points on a grid.

Compressive Sensing

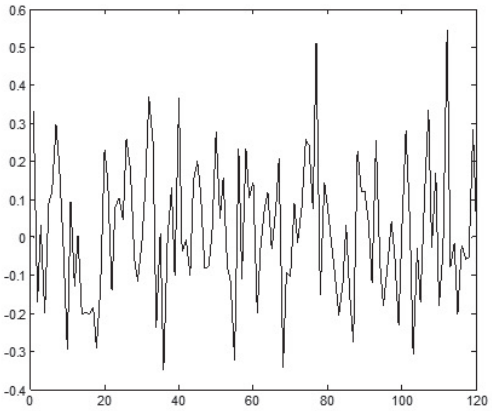

=

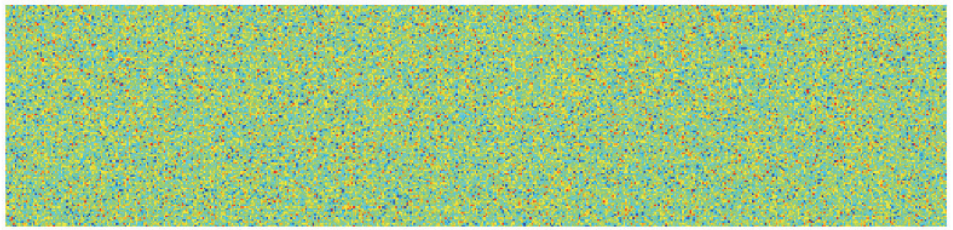

120 x 512

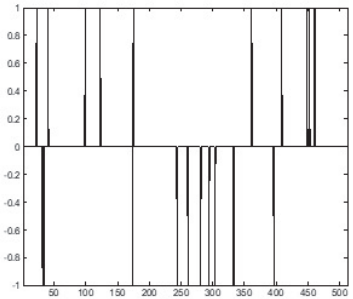

512 x 1

Initial guess - minimum energy

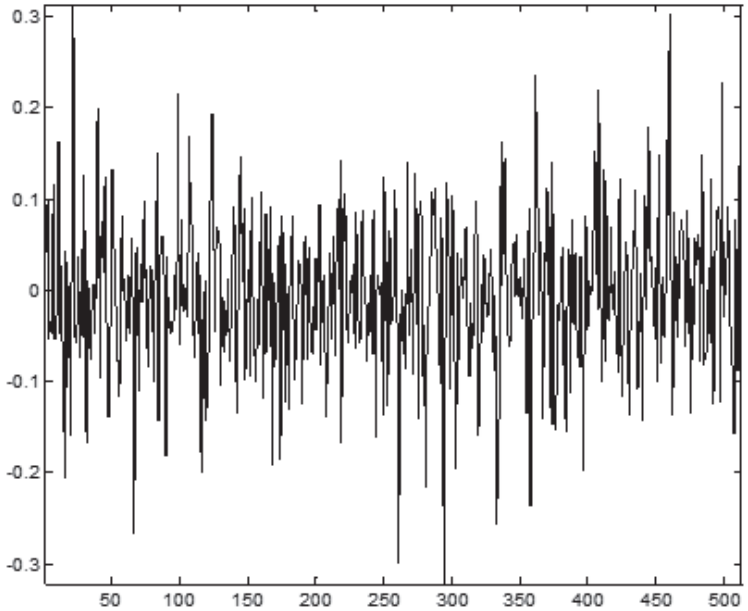

=

512 x 120

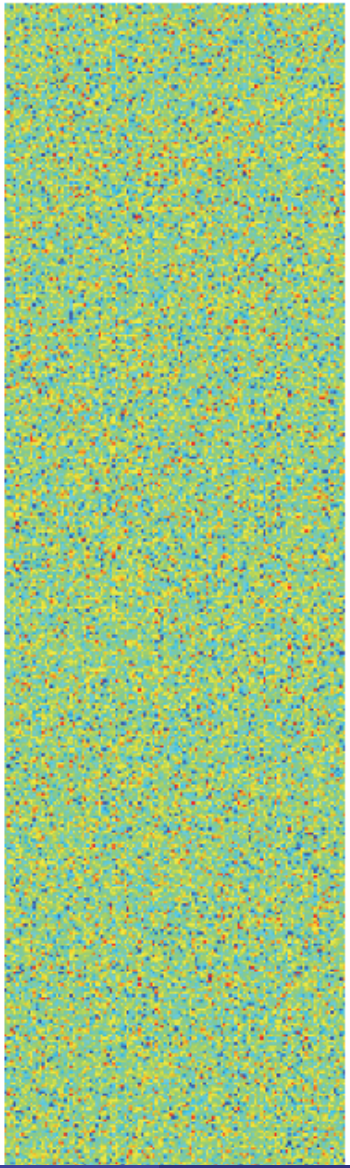

120 x 1

Compressive Sensing - linear programming

```
20      % signal length
21 -    N = 1024;
22      % number of spikes in the signal
23 -    T = 10;
24      % number of observations to make
25 -    K = 500;
26
27      % random +/- 1 signal
28 -    x = zeros(N,1);
29 -    q = randperm(N);
30 -    x(q(1:T)) = sign(randn(T,1));
31 -    figure,plot(x)
32      % measurement matrix
33 -    disp('Creating measurment matrix...');
34 -    AA = randn(K,N);
35 -    A = orth(AA')';
36 -    disp('Done.');
37 -    figure,imagesc(AA)
38 -    figure,imagesc(A)
39      % observations
40 -    y = A*x;
41 -    figure,plot(y)
42      % initial guess = min energy
43 -    x0 = A'*y;
44
45      % solve the LP
46 -    tic
47 -    xp = l1eq_pd(x0, A, [], y, 1e-5);
```

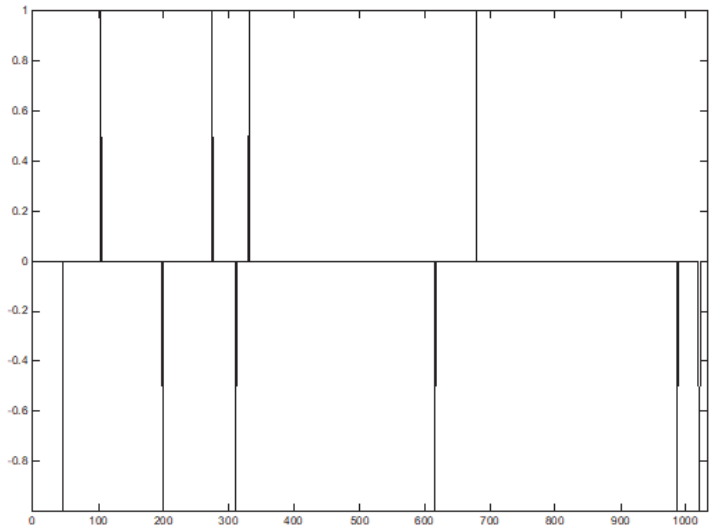

Compressive Sensing - error

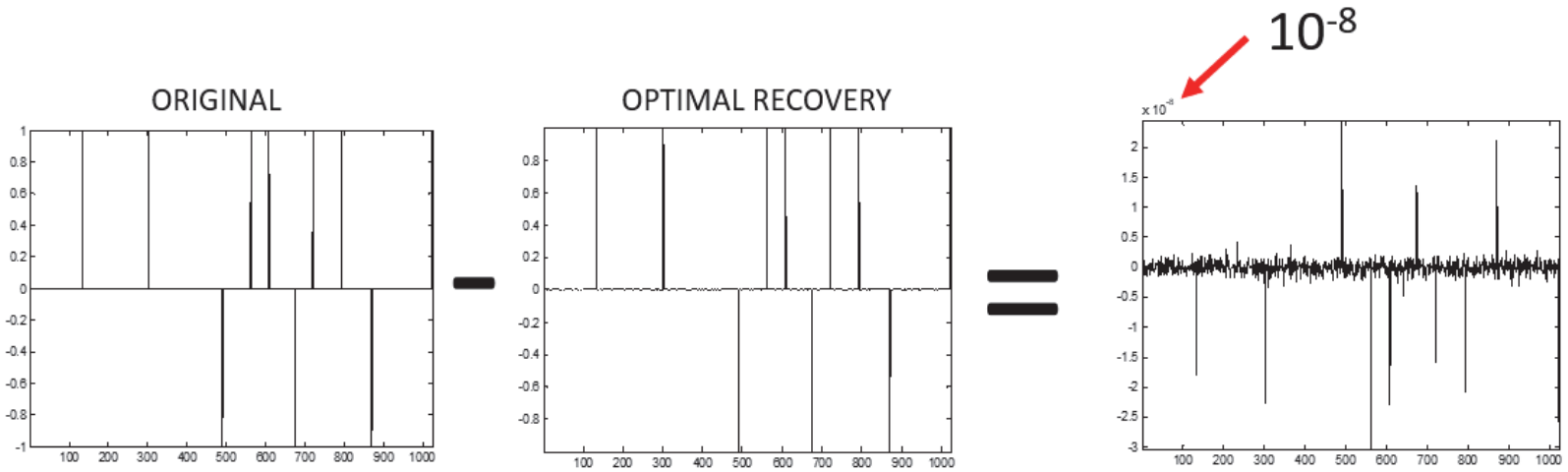

Linear Programming - QUICK!

Solve one or a set of linear equations subject to some constraint. In the case of Compressed Sensing, we are trying to solve $\mathbf{x} = Ay$ such that the $\|x\|_1$ distance is a minimum. More correctly, we are solving the inverse of this ... minimize $\|x\|_1$ distance such that $\mathbf{A}x = y$. The "how" part of this problem is a course unto itself in a whole slew of mathematics.

Bragg Peak - Proton Therapy

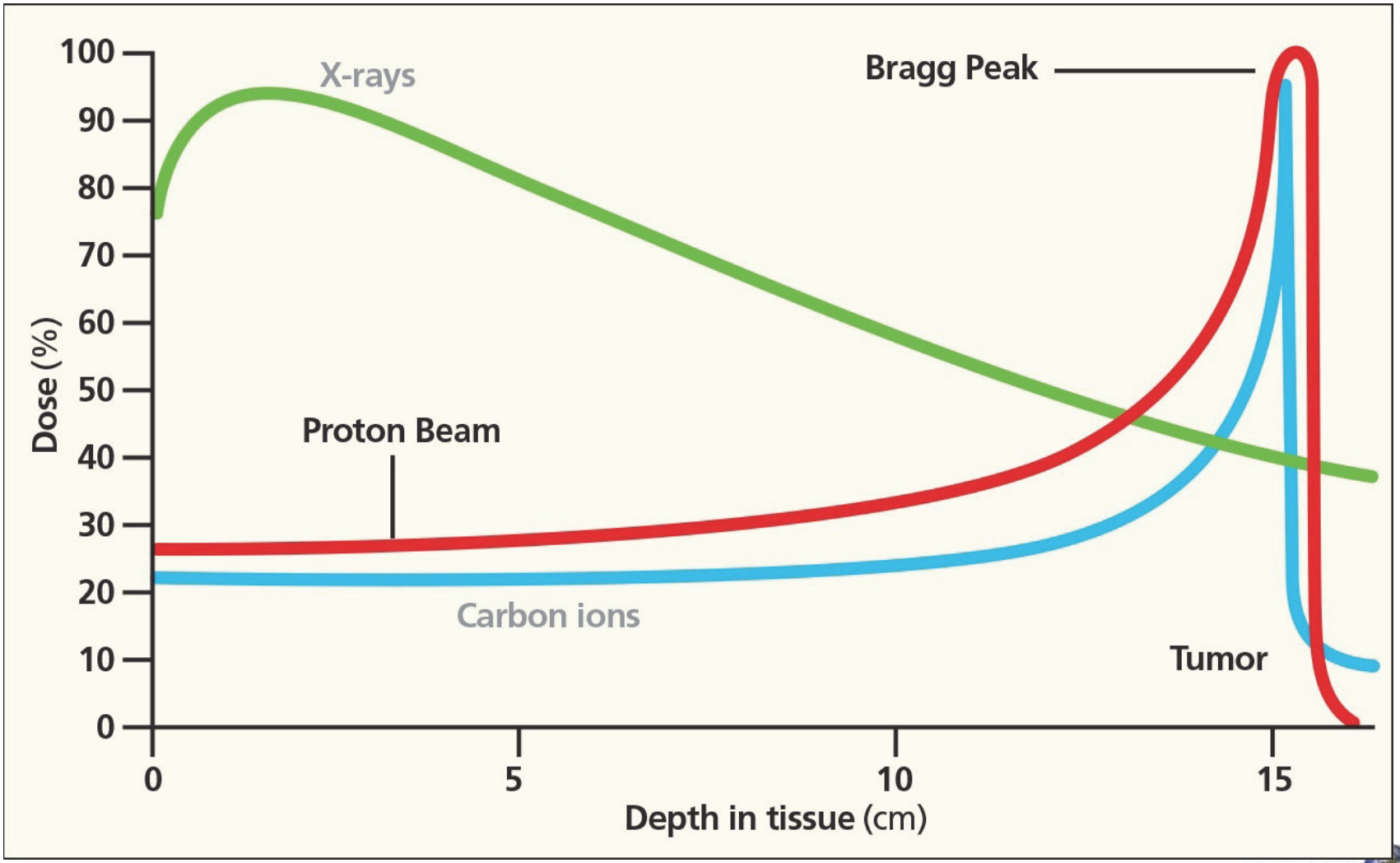

https://www.scripps.org/services/cancer-care

Bragg Peak - Proton Therapy

Bethe Formula (or Bethe Equation, or Bethe-Bloch Formula or ... Let's go with Stopping Power or Energy Loss Formula)

$$-\left\langle \frac{dE}{dx} \right\rangle = \frac{4\pi}{m_e c^2} \cdot \frac{nz^2}{\beta^2} \cdot \left(\frac{e^2}{4\pi\varepsilon_0} \right)^2 \cdot \left[\ln\left(\frac{2m_e c^2 \beta^2}{I \cdot (1-\beta^2)} \right) - \beta^2 \right] \tag{33}$$

where c is the speed of light and e_0 the vacuum permittivity, $\beta = \frac{v}{c}$, e and m_e the electron charge and rest mass respectively.

The key takeaway here is $-\left\langle \frac{dE}{dx} \right\rangle \propto \frac{z^2}{v^2}$ (because $\beta = \frac{v}{c}$), which means the loss of energy in inversely proportional to speed squared.

Proton Therapy

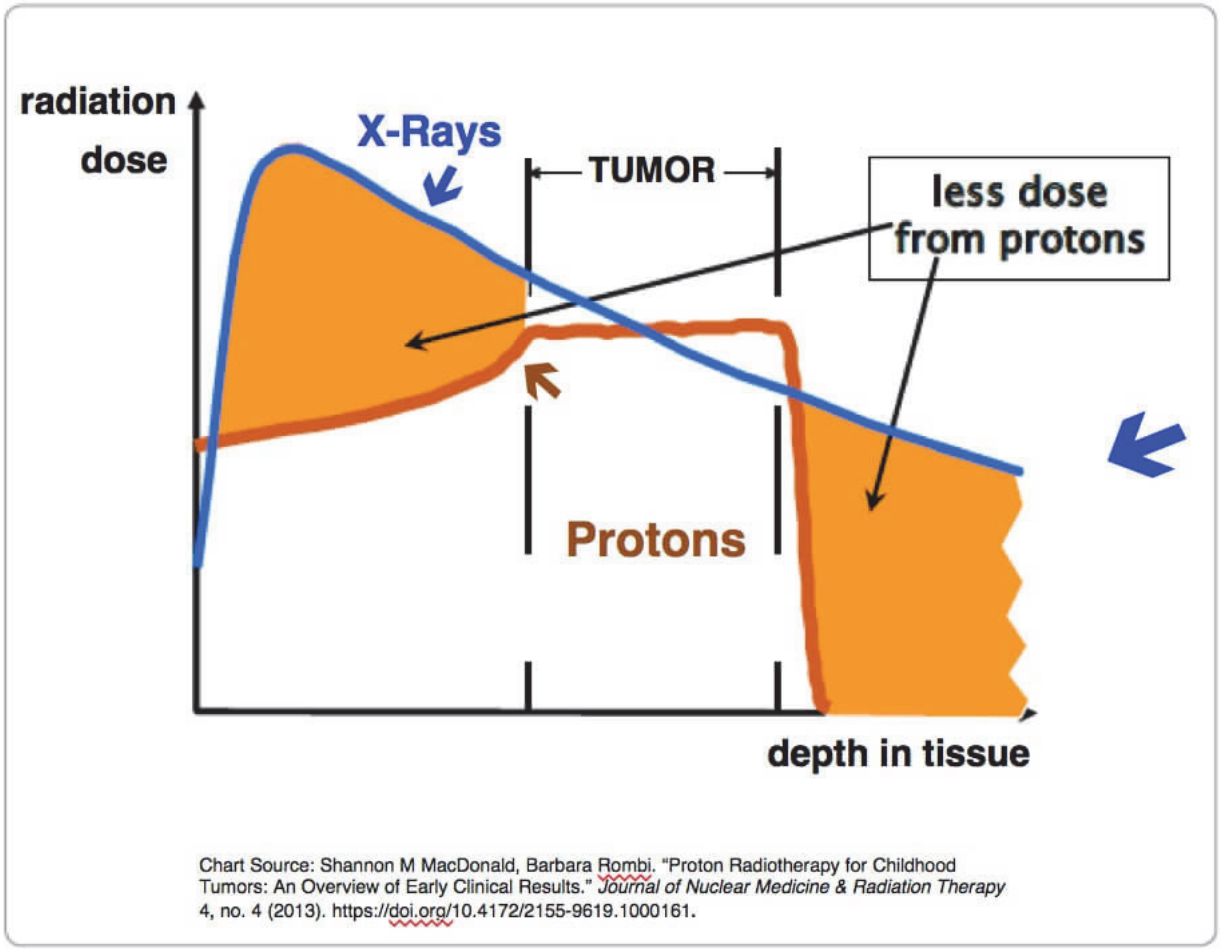

Chart Source: Shannon M MacDonald, Barbara Rombi. "Proton Radiotherapy for Childhood Tumors: An Overview of Early Clinical Results." *Journal of Nuclear Medicine & Radiation Therapy* 4, no. 4 (2013). https://doi.org/10.4172/2155-9619.1000161.

Protons STOP

X–Rays Do Not

Excess radiation to healthy tissue results in costly side effects and secondary tumors

THINK BIG WE DO™

Proton Therapy

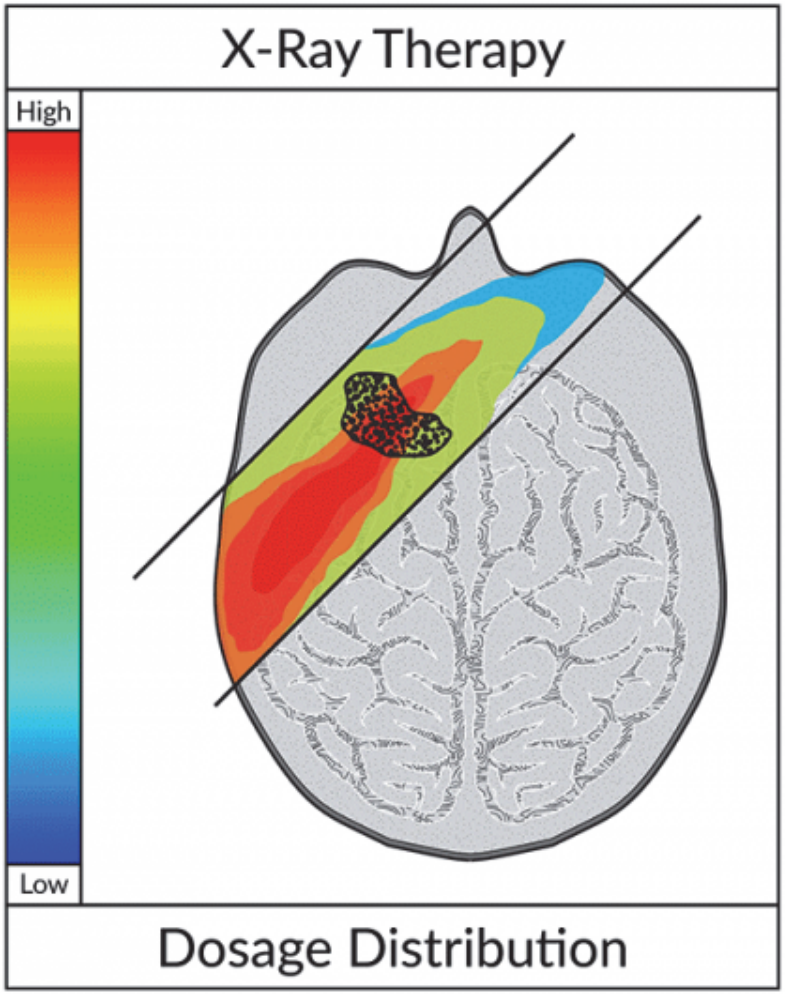

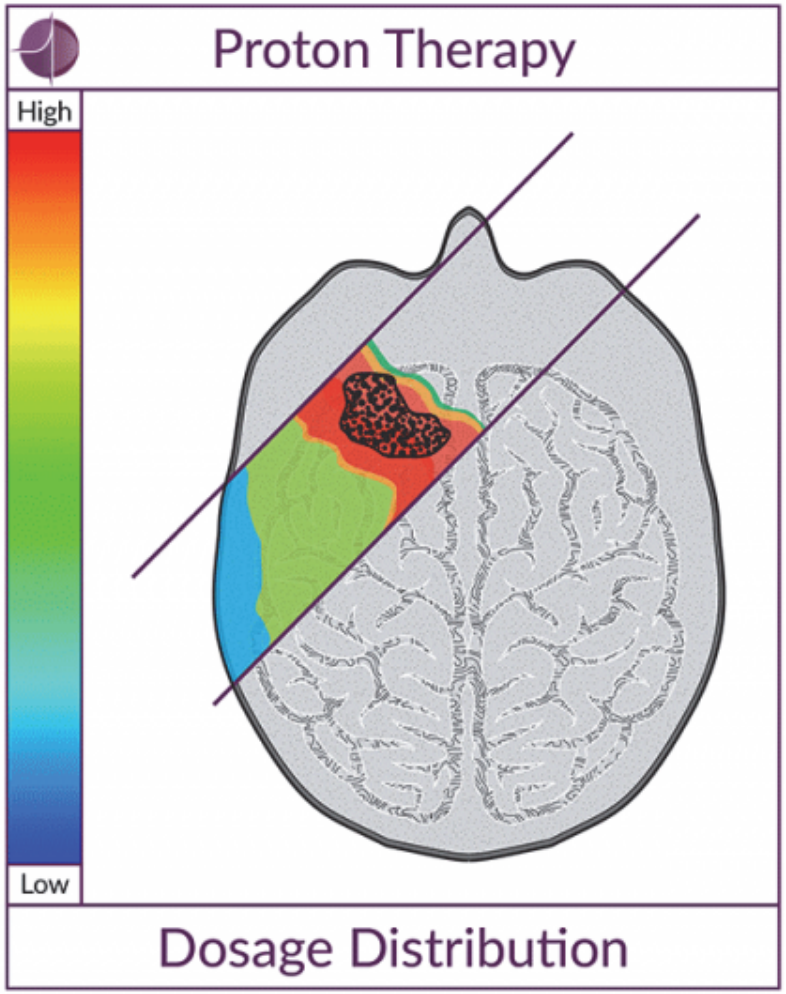

THINK BIG WE DO™

https://www.protominternational.com/proton-therapy/proton-

MRI-guided Proton Therapy

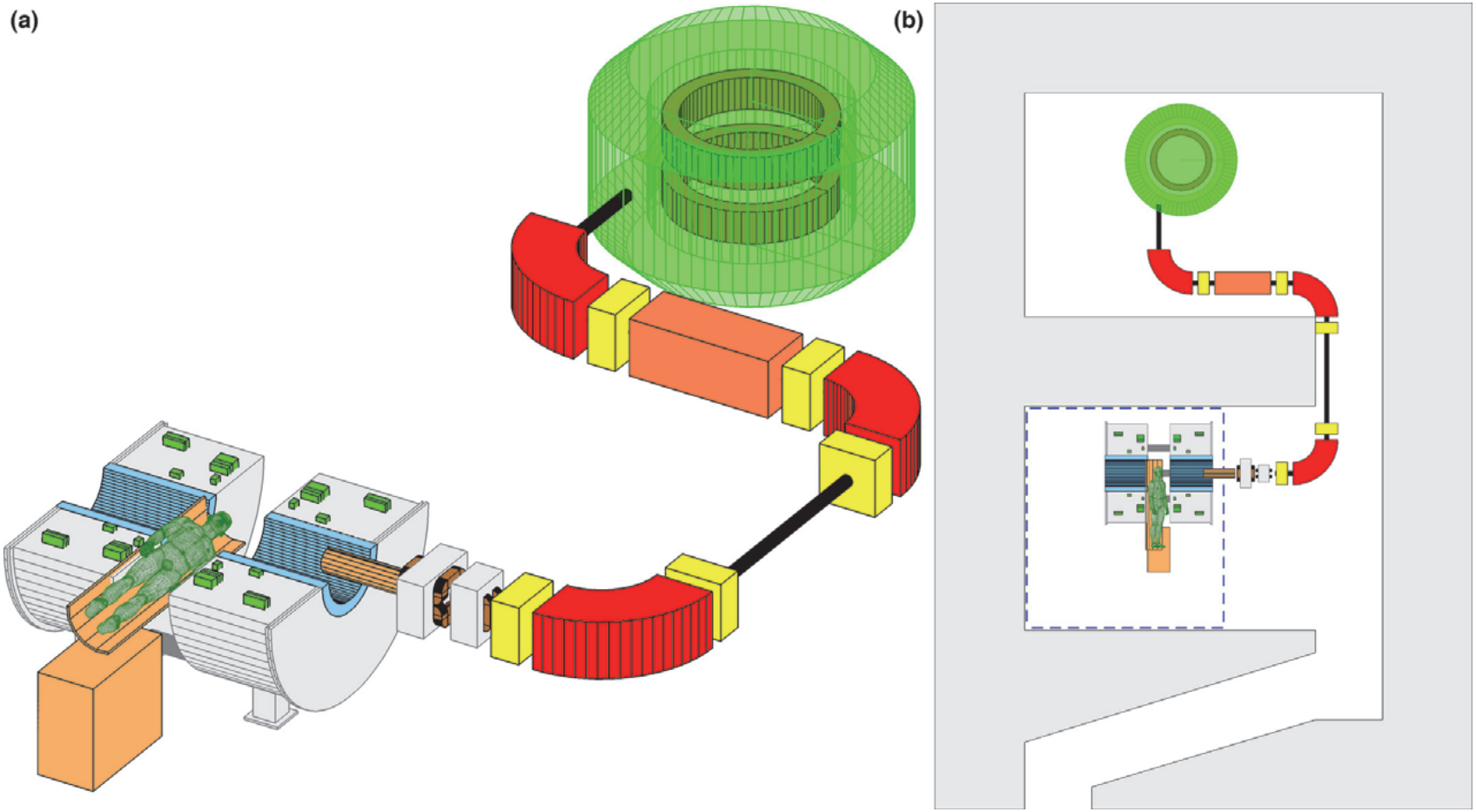

https://aapm.onlinelibrary.wiley.com/doi/full/10.1002/mp.1

MRI-guided Proton Therapy

https://www.aapm.org/meetings/09prs/documents/slopsema.pdf
https://indico.cern.ch/event/647153/contributions/2632004/a

S. Webb, *The Physics of Medical Imaging*.
Taylor and Francis, 1988.